LETTER REPRESENTATIONS IN THE MIND AND BRAIN

by
David Rothlein

A dissertation submitted to Johns Hopkins University in conformity with the requirements for the degree of Doctor of Philosophy

Baltimore, Maryland

September, 2015

ABSTRACT

Letter identification imposes numerous challenges on the brain's visual system. Identification processes must be flexible enough to recognize that **ear** and EAR refer to the same word while being precise enough to recognize that **lend me your ear** and **lend me your car** have different meanings. At the core of this dissertation is the assumption that the flexibility and precision which enables us to effortlessly recognize letters is based on our mental representations of letters. The experiments presented focus on two types of letter representations: font-invariant allographs and amodal abstract letter identities (ALIs). First, a set of behavioral experiments demonstrated that stored, font-invariant letter shape (allograph) representations influenced the visually similarity judgments participants made to pairs of letters presented in an atypical font. Following this result, an fMRI experiment was performed in which the neural response to visually presented single letter stimuli was analyzed using Representational Similarity Analysis (RSA). This analysis yielded evidence for allograph representations encoded within the left middle occipital gyrus and left fusiform gyrus. Finally, MVPA RSA analyses were employed to compare the patterns of neural responses to visually presented letter shapes and aurally presented letter names. This experiment revealed a region in the left fusiform gyrus that represented amodal ALIs (e.g., **a**, **A**, and /eI/ access the same amodal ALI). The research in this dissertation furthers our understanding of the representations that mediate letter identification and the results touch upon fundamental issues about the nature of information processing in cognitive science.

CANDIDATE:

David William Rothlein

READERS:

Brenda Rapp (Advisor), Cognitive Science

Michael McCloskey, Cognitive Science

Soojin Park, Cognitive Science

Marina Bedny, Psychological and Brain Sciences

Howard Egeth, Psychological and Brain Sciences

ACKNOWLEDGEMENTS

First and foremost I am extremely grateful to my committee—Brenda Rapp, Michael McCloskey, Soojin Park, Dr. Egeth, and Marina Bedny—for their willingness to read this dissertation and provide feedback. I would like to especially thank my advisor, Brenda Rapp, for the countless hours she has put towards helping me organize my thoughts. This includes the numerous rounds of revisions she provided for this dissertation and the amazing speed which she returned each draft. I absolutely could have not done it without you. Beyond the dissertation, she gave me the freedom to go from no fMRI experience straight to complicated MVPA analyses. Without that opportunity and her constant and brilliant guidance along the way I doubt I'd be where I am now. I would also like to thank Mike McCloskey for his willingness to tolerate my "ideas". More importantly, throughout my time at Hopkins he has constantly been a great role model, not just for his inhuman ability as a scientist and a critical thinker, but for his incredible generosity and willingness to help out those in need.

I would also like to thank all the faculty, staff, current undergraduate, graduate and recently graduated students in the Cognitive Science dept. for creating such a wonderful environment. If what the all the Alumni say is true, I will miss it dearly.

Finally I would like to thank my family—Lila for her constant support and "nudging" to finish, Hooper for tolerating me, my sister Lisa, my Mom and finally my Dad who inspired me to be a scientist in the first place. This dissertation is dedicated to him.

TABLE OF CONTENTS

LIST OF TABLES

LIST OF FIGURES

Chapter 1 - The multiple representations of letters in the mind and brain

Letter identification is a critical and often underappreciated cognitive process, both in terms of its importance for literacy and for the challenges it imposes on the brain's visual system. Like many other visual objects, letters are often easily identified despite large changes in size, position, and to some degree, orientation on the retina. Given that letters that share the same identity can vary in font[1] (see Figure 1) and case, the stimulus shape—even after correcting for changes in size and position—can vary dramatically. At the same time, while large changes in the visual shape of a character can be irrelevant (**ear** and EAR), tiny visual changes need to be processed for letters and ultimately words to be identified correctly (**lend me your ear** vs. **lend me your car)**. To deal with this need for visual specificity in the face of near infinite variability, many models of reading assume a series of increasingly abstract representations stored in memory that minimize dimensions of variability that are irrelevant for downstream processing while magnifying those features that are highly informative (see Figure 2 for overview) (e.g., Dehaene, Cohen, Sigman, & Vinckier, 2005; Grainger, Rey, & Dufau, 2008; Miozzo & Caramazza, 1998; Schubert & McCloskey, 2014).

---

[1] Classically, a typeface is a named set of letter shapes (e.g. New Times Roman or Comic Sans) and the font refers to the particular implementation of a typeface specifying parameters like size, boldness, or italics. In this paper, font will be used instead of typeface.

Figure 1. What is the nature of the internal representation that unifies the above forms as font variants of the basic shape **a**? Image from Hofstadter & McGraw (1995).

At the core of this dissertation is the assumption that the flexibility and precision with which we recognize letters is based on our mental representations of letters and the processes involved in connecting these stored letter representations together. Therefore, determining how we represent letters is critical to furthering our understanding of letter processing. Furthermore, understanding the representations, transformations, and processes involved in letter recognition could provide more general insights into how the mind/brain comes to comprehend the massive variation it regularly encounters in the world. This research will investigate both the ways we represent letters and the neural substrates encoding these representations by examining both behavioral and neural response patterns across variations in font (**a, a**), shape (**a**, **ɑ**, **A**), and modality (**a**, /ei/). In particular, I will present results from a novel paradigm demonstrating the role of stored (font-invariant) letter shape knowledge (allographs) in processing letters presented in an atypical font (Chapter 3). Additionally, I will identify the neural substrates of this stored letter shape knowledge (Chapter 4). Finally, I will investigate the role of multiple types of stored letter representations across visual vs. auditory stimulus presentations, with specific interest in localizing substrates that represent letter identity independent of sensory modality (Chapter 5).

1.1 A cognitive architecture for visual letter processing

In the following section I present a cognitive architecture for letter processing that is adapted from Rothlein and Rapp (2014), and motivated by a number of very similar proposed architectures (Brunsdon, Coltheart, & Nickels, 2006; Dehaene et al., 2005; Miozzo & Caramazza, 1998; Schubert & McCloskey, 2014). The box-and-arrow diagram in Figure 2 schematizes representational transformations from the light of the letter image hitting the retina to lexical access (reading), motoric production (writing or copying) and letter naming/oral reading. Within each box is a bank of representational features. I will describe each of these levels of representation in more detail below.

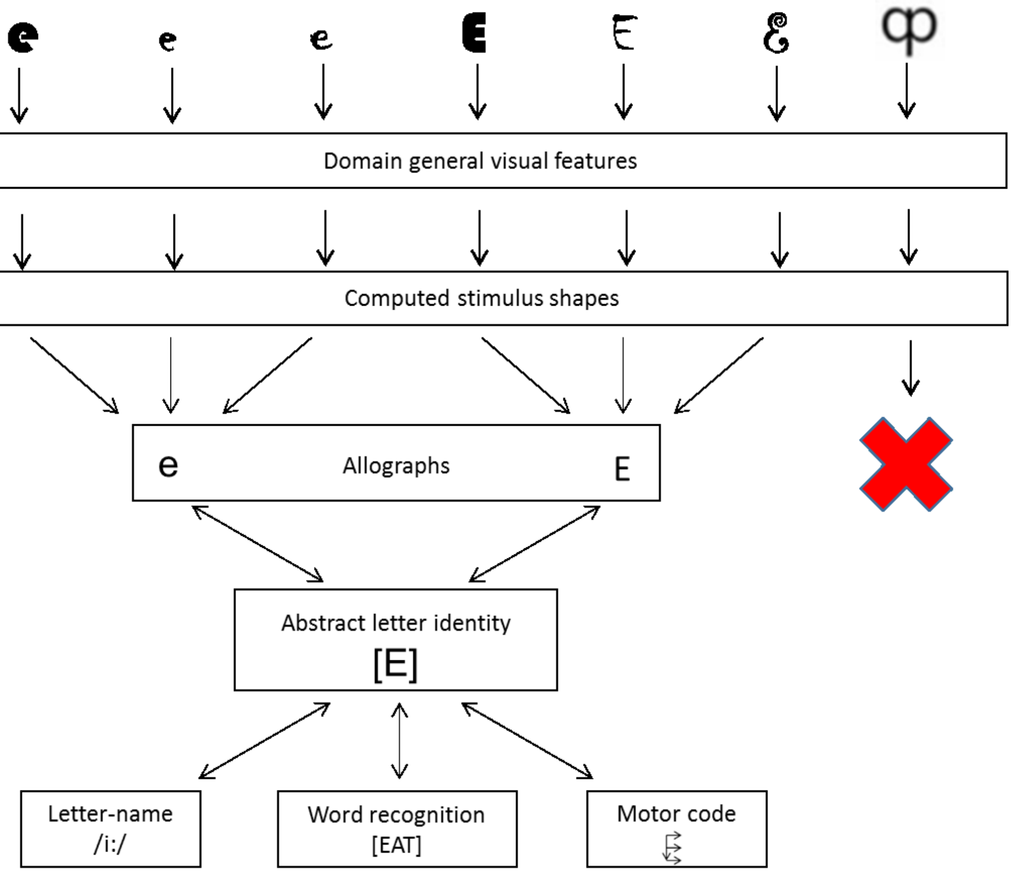

Figure 2. Various different fonts of the letter E and one pseudoletter are initially processed through domain general visual features (e.g. Simple and complex cells representing oriented bars). Many models also posit a font-specific computed stimulus shape level of representation that computes the shape of the stimulus independent of its identity (Caramazza & Hillis, 1990; Dalmás & Dansilio, 2000; Hillis & Caramazza, 1991; Rapp & Caramazza, 1989; Schubert & McCloskey, 2014). For example, we can perceive the shape of the letter R as well as the shape of a pseudoletter we have never seen before. This level of representation would allow us to describe the shape of the letter R as well as the shape of any given pseudoletter but importantly it does not encode any information regarding the identity of the shape or even whether the shape is a letter or not (e.g., Miozzo & Caramazza, 1998). These computed stimulus shape representations go on to access stored font-invariant allograph representations. While the precise format of allograph representations will not be specified throughout these studies, it presumably encodes letter shapes in a manner that abstracts away from at least certain differences in stimulus font. For example, **a** and a will activate the same allograph while ***a*** will activate a different allograph. These representations allow us to recognize that all the shapes in Figure 1 approximate the same shape—a lowercase a. The allographs in turn activate abstract letter identity (ALI) representations that represent the identity of letters in a manner that abstracts away from visual information altogether. ALI representations serve as input to lexical and sublexical reading processes and they also serve as a conduit to cross-modal letter representations like phonological letter names.

1.1.1 Domain general visual features

At the earliest stages of visual processing, internal representations will be largely isomorphic with the pattern of light-energy that the sensory organs transduce. If the stimulus is a visual object, these representations encode image properties like intensity values assigned to retinotopic positions. Changes to any of the image properties will result in changes to these early representations. Image representations of letter stimuli (as well as any other objects) could be approximated by pixel configurations.

According to many predominant views of visual-spatial processing (see Riesenhuber & Poggio, (1999) for review), the low-level retinotopic input will undergo a series of transformations in which the stimulus is represented as a set of increasingly more complex visual features which often are composed of conjunctions of simpler complex representations. For example, at the lowest level, the stimulus may be represented as a set of oriented bars, which would serve as input to simple visual feature detectors (e.g., right angles, crosses and curves). From these features, the shape of an object is computed.

1.1.2 Computed stimulus shape representations

The lines, curves, and angles that compose the low-level, domain general visual features are integrated into a unitary shape at the level of computed stimulus shape representations. Critically, the shape that is computed may or may not correspond to an actual stored alphanumeric form (a.k.a allograph). For example, the rightmost stimulus in Figure 2 does not correspond to any real alphanumeric character. So while the shape will be represented as a unitary form at this level of representation, the computed shape will fail to activate any stored letter representations. Therefore, while information from computed stimulus shape representations will presumably distinguish a coherent and unitary character-like form from a random scatter of disconnected lines and dots, knowledge of character shape alone is not sufficient to determine if the stimulus is a real alphanumeric character or a pseudoletter[2]. It is important to know that the shapes at this level of representation are sensitive to changes in font. For example, information at this level would not represent **a** and **a** as font variants of the same allograph. Furthermore, our ability to perceive the difference between **a** and **a** is likely in virtue of the (font-sensitive) computed stimulus shape representations.

1.1.3 Allograph representations

A character's basic shape (Herrick, 1974) is a font invariant description of a spatial letter-form. Allographs consist of basic shape representations **that are learned and stored in long-term memory**. Under this definition, **a** and **a** (as well as all the letter tokens in Figure 1) are examples of the same allograph, whereas **a**, **ɑ**, and **A** are 3 different allographs. A key question for this dissertation is how our prior knowledge of letter identities and shapes influences letter identification.

While allograph representations provide a computational means to reduce the variability of stimulus shapes for downstream processes, alternative word recognition models without allograph representation are conceivable. For example, exemplar-based models propose to account for letter and word recognition without allograph representations (Marsolek, 2004). These models rely on large storage capacities that can encode memory traces of every instance a letter exemplar is viewed. When a novel letter

---

[2] A letter-like form that does not correspond to an actual symbol

stimulus is viewed, it is identified by computing the similarity of the stimulus to each of the stored exemplars. The viewed stimulus would be identified by assuming the label of the nearest stored exemplar (see Goldinger, (1998) for an exemplar model of spoken word recognition). As opposed to abstractionist accounts of cognition, these models are consistent with grounded and embodied cognitive theories that rely solely on sensory and motor representations (Barsalou, 2008; Tulving, 1983; Wilson, 2002). Accordingly, in an exemplar-based letter recognition model, the content and format of the representation of letter stimuli undergo minimal transformation in order to be identified so that the distinction between sensory processing and higher-level cognition is blurred. Evidence in favor of exemplar-based accounts visual word recognition comes largely from font-specific priming effects (see Tenpenny, (1995) for review, but see Bowers, (2000) for an alternative explanation). Therefore, determining whether allograph representations are used for letter identification, in addition to furthering our understanding of word recognition, contributes to more fundamental debates regarding abstractionist vs. episodic views of human cognition.

Arguments in favor of allographs generally rely on demonstrating that the letter processing system has three properties: (1) shape sensitivity—that the system is sensitive to whether a visual form depicts a familiar alphanumeric character or not (e.g., **a** vs. ϡ[3]); (2) shape specificity—that the system will respond differently to different allographs, even if they shares the same abstract letter identity or ALI (e.g., **a, ɑ** and **A**); and (3) font-invariance—that the system will respond identically to different computed stimulus shapes depicting the same allograph (e.g., **a** and **a**).

---

[3] Assuming the cognitive system is unfamiliar with this version of the Greek character Sampi.

Cognitive neuropsychological studies

To date, evidence for allograph representations comes primarily from single-case studies (Brunsdon et al., 2006; Chanoine, Ferreira, Demonet, Nespoulous, & Poncet, 1998; Dalmás & Dansilio, 2000; Miozzo & Caramazza, 1998; Rapp & Caramazza, 1989; Schubert & McCloskey, 2014). For example, GV (Miozzo & Caramazza, 1998), following a stroke, had a deficit in letter processing that demonstrated both shape sensitivity and specificity. Specifically, GV demonstrated she was sensitive to a letter's shape by performing perfectly in a task where letters and pseudoletters (invented letter forms) were presented and GV had to decide whether the shape was a letter or not. In order to perform this task, GV had to access stored representations that could differentiate real from invented letters. Such a decision could be made by accessing many types of stored representations of letters; therefore, in order to identify the specific type of representation used in the pseudoletter decision task, Miozzo and Caramazza (1998) had GV perform tasks that required accessing a letter's ALI. They found that GV was severely impaired in such a task where she had to correctly match identical cross-case letters like **a** and **A** (accuracy 63%). On this basis, they reasoned that since GV's deficit impairs access to ALIs, her ability to perform the letter/pseudoletter decision task was likely based on intact processing at the level of allograph representations. While font-invariance was never tested with GV, ET, who had a developmental reading deficit (Brunsdon et al., 2006), and LHD, whose reading difficulties followed a stroke (Schubert & McCloskey, 2014) showed patterns similar to GV but were also capable of matching letters across differences in font. These results demonstrate font-invariant representations in individuals with impairments in forming/accessing ALIs in a normal manner. The pattern of results from ET is consistent with a system in which there are allograph representations that can be used to abstract over font variations. It is also worth noting that LHD had difficulty matching letters when they changed from print to cursive (see also Rapp & Caramazza, 1989) suggesting there are separate cursive and print allographs for the same letter.

Behavioral studies

Unlike the patient studies, behavioral evidence from studies with neurotypical individuals in support of allograph representations is quite limited. One study found evidence for a level of letter representation that is consistent with allographs by examining the memory for color-shape conjunctions (Walker & Hinkley, 2003). Walker and Hinkley found that, when articulatory suppression techniques were employed, participants were better at remembering color-letter associations when the letter itself was colored vs. when the letter was white on a colored background. Crucially, they found that this color-letter association would generalize across changes in font but failed to generalize across changes in case. This effect was true even when certain changes in font were judged to be more visually dissimilar than changes in case demonstrating that this effect was not solely based on the degree of visual differences. These results were interpreted as showing that the colors were linked to letter representations that were abstract enough to survive changes in font but not abstract enough to survive changes in case—in other words, the colors were linked to allograph representations.

Neuroimaging studies

Neuroimaging evidence supporting the existence of allograph representations is limited as well. Studies have only investigated this possibility by examining either priming effects (Gauthier, Tarr, et al., 2000; Qiao et al., 2010) involving single letters or words presented in different fonts. These studies found different-font priming effects in the left fusiform gyrus. The challenge in interpreting these results is pinpointing the type of representation that was driving these priming effects. Since single letter stimuli were used in the Gauthier et al. (2000) study, priming could have been driven by ALI representations or even low-level visual similarity. Word stimuli were used in the Qiao et al. (2010) study and while these priming effects could have arisen at the level of allograph representations, they also could have arisen at the level of abstract letter identity, lexical, semantic, or phonological representations as these are all shared across changes in font. These confounded types of representations are rarely distinguished in neuroimaging studies of letter and word recognition.

Rothlein and Rapp (2014) explicitly set out to deal with this issue by examining the similarity of multi-voxel patterns of neural responses evoked by viewing single letters and examining if there were neural response similarity patterns best explained by ALIs and/or visual, motoric, and/or letter name similarity. They found neural substrates selectively sensitive to visual similarity in the posterior occipital cortex and abstract letter identity left-lateralized along the ventral occipital and temporal cortex. However, with regard to visual similarity they did not distinguish between similarity effects due to low-level visual features, computed stimulus shape representations, or more abstract allograph representations. The research in Chapter 4 builds on Rapp & Rothlein (2014) by specifically examining if there are distinct neural substrates that are sensitive to computed stimulus shapes and/or allograph representations.

1.1.4 Abstract letter identity (ALI) representations

A starting assumption about ALI representations is that they encode a letter's case-invariant identity, regardless of the letter's surface/perceptual properties (Besner, Coltheart, & Davelaar, 1984; Coltheart, 1981; Kinoshita & Kaplan, 2008; McFarland, Frey, & Landreth, 1978; Polk & Farah, 1997). This can be unpacked into 2 claims about ALI representations: that they are case-invariant and that they are amodal—meaning the same representation is accessed whether the letter is seen, heard, or touched. Most empirical research has focused on the case-invariant criterion and that will be the primary empirical criterion for ALI representation in this paper however in Chapter 5 I will also explicitly test the latter claim as well.

Behavioral studies

The evidence in support of ALIs is not without its controversies. Behavioral studies have shown that participants can be induced to remember the identity of words while being unaware of the letter case in which the word was presented (Adams, 1979; McClelland, 1976). While this is clearly evidence for case-invariant word representations, this is not sufficient evidence for ALIs since both uppercase and lowercase versions of a word should activate the same lexical unit, phonological code, and semantic network. Given that all of these possible representations support case-invariant behavior with words, to attribute these findings to ALIs requires further experimentation. Studies that have demonstrated cross-case word priming (Bowers, Vigliocco, & Haan, 1998; Dehaene et al., 2001) even when controlling for the visual similarity of cross-case letter pairs (Dehaene et al., 2004), have the same ambiguity of interpretation. Importantly, Kinoshita and Kaplan (2008) showed cross-case priming to single letters which, presumably, was not based on lexical or semantic representations. Furthermore, Carreiras et al. (2012) showed cross form priming for single Arabic letters. While these studies certainly provide compelling evidence for ALIs, there is still a possibility that the letter name code—which is case and form invariant—is driving the priming effects in these studies. In other words, in the word-based experiments, priming may have occurred at the level of word or semantic representations and in the letter-based experiments, priming effects may have involved letter name representations.

Cognitive neuropsychological studies

The strongest evidence for ALIs comes from individuals with acquired deficits who, while unable to name individual letters, were still capable of matching letters across case—even when they were visually distinct (Mycroft, Hanley, & Kay, 2002). That they were unable to name them largely rules out the possibility that the cross-case matching was performed based on shared letter name representations. Furthermore, they could understand aurally presented letter names suggesting the deficit was limited to visually presented letters. Another individual who provides unique source of evidence for ALI representations is LHD (Schubert and McCloskey, 2014). Although her deficit was believed to involve difficulty in accessing ALIs from allograph representations, the particular letter errors she made provided compelling evidence for the existence of ALIs. When reading a list of words, LHD would often substitute letters towards the end of the word (e.g., in reading CAR she would have been more likely make an error on the R, perhaps reading CAG instead). Particularly relevant was that the incorrect letter substitution often appeared in the previous word in the list (letter perseverations). Relevant to the issue of ALIs was the finding that when LHD was performing a delayed copy task for mixed-case words (CaR), letter identities from previous word would perseverate into later words independently from the case in which they had appeared. For example, with a prior word such as C-a-R the identity of R but not the case, might have perseverated into the following stimulus m-A-t which LHD might copy as m-A-r. What is critical is that the allograph itself did not perseverate otherwise one would predict the response m-A-R. Instead the best explanation was the ALI representation perseverated independently of the case representation.

Neuroimaging studies

Most of the neuroimaging studies that support the existence of ALIs are subject to the same ambiguities as the behavioral studies. Polk & Farah (2002) showed that the left inferior occipitotemporal region became active in response both to mixed-case words as well as to uniform-case words (e.g., APpLe vs. APPLE). A similar brain region has also been shown to exhibit cross-case word priming while being insensitive to the visual similarity of the cross-case pairs (e.g.. red primes RED just as much as cow primes COW) (Dehaene et al., 2001, 2004). While these results suggest representations in this region are not purely visual, the exact nature of the representations responsible for the priming effects remains unclear because while these results are consistent with a region that represents the abstract identities of letters, they are also consistent with a region that encodes lexical, semantic and/or phonological representations of the word stimuli. Dehaene et al. (2004) more directly tested for ALIs by examining the amount of priming between anagram pairs that are identical except that the last letter of one word is moved to the first letter of the other (e.g. pines/SPINE); the logic was that this paradigm could reveal cross-case priming while varying the lexical identity of the prime and target..

Cross-case priming effects were found in the posterior extent of the left occipitotemporal region only when the stimuli were aligned so the prime and target cross-case pairs fell on the same retinal position (e.g., #pines primes SPINE#), leading the authors to argue for ALIs that are specific to retinal position. These priming effects cannot be explained at the level of lexical or semantic representations. While this study addressed some of the shortcomings of previous studies, it was not clear if the cross-case prime-target pairs were controlled for visual similarity. Therefore it could be the case that the priming results were driven by visually similar cross-case letter pairs (e.g., p-P, o-O, u,U).

Rothlein and Rapp (2014) provided some of the strongest evidence to date for ALI representations by identifying neural substrates that were specifically and selectively sensitive to cross-case letter identity. They found that the multi-voxel patterns of neural responses evoked by single letters were more similar when letters shared the same identity than when they did not and, importantly, the same neural responses were not sensitive to visual form, letter name, or motoric production feature similarity. Identifying selective sensitivity to ALI representations provided evidence that the identity effects could not be explained by other confounding letter representations. The neural substrates identified as selective to ALI representations were localized along the left ventral occipital and temporal cortex. These results are explained in more detail in Chapter 2 and replicated in Chapter 5.

1.1.5 Other modality-specific representations

Motoric

Motoric representations are the stored set of motor codes one uses to produce letter forms. Instead of encoding the allograph **A** in terms of visual features, a motor code representation of the allograph is composed of an ordered sequence of actions, such as: <**vertical-up**, **vertical-down**, **horizontal**> (Rapp & Caramazza, 1997). The relationship between the motoric representations of letters and visual letter expertise has been investigated in a number of neuroimaging studies (James & Atwood, 2009; James & Gauthier, 2006; Longcamp et al., 2008; Longcamp, Anton, Roth, & Velay, 2003). As these studies showed, brain regions involved in the motoric production of letter forms (e.g., Exner's area) were also activated when viewing familiar letter-forms. In fact, the learning of alphanumeric symbols resulted in an increase of activation in these brain regions (James & Gauthier, 2006). Of course motor features cannot be necessary for letter recognition as people often recognize symbols they may have difficulty producing (e.g., **&**). The relationship between motor features and allograph representations are explored further in Chapter 3.

Letter name

Each letter is associated with a name and that name must be stored such that it can be accessed to name visually presented letters. The format of such stored representations could be a phonological, or acoustic. The work in this dissertation will remain largely noncommittal with regard to these two possibilities but will instead, investigate the relationship between letter name representations and abstract identity representations. Specifically, do heard letter names access the same letter identity representations as seen visual letter shapes? This question along with an experiment that addresses this question will be expanded on in Chapter 5.

1.1.6 Other abstract letter representations

Letter case

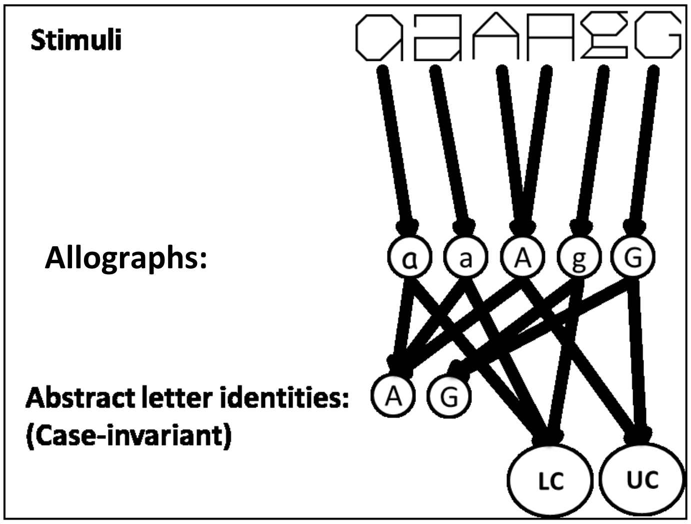

Figure 3. A diagram depicting a letter processing scheme whereby case is represented independently from identity.

While ALIs may be case-invariant, information about a letter's case cannot be entirely disregarded by the processes that mediate word (and letter) recognition. This is because two words can be composed of the same ALIs but have different meanings based on the case of the first letter. For example, the meaning of the sentence *I hate all these bills* changes dramatically if the *b* in *bill* is capitalized.

Evidence for identity-independent case representation comes from LHD (McCloskey, Fischer-Baum, & Schubert, 2014; Schubert & McCloskey, 2014), who, as previously discussed, perseverated letter identities that would assume the case of the letters they were substituting (e.g., if the R in c-A-R perseverated into the word M-a-t it would be copied as M-a-r but had it perseverated into the word M-a-T it would become M-a-R). That the identity of the [R] in c-A-R can perseverate independently of case suggests case representations that exist independently of identity representations (Figure 3). We examine this hypothesis more explicitly in Chapter 3.

Consonant vowel status

Each letter identity can be characterized as being either a consonant or a vowel. These categories place important constraints on the role the letters play in constructing words and the set of possible sounds that are associated with a given letter. While there is considerable evidence that a letter's orthographic consonant/vowel status (c/v status) is represented independently of letter identity in spelling (Buchwald & Rapp, 2006), there is less such evidence in reading (but see Berent & Van Orden, 2000; Carreiras, Gillon-Dowens, Vergara, & Perea, 2009; Carreiras & Price, 2008). The most direct evidence in spelling comes from individuals with acquired dysgraphia. Some of these individuals make letter substitutions errors ("GLOW" misspelled as GLOT) such that the substituted letters maintain the orthographic c/v status of the target letters more than would be expected if the substitutions occurred by chance (Buchwald & Rapp, 2006; McCloskey, Badecker, Goodman-schulman, & Aliminosa, 1994). Therefore, in these letter substitutions, the ALI of a letter in a word is lost, but the independent c/v representation is maintained. This spared c/v representation is used to constrain the set of possible letters that will be produced in substitution errors. The work in this dissertation will examine the possibility of the automatic activation of c/v representations in letter recognition. Specifically, in chapters 3 and 4 we will investigate the possibility that each letter activates a consonant or vowel representation that is shared with other letter stimuli.

Alphanumeric symbol category

Another issue of interest concerns the level of representation at which the distinction between letters and digits occurs. There is limited evidence, largely based on neuroimaging studies, that there are different neural substrates selectively involved in letter recognition and digit recognition (Cantlon et al., 2011; Hannagan, Amedi, Cohen, Dehaene-lambertz, & Dehaene, 2015; Park, Hebrank, Polk, & Park, 2011; Polk et al., 2002; Price & Ansari, 2011; Shum et al., 2013). However, there is little agreement as to which specific neural substrates are selective for digits vs. letters. Perhaps most consistent is the finding that the right mid fusiform tends to be more active for digits and the left mid fusiform tends to be more active for letters (Hannagan et al., 2015; Park et al., 2011; Polk et al., 2002; Shum et al., 2013). While these studies suggest that letters and digits are differentiated at some point, none of these studies investigated the representational content at the level at which letters and digits diverge. While it is generally agreed letters and digits rely on the same low-level visual mechanisms, and letters and digits ultimately serve very different functional purposes (e.g., reading in the former case and representing and manipulating quantities in the latter), it is unclear whether intermediate representations distinguish between letters and digits. For example, would a region that represents ALIs also represent digit identity or would digit identity be represented elsewhere? These issues will be explored in Chapters 3 and 4.

1.2 Letter representation and modality

So far I have discussed a number of representations that may mediate the journey of a letter from a visual stimulus to an abstract orthographic representation. The dissertation includes experiments that will attempt to localize these representations to their neural substrates, with the goal of creating a comprehensive neurotopography of letter representations. Thus far, the discussion has involved visual letter stimuli. While considerable research has dealt with the abstraction of the visual letter stimulus, remarkably little research has investigated the representations that mediate recognizing and processing spoken letter-names.

Rothlein and Rapp (2014) identified a cluster in the left posterior STS that was sensitive to letter name similarity evoked from the visual presentation of letters. This finding was interpreted as evidence for modality-specific phonological letter name representations. While it was not explicitly addressed, the presumption is that these regions should respond to spoken letter name stimuli in a similar fashion. A more important assumption of the framework depicted in Figure 2, is that abstract letter identities are a necessary gateway between modality-specific letter representations and further orthographic processing. As Figure 2 shows, spoken letter names—like visual letters—must access the same ALIs in order to be visualized, written, or used for word recognition. While coherent, this view of letter name processing is largely speculative because of the dearth of empirical results addressing this topic.

The experiment in Chapter 5 tests the hypothesis that ALIs mediate letter identification regardless of whether the letters are presented visually or aurally. Evidence for this would specifically address the issue regarding the amodal nature of ALIs. In addition to representing a seen letter in a case-independent manner (as shown in Rothlein and Rapp, 2014), this experiment will determine if ALIs are accessed in a modality-independent manner as well.

1.3 Summary and conclusions

The goal of this dissertation is to investigate both the types of letter representations involved in letter processing as well as the neural substrates encoding these representations by examining both behavioral and neural patterns in response to letters that vary in font (**a, a**), allograph (**a**, ***a***, **A**), and modality (**a**, /ei/). I have briefly reviewed the literature regarding a set of stored letter representations that have been proposed to allow both visual tolerance and precision in the identification of visual letters. The questions addressed in this dissertation and brief statements of findings are listed below:

1. *Do font-invariant allograph representations mediate letter recognition?* While there is evidence for allographs from patient case-studies, evidence from other methodologies is lacking. Furthermore the neural substrates of these representations have not been carefully investigated. Findings from the experiments carried out in this dissertation will provide behavioral evidence (Ch. 3) for the existence of allograph representation and localize their neural substrates (Ch. 4).
2. *Are abstract letter identities involved in letter identification?* The work presented in Ch. 3 and Ch. 5 will replicate and build upon previous evidence for font and case-invariant ALI representations.
3. *Are the neural regions that encode case-invariant letter identity amodal as well?* Specifically, do visual letter stimuli and auditory letter names access the same ALI representations? The results reported in Ch. 5 will provide novel evidence supporting the existence of amodal ALIs.

4. *Are task irrelevant sensorimotor representations such as phonological letter names or motor production patterns automatically activated during visual letter processing? Likewise, do aurally presented letter names activate task-irrelevant visual/spatial letter representations?* Ch. 3 addresses the former question while Ch. 5 addresses both questions.
5. *Is a letter's c/v status or case automatically represented in tasks that do not explicitly require this information?* These issues are addressed in Ch. 3 and Ch. 4.

Chapter 2: Representational similarity analysis

The methodology employed in the research in this dissertation follows and expands upon a growing trend to take advantage of the multivariate (multivoxel) aspect of fMRI data. As I will demonstrate in the following sections, harnessing the multivariate richness available in fMRI data allows us to investigate the cognitive phenomena underlying letter recognition to a degree of precision that not only identifies neural networks that are activated during letter recognition, but begins to decipher the representational contents of these letter activations. To this end, I use Multi-Voxel Pattern Analysis, Representational Similarity Analysis (MVPA-RSA) (Kriegeskorte, Mur, & Bandettini, 2008) methods to link theories of representational content to neural and behavioral data by measuring the degree of second-order isomorphism between predictions about representational content and observed patterns of brain and behavioral responses.

2.1 First order isomorphism

Isomorphism, in the context of cognitive neuroscience, refers to the "extent that there is some structural resemblance between an individual internal neurophysiological event and the individual external object that it represents" (Shepard, 1975). To illustrate this idea, imagine an experiment where a researcher is measuring the neural response across 4 neurons in response to an externally presented square. The researcher already discovered that each neuron has 4 different firing rates, each indicating a different position of an oblique line. In response to visually presented square (Figure 4, left), the researcher records firing rates indicating the presence of each of the different possible line orientations across the four neurons (Figure 4, right). That such a mapping exists demonstrates a first-order isomorphism between the image and brain space. If you knew precisely how the brain space maps on to the image space (i.e. you knew the functions that mapped between the two isomorphic spaces), you could reverse engineer any brain response to reconstruct the actual picture shown without ambiguity.

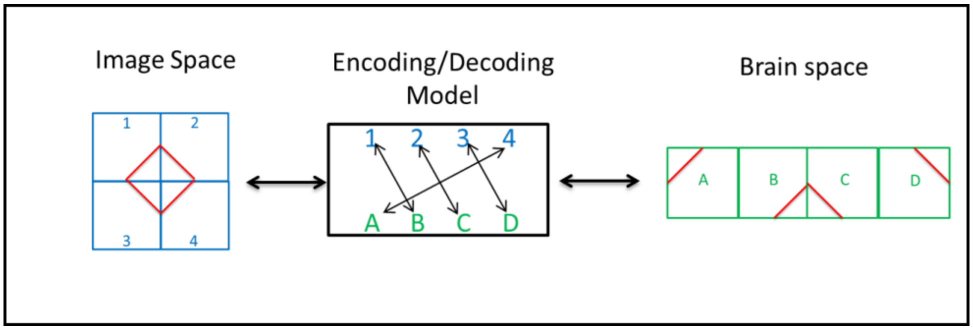

Figure 4. An example of a first order isomorphism between the representation of a diamond shape in two systems. The first order isomorphic relationship means that each feature in image space has a one-to-one mapping with a feature in "brain space". The formal description of this mapping serves as an encoding model that can translate information between the two spaces. At this point, encoding models are quite scarce, particularly for brain regions believed to underlie higher-level cognition.

A first order isomorphism between cognitive representations and processes and brain activation entails that changes in cognitive processes and representations will result in functionally equivalent neural changes. A description of this cognition-to-brain mapping is a neural encoding theory (see Figure 4, center). A neural encoding theory is successful to the extent that it can predict neural behavior resulting from a set of cognitive operations (processes and representations) and conversely predict the cognitive operations being carried out based on observed neural behavior (decoding) (Kriegeskorte, 2011)[4]. For neural encoding theories to be tested, such theories require a description of: (1) the cognitive representations and processes involved in recognizing a given stimulus or performing a specific task; (2) the mapping between cognitive representations and processes and neural behavior; and (3) a mapping between the neural behavior (e.g., the firing rate of neurons) and the measured signal generated from the neural behavior (e.g., the BOLD signal from an fMRI scanner). A description of (3) entails properly modeling the influences of noise and spatial/temporal resolution specific to the recording device. Description (3) is necessary because encoding theories, to be testable, must predict the expected *measured* neural activation using some imperfect imaging device. Only once the technology exists that can measure the cognitively relevant signals from the brain—noise-free and at the perfect resolution—will (3) become unnecessary. Given that I am largely interested in identifying the representations that mediate letter recognition, a method that can utilize neural data in service of (1) while minimizing the necessary assumptions about (2) and (3) is ideal. Representational Similarity Analysis achieves this by measuring the second order isomorphism between theoretical representations and measured brain activation.

---

[4] Many encoding models can successfully predict patterns of neural activity in response to a given stimulus, but these models are not cognitive insofar as they generally rely on the first-order isomorphism between neural activity and surface image properties, or even learned stimulus-to-neural response regularities of unknown content. Such encoding models are successful in predicting patterns of neural activity in brain regions where the internal organization is somewhat understood (e.g., primary sensory areas), but are far less successful for regions associated with higher-level cognitive processing. This is likely because primary sensory areas represent easily measured surface properties of the stimulus whereas higher-order brain regions represent more abstract stimulus properties that cannot be inferred from the stimulus image alone, but require assumptions about the content of these internal representations.

2.2 Second order isomorphism

A second order isomorphism between cognitive processes/representations and patterns of brain activation entails that the *similarity structure* predicted by a cognitive theory is equivalent to the similarity structure observed from neural behavior (Edelman, 1998; Shepard & Chipman, 1970). By similarity structure, I am referring to the pairwise similarity of every stimulus within a domain of interest at a given level of representation. Given a stimulus set, similarity structures are often depicted as 2-D grids that index the similarity between each possible stimulus pairing. This grid is referred to as a Representational Similarity Matrix (RSM). Representational Similarity Analysis (RSA) involves comparing the RSMs derived from two different sources to see the extent to which the two RSMs are equivalent.

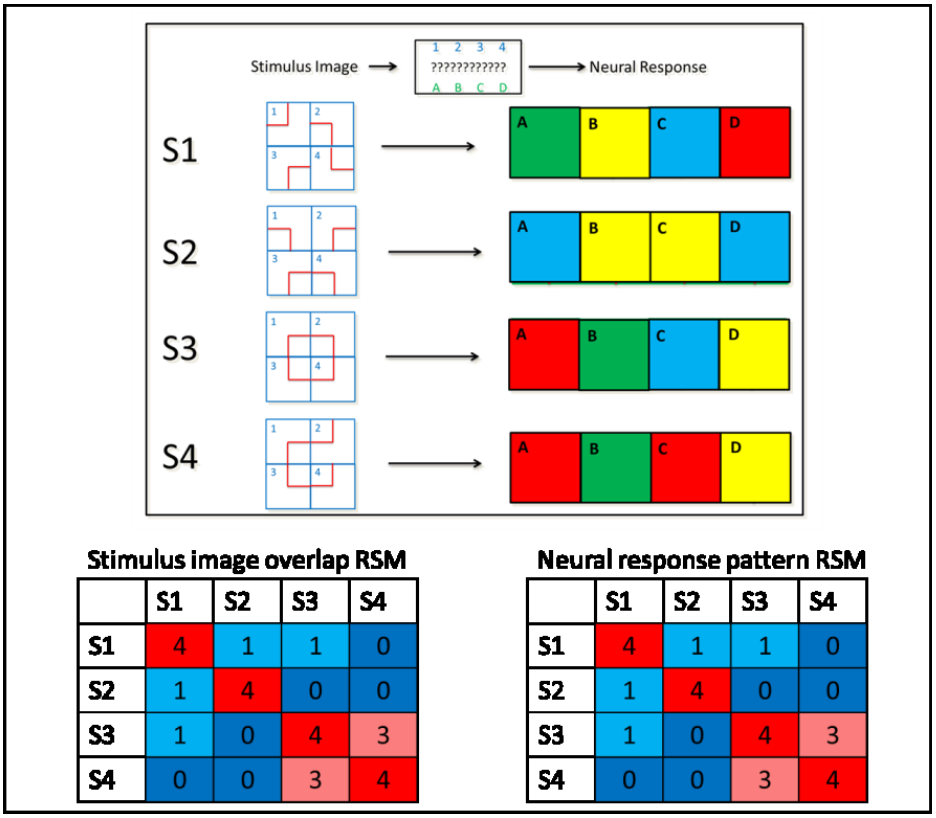

Stimulus image overlap RSM

	S1	S2	S3	S4
S1	4	1	1	0
S2	1	4	0	0
S3	1	0	4	3
S4	0	0	3	4

Neural response pattern RSM

	S1	S2	S3	S4
S1	4	1	1	0
S2	1	4	0	0
S3	1	0	4	3
S4	0	0	3	4

Figure 5. A depiction of a second order isomorphism between to representational spaces—image or feature space on left and neural response space on right. The top image shows how four stimuli S1-S4 are encoded in each space (see text for details). The colored blocks (top right) indicate measurements from 4 different neural units in response to the 4 stimuli. Each unit (A-D) is known to have 4 different levels of activation indicated by the depicted color (green, yellow, blue, or red). The similarity structure between each space is computed and shown as RSMs on the bottom of the figure. Second order isomorphism is operationalized as the degree of similarity between the two RSMs. Even though an encoding model is unavailable, we can still be reasonably confident that the neural activity reflects the encoding of the same representational content as the image/feature space.

The claim is that analysis of second order isomorphisms can allow us to reach detailed cognitive conclusions from fMRI data with few assumptions about how the stimulus information is encoded in the neural tissue[5]. Looking at the example in Figure 5, we see four stimuli encoded in image space (left) and brain space (right). Instead of image space, we can also hypothesize that the image is represented as a set of 4 visual

---

[5] RSA, as applied to Multi-voxel pattern analysis (depicted in the example on figure 5), requires that information be sufficiently distributed to be detectable in a multi-voxel signal. If RSA fails to reveal that a set of voxels encodes a particular representation this could always be due the nature of how the representation is encoded (too local) or the nature of the signal (too noisy) as opposed to the null hypothesis that the neural tissue does not encode that particular representation.

features that can exist in 4 positions. Accordingly we would like to know if these features are neurally and cognitive represented and if so, where in the brain they are represented. Given the response from four voxels to each of the four stimuli (S1-S4), we can determine if those four voxels are encoding the stimuli in similar manner as would be predicted by this hypothesized feature representation. To do this we create an RSM that represents the pairwise similarity of S1-S4. The similarity between two stimuli (in this example) is determined by counting the number of identical position-specific features for each stimulus pairing. In image/feature space, S1 and S2 share position 3 so the stimulus pair is assigned a similarity value of 1 in the RSM while S3 and S4 share positions 1, 3, and 4 so they are assigned a similarity value of 3. Since there are only four positions, the identity relationship would be a similarity value of 4. The full mapping of all the pairwise similarity values for the image space constitutes the predicted RSM (pRSM). Since there is no encoding theory we cannot predict how the stimuli should translate to neural activation. To get around this limitation we examine the similarity structure of the brain space as well. In this example, we have 4 voxels and each color depicts a level of activation[6]. The voxel response patterns to each stimulus are compared such that we have an RSM depicting the pairwise similarity of the observed activation patterns in response to S1-S4 (oRSM). We compute the correlation between the feature-overlap pRSM and the neural response oRSM to determine the degree of second order isomorphism that exists between these two spaces. If the pRSM is designed to model the similarity of S1-S4 that a cognitive theory would predict, then a high degree of second order isomorphism with neural responses provides evidence in support of this cognitive theory. Additionally,

---

[6] In reality there is not a clean mapping between the number of positions/features in theoretical space and the voxel-space of fMRI data. Furthermore, the most relevant set of voxels is generally unknown. A lot of effort is spent selecting the best voxels to analyze for second-order isomorphism.

the neural substrates of the representations or processes predicted by the cognitive theory correspond to the set of voxels that demonstrate the high-degree of second order isomorphism.

2.3 Using second order isomorphism to uncover content in an opaque medium

2.3.1 Rothlein and Rapp (2014)[7]

Previous neuroimaging work by the present author and Brenda Rapp used MVPA-RSA to uncover multiple types of letter representations from patterns of brain activity. Using this approach we identified patterns of neural activity consistent with representations of different modality-specific letter features—specifically, visual-spatial, phonological/acoustic, and motor representations—as well as representations of case-invariant abstract letter identity (ALIs). Abstract letter representations, we posited, should represent case-invariant identity to the exclusion of all of the modality-specific features. Therefore, neural activation patterns consistent with ALIs and not consistent with the modality-specific representations of letters, would constitute evidence that ALIs are, in fact, represented and it would allow us to localize them to a specific neuroanatomical location or locations. RSA allowed us to determine the extent to which a given pattern of brain activation was consistent with a given representational type by measuring the second order isomorphism between the representational similarity structure and the neural activation similarity structure evoked by a set of individually presented letters. The degree of second order isomorphism was operationalized as the correlation between a

---

[7] Some of the language in the methods is taken from Rothlein and Rapp (2014).

theoretically motivated (predicted) similarity structure (pRSM) for each letter stimulus and an observed similarity structure (oRSM) derived by taking all possible pairwise correlations of letter-stimulus evoked patterns of activation across voxels in some brain region.

While there are many variants, RSA involves 3 basic steps: (1) obtain an oRSM by computing (or measuring) the similarity of the neural (or behavioral) responses to pairs of stimuli within a stimulus set; (2) operationalize hypotheses of representational content by generating one or more representation-specific pRSMs for a set of relevant stimuli; and (3) estimate the degree of second order isomorphism between a pRSM and oRSM by computing the correlation (or distance) between them. Of course each of these steps introduces a number of considerations that I will discuss below in the context of Rothlein and Rapp. I discuss this work in considerable detail as the work in this dissertation relies heavily on these methods.

Generating pRSMs

We selected 24 letter stimuli (Aa, Bb, Dd, Ee, Ff, Hh, Kk, Oo, Pp, Rr, Tt, Uu, Arial size 88 font) as a representative sample of the alphabet and created 4 pRSMs that characterized letter similarity for visual-spatial, letter-name, motoric, and ALI feature dimensions.

To estimate visual-spatial letter similarity, we used subjective letter similarity judgments taken from an experiment in which participants were shown every possible letter pair and asked to rank the visual similarity of each letter pair on a scale from 1 (dissimilar) to 5 (similar) (Boles & Clifford, 1989). It is worth noting that visual similarity judgments, while providing an estimate of the stimulus similarity of the letters, may also be biased by non-visual representational similarity like letter identity (e.g., one might judge **a** and **A** to be more visual similar than they would if they did not know that **a** and **A** shared the same identity). This issue is examined in detail in Chapter 3 and is used to draw a number of conclusions about the representations used in letter processing.

Letter-name similarity values were also derived experimentally. Letter-name confusions were elicited by Hull (1973) asking participants to report spoken letter names presented in a noisy environment. The noise increased the likelihood that the letter names would be misheard and confused for similar sounding letter names. The number of such confusions was used as a metric of letter-name similarity—the logic being that letter names that are highly confusable (a, k) are more acoustically/phonologically similar that non-confusable pairs (a, z). One could also approximate letter-name similarity theoretically by reference to phonemic and phonetic feature overlap, but this involves committing to a specific level of representation and for the purposes of this study, we wanted a more inclusive metric of letter-name similarity (that could include both acoustic and phonological similarity).

Motoric similarity was based on a stroke feature metric that was validated experimentally on the basis of written letter confusions produced by dysgraphic participants (Rapp & Caramazza, 1997). For example, in this pRSM, E and H have similar stroke patterns and therefore were similar, whereas B and E, while visually similar, were motorically dissimilar.

Finally, for the ALI pRSM, case-invariance was used as a proxy for abstract letter identity. Therefore, in the ALI pRSM, any letter pairs that shared the same identity, regardless of case and letter shape, were identical and all other pairs were assumed to be unrelated. For example, in this pRSM, e and E were identical whereas e and B were not.

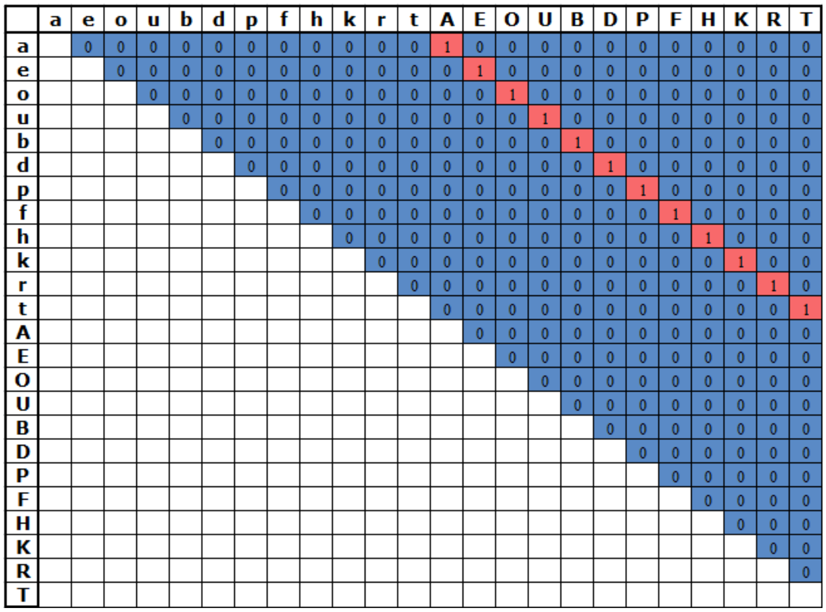

	a	e	o	u	b	d	p	f	h	k	r	t	A	E	O	U	B	D	P	F	H	K	R	T
a		0	0	0	0	0	0	0	0	0	0	0	1	0	0	0	0	0	0	0	0	0	0	0
e			0	0	0	0	0	0	0	0	0	0	0	1	0	0	0	0	0	0	0	0	0	0
o				0	0	0	0	0	0	0	0	0	0	0	1	0	0	0	0	0	0	0	0	0
u					0	0	0	0	0	0	0	0	0	0	0	1	0	0	0	0	0	0	0	0
b						0	0	0	0	0	0	0	0	0	0	0	1	0	0	0	0	0	0	0
d							0	0	0	0	0	0	0	0	0	0	0	1	0	0	0	0	0	0
p								0	0	0	0	0	0	0	0	0	0	0	1	0	0	0	0	0
f									0	0	0	0	0	0	0	0	0	0	0	1	0	0	0	0
h										0	0	0	0	0	0	0	0	0	0	0	1	0	0	0
k											0	0	0	0	0	0	0	0	0	0	0	1	0	0
r												0	0	0	0	0	0	0	0	0	0	0	1	0
t													0	0	0	0	0	0	0	0	0	0	0	1
A														0	0	0	0	0	0	0	0	0	0	0
E															0	0	0	0	0	0	0	0	0	0
O																0	0	0	0	0	0	0	0	0
U																	0	0	0	0	0	0	0	0
B																		0	0	0	0	0	0	0
D																			0	0	0	0	0	0
P																				0	0	0	0	0
F																					0	0	0	0
H																						0	0	0
K																							0	0
R																								0
T																								

Figure 6. The pRSM used to model ALI representations. Cells assigned 1(red) are predicted to be similar while 0 (blue) are predicted to be dissimilar.

Generating oRSMs

In order to record letter-specific activation patterns, Rothlein and Rapp had 9 participants view single letter stimuli in an event-related fMRI experiment. Each trial consisted of a 200ms fixation dot followed by a 300ms stimulus presentation and a 3500ms rest period. The stimulus was either one of the 24 letter shapes, a non-letter symbol, or a blank screen. Each stimulus was presented 12 times over the course of 6 runs (2 tokens per run). Participants were instructed to press a button in both hands if the stimulus was a non-letter symbol. This simple task ensured that participants were awake and processed the content of the stimuli while not directing attention to specific aspects of the letter stimuli. The general linear model approach (Friston et al., 1995) was used to compute the stimulus-specific activation pattern for each letter stimulus at each voxel. There were 26 experimental regressors; one regressor for each of the 24 letter stimuli, one for all the fixation timepoints and one for all the trials where a non-letter symbol was shown. The experimental regressors were created by convolving a boxcar function of the time-course for all the 200ms periods when a fixation was displayed, or the 300ms durations when each letter stimulus was shown and finally all the 4000ms trials when a non-letter symbol was convolved with a Boynton hemodynamic response function (Boynton, Engel, Glover, & Heeger, 1996). The six runs of trials were concatenated so that each experimental regressor included the 12 presentations of each letter stimulus over all six runs. A number of motion and confound regressors were included as well. The output of the GLM analysis is a map of activity estimates (beta-weights) which estimate the extent to which the signal from each voxel can be explained by the predicted signal associated with each regressor. The beta-maps for each of the 24 letter regressors were used as the activation pattern estimates in the Representational Similarity Analysis. The resulting participant-specific multi-voxel pattern of activity for each letter stimulus was then used to derive the observed RSMs).

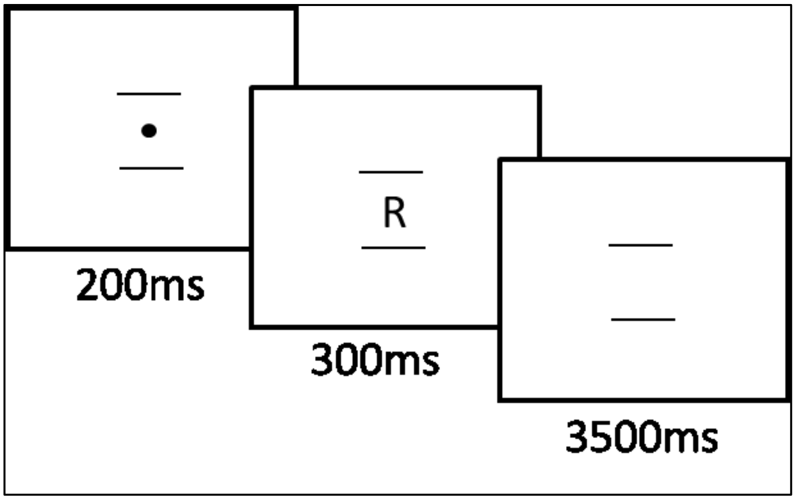

Figure 7. A depiction of a trial sequence from Rothlein and Rapp (2014). The example shown here is for a letter trial.

A searchlight analysis (Kriegeskorte, 2006) was used to exhaustively examine brain regions throughout a bilaterally symmetric searchspace. This searchspace was derived from an Orthographic Network Localizer task that identified brain areas that were more responsive to words and consonant strings than a checkerboard stimulus and fixation baseline. Spheres were drawn at the peaks of the responsive regions and these spheres were reflected across the mid-sagittal plane in order to ensure the space was bilaterally symmetric. The voxels contained within the spheres served as the searchspace.

An oRSM was computed for each searchlight region (a 7 voxel sphere) within the searchspace (See step 2 in Figure 8). An oRSM was computed by taking the Pearson correlation of the pairwise beta-values across the 7 voxels for each letter pair. This correlation was used to estimate the neural representational similarity of a given letter pair for the searchlight region. The set of all letter-pair correlations within the searchlight region corresponded to the oRSM for that particular searchlight region. An oRSM was computed for each searchlight region within the searchspace. The set of oRSMs derived in this manner will be referred to as an oRSM-Map.

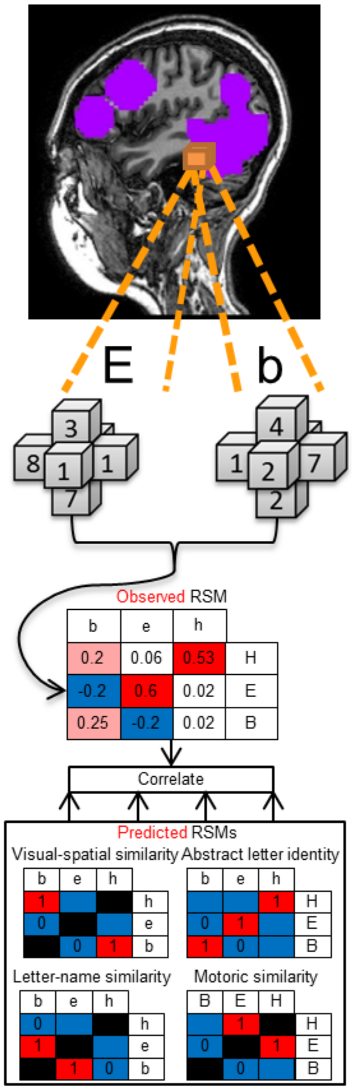

Step 1: The search space is evaluated by means of a searchlight volume (orange) corresponding to a 7 voxel sphere with a diameter of 9 mm. For each participant, the searchlight volume is moved through the entire search space by moving the center of the volume one voxel at a time.

Step 2: For each voxel in a searchlight volume, beta weights (or their equivalents) from a univariate GLM analysis are extracted for each letter viewed.

Step 3: An Observed Representational Similarity Matrix (oRSM) is generated for each searchlight volume. Each oRSM contains cells corresponding to all pairwise combinations of the letter stimuli that were viewed (e.g., b/E, e/H, etc.). Each cell contains a correlation of the beta weights from all the voxels in the searchlight volume for one pair of letters. In this way, each oRSM depicts the similarity structure of that searchlight volume's response to the set of viewed letters.

Step 4: The values in each oRSM are correlated with the values in each of four predicted RSMs (pRSMs). A pRSM represents the similarity structure predicted for a brain region sensitive to a specific feature dimension: abstract letter identity (ALI), visual-spatial, letter-name or motoric. The correlation of an oRSM and pRSM provides a measure of the degree to which a particular brain region is sensitive to a specific feature dimension. This is repeated for all searchlight volumes. The oRSM/pRSM correlations are then assigned to voxels, evaluated for statistical significance, thresholded and the resulting map represents an individual participant's spatial distribution of sensitivities to a specific feature dimension. These individual participant feature maps form the basis for subsequent analyses.

Figure 8. (Taken from Rothlein and Rapp, 2014). **A** depiction of the four basic steps of the MVPA-RSA Searchlight Analysis. BOLD response is measured while participants viewed single (upper and lower case) letters during a symbol detection task. The search space for the analysis, depicted in purple, was derived from a functionally localized reading network**.**

Comparing pRSMs to oRSMs

In order to infer the representational content of each searchlight region, each oRSM was correlated using a Pearson correlation with each of the four pRSMs. A Fisher's r-to-Z transformation was applied and the resulting Z-score served as a measure of representational fit of the observed to predicted RSM (see step 2 in Figure 8). The z-scores were assigned to the central voxel of the searchlight region for each oRSM in the oRSM-Map. The result was 4 maps depicting the degree of second order isomorphism (as measured by z-values) between a feature specific pRSM and all the oRSMs from the oRSM-map. Each feature-specific map was referred to as a Participant Feature Sensitivity Map; each participant had 4 sensitivity maps.

Sensitivity analysis

For each feature dimension, we generated group sensitivity maps by first smoothing (2 full-width half-mass or FWHM) and normalizing the Participant Feature Sensitivity Maps into Talairach space. We then combined the maps across participants by performing a one-way t-test (null hypothesis of sample mean = 0) over the participant feature sensitivity z-values at each voxel, generating a Group Feature Sensitivity Map.

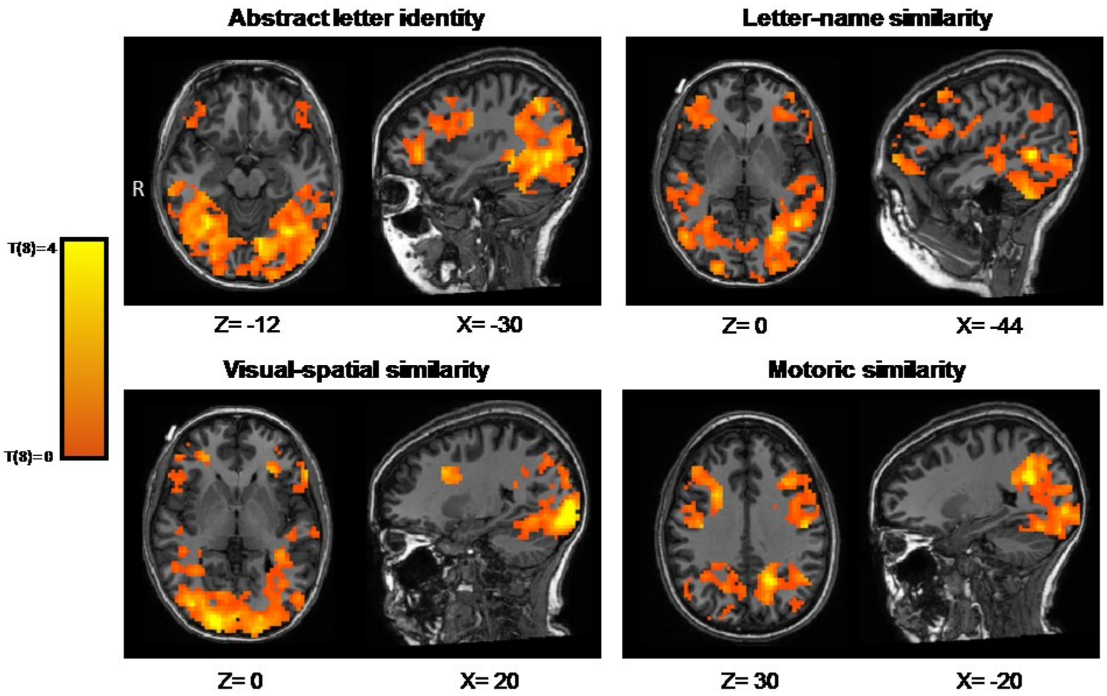

Figure 9. Unthresholded Group Feature Sensitivity Maps depicting brain regions sensitive to each feature dimension. Each Group Feature Sensitivity Map was obtained from combining Individual Sensitivity maps (after Talairch normalization and Gaussian smoothing at 2 FWHM) and then carrying out a one-way, two-tailed, t-test at each voxel. These unthresholded t-maps depict the topography of feature-sensitivity for each of the four feature dimensions.

responsive to one feature dimension only. We evaluated selectivity with 3 analyses: (1) An **ANOVA Selectivity Comparison Analysis** that identified voxels with greater sensitivity to one feature dimension compared to the other three; (2) A **Permutation Selectivity Analysis** that evaluated the number of participants with feature-selective responses at each voxel and (3) A **Regression Analysis** that determined the relative contributions of each feature dimension pRSM to the similarity structure of each oRSM.

As seen in Figure 10, the results of the selectivity analyses revealed a right posterior occipital cluster that was selectively responsive to visual-spatial similarity in all 3 selectivity analyses (TAL: 20, -86,-3). For ALI, there was a region in the left-mid fusiform gyrus (TAL: -31, -58, -12) that was consistently selective across all 3 analyses.

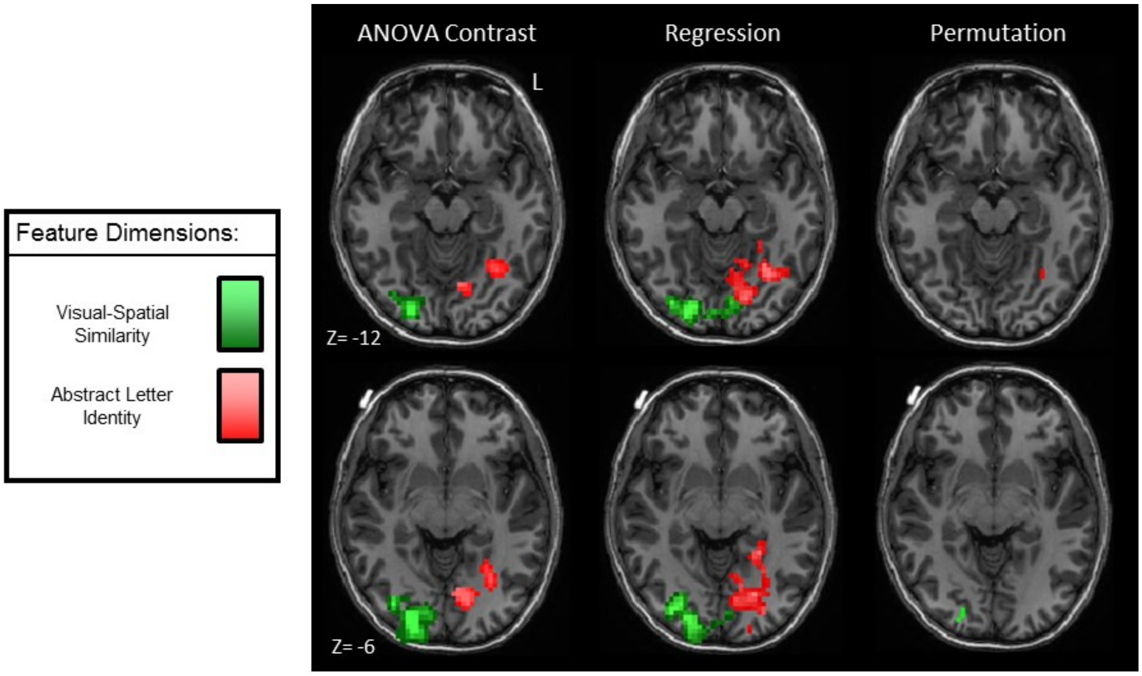

Figure 10. The significant clusters identified in each of the three selectivity analyses. For each of the maps, visual-spatial selectivity is depicted in green and abstract letter identity is depicted in red. For the ANOVA comparison significant clusters (uncorrected voxelwise threshold $p<0.05$; corrected cluster size threshold $p<0.05$) are shown in a scale where the darker colors indicate lower f-values and lighted colors indicate higher f-values. For the regression analysis significant clusters (uncorrected voxelwise threshold $p<0.10$; corrected cluster size threshold $p<0.05$) are shown in a scale where the darker colors indicate lower t-values and lighted colors indicate higher t-values. For the permutation analysis, selectivity maps were thresholded to depict only voxels where all 9 participants showed selective tuning with cluster-size correction for multiple comparisons ($p<0.05$). The letter-name and motoric feature dimension are not depicted because significant clusters were not identified for these feature dimensions in these analyses.

Rothlein and Rapp (2014) demonstrated that a searchlight implementation of MVPA-RSA can be used to evaluate the inherently multivariate fMRI data to examine the representational content of letters. While the experiments in this dissertation follow the logic of RSA analysis, I will use the next section to briefly discuss alternatives to the searchlight approach.

2.3.2 Further considerations

An important step in using MVPA analyses is identifying the set of voxels to include in the analysis. The searchlight approach described above attempts to minimize assumptions regarding selection of voxels used to derive an oRSM by systematically sampling groups of voxels from the whole brain or a large searchspace. The advantage of this approach is that it paints a fairly complete picture of sensitivity to a specific pRSM across much or all of cortex. The downside to searchlight analyses is that they require many statistical tests and corresponding corrections for multiple comparisons. Furthermore, combining results across participants typically involves linking a set of voxels from participant A to a set of voxels in participant B merely on the basis of shared Talairach (or other spatially normalized) coordinates. Given that RSA analyses produce relatively weak and noisy effects, the "approximate" voxel-to-voxel mapping across subjects results in high variance due to spatial uncertainty that may be problematic in testing pRSMs against oRSM at the group level. Finally, while searchlight analyses make few assumptions about where an effect occurs in the brain, they do require arbitrary decisions about the shape and number of voxels that best represent a given feature (Etzel, Zacks, & Braver, 2013). For example, we assumed a 7 voxel sphere for a searchlight region, but this decision was arbitrary.

One way to bypass some of the complications associated with a searchlight analysis is to select a set of voxels of interest in each individual in an experimentally or theoretically motivated manner. The volume-of-interest or VOI approach involves carrying out RSA analysis on a set of selected voxels. The two most common ways of defining VOIs are by either using anatomical landmarks or functionally relevant regions identified from a different experiment (functional localizer). VOI avoids complications induced by spatial normalization when combining data across participants. We can then perform RSA within each participant's VOI. While this approach is ideal for combining data across participants, it is not without its own drawbacks. There may be relevant voxels that are not included in the analysis and the size of the VOI is still largely arbitrary because it is sensitive to statistical thresholding. Also, the univariate activation magnitude comparisons typically used in functional localizers may not be the optimal way to define VOIs for MVPA-RSA[8]. Activation magnitude in a functionally identified VOI might be only indirectly related to the question at hand and therefore investigating the representational content of a VOI identified in this manner could be misleading.

2.4 Chapter 2 summary

In Chapter 2, I discussed how second order isomorphism can be used to test hypotheses about the representational content of any brain region using fMRI and Representational Similarity Analysis (RSA) (Kriegeskorte et al., 2008). RSA compares the similarity structure that would be predicted if a brain region encoded a particular type of representation with the actual similarity structure of the multivoxel activation patterns from that region. I discussed previous research that successfully used this method to identify both modality specific and abstract representations of letters (Rothlein & Rapp, 2014). This is the primary methodology used in the behavioral studies in chapter 3 and fMRI studies in chapters 4 and 5.

---

[8] Searchlight RSA could be used to define VOIs based on representational content instead of univariate activation. A VOI is defined in this manner in the experiment presented in Ch. 5 of this dissertation.

Chapter 3 - The influence of visual and non-visual letter representations on behavioral measures of visual similarity

As discussed in the introductory chapter, models of reading often propose a series of increasingly abstract representations to deal with the computational challenges that stimulus variability imposes on the identification process. Two such proposed levels of abstraction are font-invariant stored letter shape representations (allographs) and abstract letter identity (ALI) representations. While arguments in support of ALI representations come from evidence from multiple methodologies—with varying degrees of success—evidence for allograph representations in reading is relatively scant. Many models of reading gloss over visual recognition processes entirely by assuming simple letter stimuli that do not vary in font or position so simple visual features can be used to accurately identify letters (e.g., McClelland & Rumelhart, 1981; Plaut & Behrmann, 2011). Other models of reading base letter identification processes on models of object recognition and assume each letter has a stored structural description that is invariant to certain changes in position and orientation (for review see Grainger et al., 2008). The series of 3 behavioral experiments that follow explicitly test for the existence of font-invariant allograph, abstract letter identity, and other types of stored letter representations (reviewed in Ch. 1) by examining the influence, if any, that these representations exert on pairwise visual similarity judgments (Experiment 1) and reaction times for physical same-different judgments of simultaneously presented letters (Experiment 2). A third experiment addresses a possible alternative account for the results from Experiments 1 and 2. Determining which types of representations influence visual judgments in these tasks provides a novel source of evidence to evaluate the types of representation that mediate letter processing.

The experiments that follow include the use of pairwise letter similarity matrices in order to draw inferences about the cognitive representations involved in visual letter processing. Similarity matrices for letters consist of matrices where the value in each cell reflects some empirical measure of similarity for a pair of letters. In the literature, similarity measures have often been derived by either tallying confusions in a letter naming task where a visual letter was presented in degraded conditions—for example short stimulus duration (e.g., Fisher, Monty, & Glucksberg, 1969; Gilmore, Hersh, Caramazza, & Griffin, 1979; Tinker, 1928; van Der Heijden, Malhas, & van Den Roovaart, 1984), low light or contrast (e.g., Geyer & Dewald, 1973; Gupta, Geyer, & Maalouf, 1983; Watson & Fitzhugh, 1989), or peripheral presentation (e.g., Dockeray, 1910; Reich & Bedell, 2000)—by measuring the reaction time involved in judging whether two letters are visually identical or not (Courrieu, Farioli, & Grainger, 2004; Podgorny & Garner, 1979), or by having participants explicitly judge the visual similarity of presented letter pairs (Boles & Clifford, 1989; Podgorny & Garner, 1979; Simpson, Mousikou, Montoya, & Defior, 2012). While the use of visual similarity matrices to make inferences about the cognitive processing of letters is not new (for review see Mueller & Weidemann, 2012), such inferences have often been used for identifying a set of visual features that mediate letter identification. Wide-spread acceptance of such feature sets has remained elusive largely due to methodological issues; namely that similarity values were sensitive to both the stimulus font used and the experimental task employed (Fisher et al., 1969; Gupta et al., 1983; Mueller & Weidemann, 2012).

Therefore, different feature sets could be and often were derived for each font and each similarity measure used. Nonetheless, much can still be inferred about the representations involved in letter processing from the information represented in similarity matrices. To expand, it is reasonable to assume that one reason both task type and font influences similarity values is because any given empirical similarity metric could be based on or influenced by similarity at multiple levels of representation. In fact, evidence that conceptual (or non-visual) information influences measures of visual perception (like visual similarity) comes from many sources (for review see Lupyan, 2012; Wiley, Wilson & Rapp, under review). In general, these findings reveal that category labels can warp similarity judgments so that items that share the same category label are judged to be more similar than items that cross a category barrier, even if the physical difference of the within category and across category boundaries is matched (Goldstone, 1994; Panis, Vangeneugden, & Wagemans, 2008). A number of studies have investigated category effects on vision with letters by presenting pairs of letter stimuli and asking participants to decide whether or not the letter pairs were visually identical or not. The underlying assumption was that similar letter-pairs required more cognitive effort to differentiate and therefore would take longer to elicit a "different" response than did dissimilar letter-pairs. These studies revealed that reaction times were longer for "different" responses when the two letter stimuli shared the same ALI, even if the cross-case pairs were visually distinct (Carrasco, Kinchla, & Figueroa, 1988; Lupyan, Thompson-Schill, & Swingley, 2010; Wiley, Wilson & Rapp, under review).

A recent study by Lupyan et al. (2010) demonstrated significantly slower response times in a visual same-different task when the two letters were case variants of the same identity than when they were different identities although the pairs were matched for visual similarity (see also Chen & Proctor, 2012). Lupyan argued that the letter identity information dynamically altered the visual representation of cross-case identity pairs (e.g., **B** and **b**) via feedback rendering their visual representations more similar than B/p, Others have argued that later decision-based processes like response competition could explain these results without the need for conceptual penetration of visual processing (Chen & Proctor, 2012). Regardless of whether the mechanism is response competition or feedback, the finding that response interference occurs at all is evidence for the level of representation that best explains the interference. The experiments that follow made use of this effect to see which representations, beyond computed stimulus shape representations, influenced pairwise visual similarity judgments and visual same-different decision errors and RTs.

Isolating the unique contribution of a given letter representation to measures of visual similarity presents a number of challenges. Most apparent is separating the influence of stored visual and nonvisual letter representation from the influence of computed font-specific stimulus shape representations on a given response. For example, if participants judge **d** and **D** to be more visually similar than **f** and **H**, would this be due to an identity similarity bias in the judgment of the former pair? Alternatively, perhaps identity has no influence and the computed stimulus shapes for **d** and **D** are actually more similar than the stimulus shapes for **f** and **H**. To get around this issue, Lupyan et al. (2010) only compared the difference between **B-b** and **B-p**, the logic being that the stimulus shape similarity between **B-p** and **B-b** is matched since **p** and **b** differ only by a horizontal reflection so any difference in RT should be attributable to the influence of identity. While this approach is sound, it severely limits the number of letter pairs that can be used. The more diverse the stimulus set, the larger the set of interference patterns that can be tested. So while **B-b** and **B-p**, worked for testing identity interference, other interference patterns such as the similarity of the letter's name, whether a letter is a consonant or vowel, or whether a character is a letter or a digit requires a larger stimulus set. One approach also comes from Lupyan et al (2010) who found that the influence of identity disappears entirely when stimuli were presented at a 90° rotation. In other words, responding "different" to the rotated **B and b** took equally long as to the rotated **B and p**. Lupyan et al. assumed that rotating the letters sufficiently disrupted the processing of letter identity to eliminate any influence identity may have had on the visual same-different task[9] (see also Egeth & Blecker, 1971). According to this logic, one could estimate the pairwise stimulus shape similarity of a large set of alphanumeric stimuli by performing the same rigid transformation (e.g. rotation or reflection) on each stimulus forming a pixelwise matched, rotated stimulus set. This transformation would reduce and ideally eliminate any contributions from stored letter representations while maintaining the stimulus shape similarity. What follows from this logic is that any differences in the similarity structure of responses to the normal, "upright" set of alphanumeric characters compared to responses to the visually matched and difficult-to-recognize "rotated" stimulus set could be attributed to one or more types of stored letter representations that were accessed when the characters were identified (in the upright presentation).

---

[9] It is worth noting that the rotated forms of **p** and **b** may be particularly difficult to differentiate as orientation information alone distinguishes these letters. Because of this, a rotated **p** is not an ideal visual control as it may activate both **b** and **p** equally (instead of activating neither). Therefore, the finding that the "different" responses to the rotated **B** and **b** pair and the rotated **B** and **p** pair took equally long could be explained by the fact that the rotated **b** and **p** both were identified as **b** and therefore lead to the same amount of interference.

Representational Similarity Analysis (Kriegeskorte et al., 2008) for behavioral data (e.g., RTs and accuracies) can be implemented to quantify the influence of stored representations over a large stimulus set by generating the predicted similarity structure (referred to as predicted Representational Similarity Matrices or pRSMs) for different types of stored letter representations and then correlating these pRSMs with an observed set of similarity measures (observed RSMs or oRSMs). Crucially, to isolate the influence of stored representations, a correlation between the oRSM obtained from the rotated letter pairs and the pRSMs can serve as a baseline correlation for computed stimulus shape similarity. The same correlations can be computed with the upright set of characters and then the degree of influence for each type of representation can be quantified as the change in the correlation between the rotated oRSM and the pRSM and the correlation between the upright oRSM and the pRSM.

A challenge arises specifically when separating the contributions of allographs from the font-specific computed stimulus shapes. Specifically, it is possible that allograph representations make a unique contribution to measures of pairwise visual similarity, but separating their contribution from similarity effects arising from lower-level visual features is difficult because the similarity structure at the different levels of representations are likely to be highly similar. For example, it could be that the visual similarity for the stimuli **e** and **E** is the same at the level of computed stimulus shape representations and at the allograph level of representation, even if the features that compose the representations are simple oriented lines for the computed stimulus shapes and more complex curves and angles for the allographs. One way to ensure that the representational similarity structure is different for the font-specific computed stimulus shapes and the font-invariant allographs is to use a stimulus font that is both atypical and novel so that the stimulus shape is substantially different from the allograph representation. Therefore, if one were to compare similarity measures derived from a typical font and an atypical font, and if allograph representations exist and “bias” similarity judgments, then the observed similarity structure of the typical font will be more similar to the similarity structure of the upright atypical font than to the similarity structure of the rotated atypical font (Figure 11). I will posit that a greater degree of similarity of the upright atypical font to the upright typical font than would be predicted by stimulus shape alone is due to the influence of font-invariant allograph representations. In order to reach this conclusion one must assume that the visual similarity of the typical font constitutes a good proxy of the similarity structure of allograph representations. This is a reasonable assumption because allograph representations would likely be tuned to the most typical and frequent letter forms in order to maximize efficiency while reading. The logic for inferring allograph representations from similarity judgments is spelled out in more detail in Figure 11.

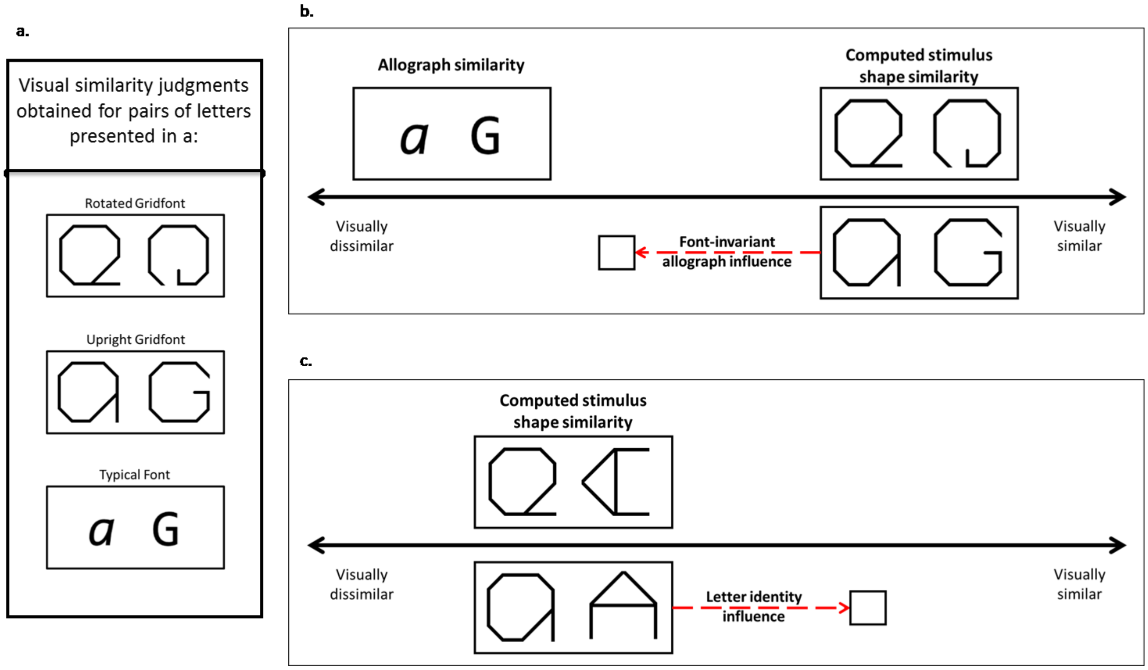

Figure 11. (a) Participants made visual similarity judgments to alphanumeric shapes presented in an atypical gridfont (a. middle), a rotated gridfont (a. top) that, while maintaining the same pixelwise image similarity as the upright gridfont, was difficult to recognize. Similarity judgments of the rotated gridfont served as a proxy for visual similarity of the upright gridfont at the level of computed stimulus shapes because the visual judgments would reflect visually matched shapes that would not be influenced by stored letter representations. A typical font (a. bottom) was also presented as a proxy for the visual similarity at the level of allograph representations. (b) Visual similarity judgments for the letter pair (***a*** and **G**) were depicted on a horizontal scale where positions on the left indicate visual dissimilarity and positions on the right indicate visual similarity. Participants judged the rotated gridfont (***a*** and **G**) to be similar suggesting the stimulus shape was visually similar while the same letters presented in a typical font were judged to be visually dissimilar. If allograph representations have no effect, when the visual similarity judgments were made on the upright gridfont, the judgment should be identical to the rotated gridfont judgment because the upright and rotated stimuli were visually matched. Instead if allograph representations were accessed and influence the similarity judgment, the judgment for the upright gridfont should be "pulled" towards the judgment of the typical font pair, in this case being judged as less visually similar than the rotated gridfont letters. (c) Following a similar logic described in (b), if ALI representations were accessed and influence the visual similarity judgment of the letter pair (***a*** and **A**), than the upright gridfont pair should be judged as more similar than the rotated gridfont pair because the identity relationship (recognized in the upright gridfont pair) would bias the participant to view the letter-pair as being more similar than the same stimulus shapes without the identity relationship (estimated by the rotated gridfont).

One issue that should be discussed is whether the existence of allograph representations is actually controversial. For example, one could argue that all the evidence that is needed to support the existence of allograph representations is the fact that we know what typical letter shapes look like and we can easily conjure up mental images of typical letter shapes. There are a number of objections to this line of argument but perhaps most relevant is the fact that the claim in this paper is not just that we have stored allographs, but that these stored letter shapes mediate letter recognition. That we can easily imagine what typical letter forms looks like in no way suggests that the same representations that guide our mental imagery are used in letter recognition or lexical access. For example, many can conjure up an image of a fancy calligraphic typeface but this does not mean that the stored knowledge that allows us to do so is utilized by letter recognition processes under normal[10] circumstances.

In order to test for the influence of stored letter representations on behavioral measures of pairwise letter and digit similarity, nine pRSMs were constructed that represent predicted similarity structures for the following representational types: allographs, ALIs, upper/lower case, c/v status, letter/digit status, motoric production features, and letter name similarity. Across 2 experiments I obtained oRSMs for pairs of novel atypical gridfont alphanumeric stimuli presented in either upright or rotated versions. I also obtained an oRSM for the same alphanumeric characters presented in a more typical font (upright presentation). Three oRSMs were developed based on three types of data: explicit visual similarity judgments, reaction times for visual same or different decisions, and counts of erroneous “same” responses in the same-different paradigm.

---

[10] There is a strong case to be made that the visual similarity judgments and same-different decision tasks do not rely on normal letter recognition processes as reading presumably does not utilize the level of visual analysis that similarity judgments and same-different decisions require. It is worth noting, however, that accessing any type of stored letter representation is not necessary and in fact detrimental to the “accuracy” of responses in these tasks. Therefore, one is forced to ask—why are these stored letter representations accessed in a task that does not require them? My explanation is that viewing letters reflexively activates the representations involved in normal letter processing (i.e., reading) in addition to the visual processes necessary for the task at hand. Under this interpretation, the normal letter recognition processes are what interfere with the abnormal, task-specific representations and processes.

3.1 Experiment 1 – Pairwise visual similarity judgments of letters and digits

Experiment 1 examined the proposal that visual similarity judgments of pairs of letters are driven by multiple levels of representation—from low level visual features to stored font-invariant allographs to conceptual properties of letters like abstract identity or consonant/vowel status. Influence from these different levels of representations on visual similarity judgments would indicate that these representations are accessed automatically during letter recognition.

Visual similarity judgments from three groups of participants were collected in this experiment. For the first group of participants, similarity judgments were obtained for pairs of letters presented in a novel and atypical gridfont (Figure 12). The set of these similarity judgments served as the observed Representational Similarity Matrix (**Upright oRSM**) and were analyzed for the influence of different types of stored letter/digit representations. In order to differentiate the influence on similarity judgments of stored letter representations from the visual similarity of the stimuli, a second group of participants made visual similarity judgments on the same gridfont, but with the stimuli rotated in a manner than rendered them difficult to recognize while maintaining the same pairwise pixelwise similarity as the upright gridfont letters (**Rotated oRSM**). These judgments provided an estimate of the font-specific visual similarity of the gridfont at the level of computed stimulus shape representations without any interference from stored letter representations. Finally, in order to provide an estimate of the visual similarity at the level of allograph representations, a third group of participants made visual similarity judgments for letter stimuli presented in a typical upright font (**Allograph pRSM**).

Additional pRSMs were constructed to detect the influence of ALIs, case-markers, c/v markers, motoric production codes, and letter name representations. The degree of influence for each type of stored letter representations was quantified in two ways: (1) the correlation difference value (r_{diff}) between the correlation r of a given pRSM with the Upright oRSM ($r_{upright}$) minus the correlation between that pRSM with the Rotated oRSM ($r_{diff} = r_{upright} - r_{rotated}$); and (2) the standardized beta-weight corresponding to each pRSM in a regression analysis where the Rotated oRSM and a set of pRSMs serve as regressors for the Upright oRSM.

3.1.1 Methods

Each experiment was run on Amazon's Mechanical Turk (AMT) and coded using HTML and JavaScript code. JavaScript code made use of the jquery1.8.3 (https://ajax.googleapis.com/ajax/libs/jquery/1.8.3/jquery.min.js) and TimTurkTools (Tim Brady - https://timbrady.org/turk/TimTurkTools.js) packages.

Participants

153 participants were recruited from Amazon's Mechanical Turk (AMT). Workers (participants from AMT) were instructed not to participate in any experiment if they had a history of reading or spelling disabilities. Furthermore, workers were instructed not to participate if they were literate in any other written script besides the Roman alphabet although there was no way to independently verify this. Workers were only recruited from the US. Participants were paid $1.00 for their participation.

The 153 participants were divided into 3 groups based on the stimuli used: the Upright Gridfont, the Rotated Gridfont, and the Typical Font Groups. For the Upright Gridfont Group, 54 participants were recruited. Participants had to have participated in at least 100 HITs (tasks on AMT) with an approval rating of at least 95%. For the Rotated Gridfont Group, 50 participants were recruited. Participants had to have participated in at least 1000 HITs with an approval rating of at least 90%. For the Typical Font Group, 49 participants were recruited. Participants had to have participated in at least 1000 HITs (tasks on AMT) with an approval rating of at least 90%.

Stimuli and design

Upright Gridfont Group

The stimuli shown above (Figure 12, left) were the alphanumeric symbols used in this experiment. The stimuli consisted of 28 letters (7 different identities) and 5 digits. In order to control for visual cues like size and curvature, all stimuli were constructed from a limited feature-set of straight lines and were matched to be the same size (see Figure 11 for more details). The limited feature set was used to ensure that features like stimulus orientation (e.g. **r**, ***r***) and line thickness would not serve as cues indicating different shapes. Furthermore, since stimuli were matched in height and width, stimulus size could not serve as a cue to letter case or identity.

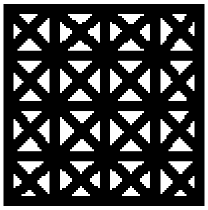

Figure 12. A depiction of the square, 100 X 100 pixel grid with all of the possible features in black. Each stimulus was required to touch all 4 sides. This ensured the height and width of each stimulus were matched.

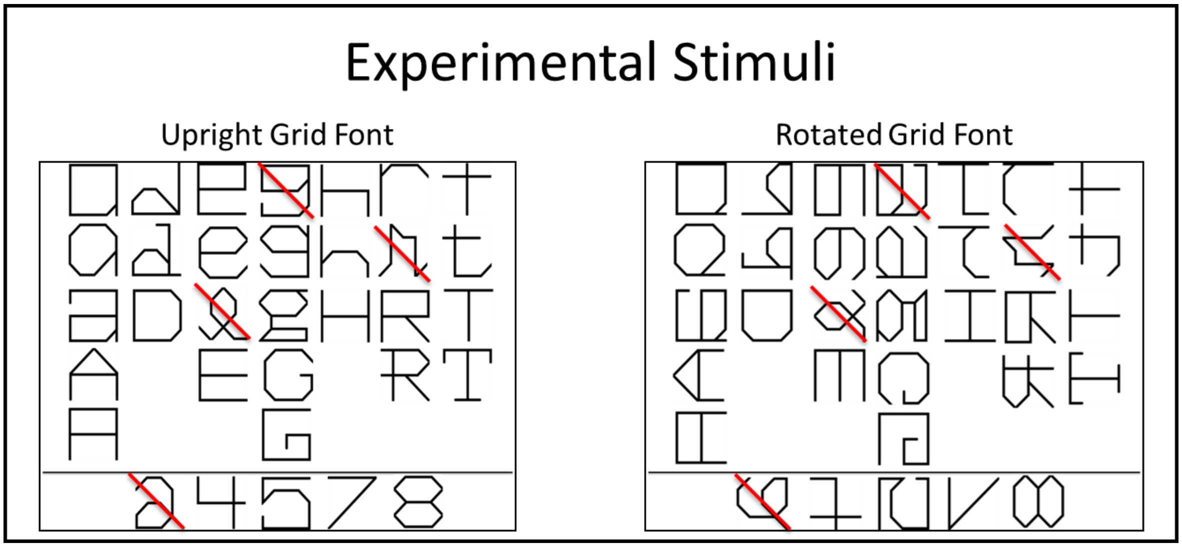

Figure 13. Left: The novel, atypical and upright gridfont alphanumeric characters used as stimuli in Experiment 1 and 2. The red lines indicate stimuli that, while included in the experiment, responses involving these stimuli were excluded from analyses due to the fact that the data analysis indicated that they were difficult to recognize. Right: the rotated gridfont stimuli used in Experiments 1 and 2. These stimuli were created by flipping the upright characters about their vertical axis and then rotating them 90°ccw. The rotation intended to render them difficult to identify. The rotated oRSM provided an estimate of the representational similarity of the upright gridfont stimuli at the level of font-specific computed stimulus shape representations.

Experimental stimuli were displayed within a 500px (width) by 600px (height) frame with a black border and were centered within a 100px by 100px stimulus space. During the stimulus familiarization portion of the Experiment, 1 stimulus within the stimulus space was centered within the display frame. The written feedback displaying the correct response was centered as well. During the similarity judgment portion of the experiment, 2 letter stimuli were displayed side by side (each within a stimulus space) and each stimulus space was centered vertically within the display frame. The center of each stimulus space was 150px away from a fixation dot that was centered both vertically and horizontally within the display frame.

The stimulus familiarization portion consisted of 66 trials, displaying each of the Upright Gridfont stimuli twice. The similarity judgment portion consisted of 22 practice trials and 528 experimental trials. The 528 experimental trials consisted of 1 trial for each possible different-stimulus pairs for the set of 33 stimuli. The 22 practice trials were randomly selected from the set of possible different-stimulus pairs. Stimulus position (left or right) was randomized for each trial and trial order was randomized for each worker.

Rotated Gridfont Group

Experimental stimuli and design were identical to the Upright Gridfont Group except for three variations. First and most importantly, in order to make the letter and digit stimuli difficult to recognize, each character stimulus was flipped around its vertical axis and rotated 90°ccw[11]. Next, there was no familiarization portion of the experiment and the stimuli were referred to as shapes instead of letters and digits. Finally, at the end of the experiment, a survey was presented asking if any of the shapes were recognized and if so to provide a few examples.

Like the Upright Gridfont Group, the similarity judgment portion consisted of 22 practice trials and 528 experimental trials. The 528 experimental trials consisted of every possible different-stimulus pair from the set of 33 rotated stimuli. The 22 practice trials were randomly selected from the set of possible different-stimulus pairs. Stimulus position (left or right) was randomized for each trial and trial order was randomized for each worker.

Typical Font Group

Experimental design was identical to the Rotated Gridfont Group except for the stimulus set used (Figure 13). The characters were presented upright in the monospaced typeface Consolas.

---

[11] For simplicity I will refer to these stimuli as rotated characters.

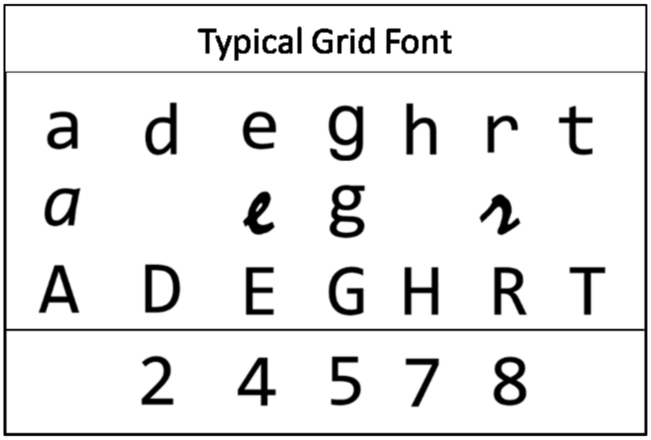

Figure 14. Font used in the Typical Font Group. The font is Consalas which is a variant of Calibri where the width of each character is matched.

The similarity judgment portion consisted of 22 practice trials and 255 experimental trials. The 255 experimental trials consisted of every possible different-stimulus pair within the set of 23 stimuli. The 22 practice trials were randomly selected from the set of possible different-stimulus pairs. Stimulus position (left or right) was randomized for each trial and trial order was randomized for each worker.

Procedure

Upright Gridfont Group

Qualified workers on AMT found the experiment by clicking on a link found on the AMT website titled “Visual Judgements about Letters”. Workers were not allowed to view or begin the experimental tasks until they both agreed to the consent form and accepted the HIT. This experiment consisted of two tasks.

The first task both familiarized the workers with, and tested the legibility of each stimulus. Workers were instructed to indicate the identity of the character by pressing the appropriate key on their keyboard. They were also told responses were not case-sensitive. A stimulus character would appear within the display frame. Once a response was given (correct or incorrect), the correct answer appeared on the screen in Arial font (e.g., “lower-case g”). Workers began the next trial by pressing spacebar. Each stimulus appeared twice. Responses and reaction times were recorded but only responses were analyzed further.

In the second task, participants were instructed to indicate how visually similar the two character stimuli were on a scale of 1 through 5 by pressing 1, 2, 3, 4, or 5 on their keyboard. Furthermore they were instructed that pressing 1 indicates the pair is less similar and increasing numbers indicate increasing similarity up to 5 which is more similar. A reminder of this scale remained visible throughout the task as well as a countdown of the number of remaining trials. Once the task began, a character pair was shown. A keyboard response immediately triggered the appearance of the next stimulus pair. Similarity judgments and reaction times were recorded but only judgments were analyzed further.

Rotated Gridfont Group

The procedure was identical to Upright Gridfont Group except there was no familiarization portion and there was a survey added on at the end that asked participants whether any of the Rotated Gridfont stimuli were recognizable. Additionally, qualified workers on AMT found the experiment by clicking on a link found on the AMT website titled “Visual Judgements about Shapes”.

Typical Font Group

Participants were instructed to indicate how visually similar the two character stimuli were on a scale of 1 through 5. A keyboard response immediately triggered the appearance of the next stimulus pair. Responses and reaction times were recorded but only responses were analyzed further.

3.1.2 Experiment 1 Analysis

Group oRSM formation

Upright Gridfont Group

For the similarity judgment portion of the experiment, visual judgment oRSMs for each participant (participant oRSMs) and 1 group oRSM were constructed. The raw participant oRSMs each consisted of a matrix where each cell contained the similarity judgment for a given stimulus pair. The values in each participant oRSM were reflected across the matrix diagonal[12] and only the upper triangle of the similarity matrix was analyzed. The diagonal had no values since similarity judgments were only made for pairs where the two stimuli were different. Finally, to minimize any influence of different similarity standards across participants, only relative similarity was analyzed by z-normalizing each of the 54 participant oRSMs.

The following procedure was employed to remove outliers: first, for each participant oRSM, a similarity-to-sample value was computed by correlating a given participant's oRSM with each of the other 53 participants' oRSMs, resulting in 53 r values. The similarity-to-sample value consisted of the mean of these 53 r values. This was computed for each participant resulting 54 similarity-to-sample values. Finally, outliers were defined as participants whose similarity-to-sample values fell 1.5 standard deviations below the mean similarity-to-sample value (0.3032). Eight participant oRSMs

---

[12] The y dimension indexes stimuli that appeared to the left of fixation and the x dimension indexes stimuli that appeared to the right. Since only one configuration of a stimulus pair (either <i,j> or <j,i>) was shown to a given participant, the resulting participant oRSM was incomplete. By reflecting across the diagonal (the response in cell_{ij} is placed in cell_{ji} as well), the resulting oRSM has a single value in each cell (except the diagonal). The assumption in performing this operation is that the left /right configuration of the stimuli makes no difference to the visual similarity judgments. Further experimentation would be necessary to verify this assumption.

were found to be outliers in this manner and removed from further analysis. The mean similarity to sample was increased to 0.3926 after it was recomputed with the remaining 46 participant oRSM.

The group oRSM was computed by taking, for each stimulus pair, the mean of the 46 participant similarity z values and placing the mean value in the appropriate cell in the group oRSM. The group oRSM was then z normalized. In further analyses it will be referred to as the **Upright oRSM.**

Rotated Gridfont Group

For the similarity judgment portion of the experiment, 50 participant oRSMs and 1 group oRSM were constructed in the identical manner to the Upright Gridfont Group. Seven outlier participants were identified and removed following the same procedure described above, increasing the mean similarity to sample value from 0.32 to 0.42. The group oRSM formed will be referred to as the **Rotated oRSM**.

Typical Font Group

For the similarity judgment portion of the experiment, 49 participant oRSMs and 1 group oRSM were constructed following the aforementioned procedure. Four outlier participants were identified and removed increasing the mean similarity to sample value from 0.23 to 0.27. Because the similarity judgments from the typical font served as a proxy for the predicted representational similarity of allographs, the group oRSM formed from the typical font will subsequently be referred to as the **Allograph pRSM**

Measuring representational influence

Correlation and regression analyses were employed to determine the types of letter representations that were activated in the processing of visually presented letters. Of particular interest was determining if allograph representations were activated. Two analysis stages were employed. The first stage was a correlation analysis used to identify stored letter representations (e.g., allographs, abstract letter identity, letter name) that influenced visual similarity judgments in a manner that could not be explained by stimulus shape similarity. The second stage was a regression analysis in which the feature dimensions determined to be significant in the correlation analysis were evaluated for their unique contribution to the similarity judgments.

Correlation analysis

The correlation analysis used an observed representational similarity matrix (oRSM) which consisted of pairwise visual similarity judgments from letter stimuli presented in an atypical grid typeface (**the Upright oRSM**). The grid typeface was intended to have a computed stimulus shape similarity structure (see Figure 2) that was substantially different from more typical typefaces in order to maximize the detectability of any bias from allograph representations. Additionally, there was a control oRSM which consisted of visual similarity judgments of the stimuli from the rotated grid typeface (**the Rotated oRSM**). These similarity judgments provided an empirical estimate of the visuo-perceptual similarity of the grid typeface uninfluenced by letter representations accessed by virtue of identifying the letter stimuli.

In addition to the upright and rotated oRSMs, a set of 9 predicted representational similarity matrices (pRSMs) were constructed so that each pRSM represented the predicted similarity structure of the upright grid letter stimuli for a given feature dimension (See Appendix 1, Figures 1-10 for sample pRSMs). Most important among these were 2 pRSMs. First was the **Allograph pRSM**, which estimated the representational similarity of allograph representations. This pRSM consisted of the visual similarity judgments of upright letters presented in a typical font. The assumption here is that the visual similarity of a typical font is a better proxy of the internal representation of stored letter shapes than upright grid font. Second, the **ALI pRSM** predicts the similarity structure at the level of abstract letter identities; specifically, it assigns 1 to all letter pairs with the same identity (e.g., **a, A**) and 0 to all other letter pairs. Practically, it predicts that similarity judgments for letters that share the same identity will be greater than the judgments of letter pairs that do not. Other pRSMs include a **Pixel-Overlap pRSM** that measures low-level (pixel-based) image similarity of pairs of letter stimuli to capture low level visual similarity that is not represented in the Allograph pRSM. As described above, each letter stimulus was composed of a black font on a white background and was constructed, cropped, and centered such that both the background size and the topmost, bottommost, leftmost and rightmost points of each letter were matched. Each pixel in the stimulus image was assigned 1 (black) or 0 (white). Each stimulus image matrix was then subtracted from one another and sum of the absolute value was taken of the difference matrix was computed. This was the sum of pixels where the two images did not share the same value (misses). Pixel Overlap was computed by the following formula: Overlap=1-(misses / total number of pixels in an image). Following Rothlein and Rapp (2014), there were 3 pRSMs that measured similarity based on similarity in the auditory and motor modalities. The auditory **Letter-Name pRSM** represents auditory similarity on the basis of an empirically derived letter name confusability matrix (Hull, 1973). The experimental task used by Hull involved participants identifying aurally presented letter and digit names. Confusions were elicited by presenting the names in a noisy background. The more confusable two names were, the more similar the name representations. A second **Phonetic Feature pRSM** was created based on the set of phonetic features corresponding to each letter name (features taken from an IPA phonetic feature chart). Phonetic feature overlap was computed by summing the features from each letter name that overlap with the features from the other letter name and dividing that sum by the total number of features across the pair of letter names. The **Motoric pRSM** was derived from a stroke-feature similarity metric (Rapp & Caramazza, 1997) that was validated against written letter confusions produced by individuals with acquired dysgraphia. Finally, there were 3 pRSMs that predicted the similarity structure of the orthographic and semantic properties of alphanumeric symbols. The **Case pRSM** tested the hypothesis that case was represented independently of letter identity. Specifically, all letters that shared the same case shared the same case marker representation (see Figure 5). Accordingly, the **Case pRSM** predicted that all letters that shared the same case (e.g., **A** and **B**) should be more similar to one another (and were assigned a 1) as compared to letters that did not (e.g., **A** and **b** which was assigned a 0). To reduce the possibility of an interaction with letters that share the same ALI, only letter pairs with different identities were included in this analysis. The **Consonant/Vowel (c/v) pRSM** tested for identity-independent consonant or vowel representation shared across letters. For example, the letters **a** and **e** shared the same vowel representation and were assigned a 1 whereas **a** and **c** was be assigned a 0. Following this, the c/v pRSM predicted that all consonants should be more similar to other consonants (that do not share the same ALI) than with vowels and all vowels should be more similar with other vowels (that do not share the same ALI) than with consonants. Finally the **Alphanumeric pRSM** predicted that all letters should be more similar to each other than to digits and digits should be more similar to other digits than to letters. Only letter pairs with different identities were included in this pRSM to account for the fact that there were no font or shape variants of the same digit identity.

The goal of the correlation analysis was to identify representations that influenced the visual similarity judgments of the upright gridfont in a manner that could not be explained by the visual similarity of the stimuli. To this end the analysis involved the following four steps: (1) each of the 9 pRSMs was correlated with the Rotated oRSM. Because the pixelwise similarity was matched between the rotated and upright gridfonts and because the stimuli in the rotated gridfont were hard to identify, these correlations served as a control condition to estimate the baseline correlations between the visual similarity of the stimulus shapes and the pRSMs without the contribution of letter recognition. (2) Each pRSM was also correlated with the Upright oRSM. (3) The difference between the correlations of each pRSM with the Upright oRSM and the Rotated oRSM was interpreted as reflecting the influence of the stored letter type represented by that particular pRSM. In other words, the degree of influence for each type of stored letter representation was quantified as the correlation difference value (r_{diff}) between the correlation r of that stored letter representation's pRSM with the Upright oRSM ($r_{upright}$) minus the correlation between that pRSM and the Rotated oRSM ($r_{diff} = r_{upright} - r_{rotated}$). (4) Significance for the aforementioned correlation difference (r_{diff}) was established using a label-scramble permutation Monte-Carlo analysis. This analysis was carried out by creating 10000 Upright and Rotated Pseudo-oRSMs in the following manner: the rows and columns of the original Upright oRSM and the Rotated oRSM were scrambled forming Upright and Rotated Pseudo-oRSMs. Importantly, the rows and the columns were scrambled identically (e.g., if the **a** column swapped places with the **d** column, then the **a** row would swap places with the **d** row). This ensured that the Pseudo-oRSMs properly estimated the null-distribution based on scrambled label permutations. Each Upright Pseudo-oRSM was matched with a Rotated Pseudo-oRSM insofar as the scrambled row and column assignments for the Upright and Rotated Pseudo-oRSM pair were identical. For each pRSM a distribution of 10000 random correlation differences were computed by taking the correlation of the Upright Pseudo-oRSM and a pRSM and subtracting the correlation between that same pRSM and the matched Rotated Pseudo-oRSM. If the actual difference between the pRSM correlated with the upright oRSM and the pRSM correlated with the rotated oRSM fell within the top 5% of correlation difference values, the correlation difference was labeled significant. Reported one-tailed p values were computed by subtracting the percentile rank of the r_{diff} value from 1.

Regression analysis

While showing that a given pRSM had a significant r_{diff} is consistent with the hypothesis that the stored letter representation quantified by a particular pRSM was influencing visual similarity judgments, it is possible that the pRSM only appeared to be influential by virtue of its correlation with a pRSM that actually is influential. For example, the Allograph pRSM is highly correlated with the ALI pRSM (r=0.66). Therefore, if both are shown to be influential, both could be genuinely influential or possibly only allograph representations are influential and ALI representations merely appear to be so based on their high correlation with the Allograph pRSM. To account for this possibility, a multiple linear regression analysis was employed where Y=the Upright oRSM and all of the pRSMs that had significant r_{diff} values were included as regressors along with the Rotated oRSM. The logic is that the beta values for each pRSM would indicate the relative contribution of the pRSM in the context of the other significant r_{diff} pRSMs while controlling for the stimulus shape (via inclusion of the Rotated oRSM). The values in the Upright oRSM were z-normalized as were the values for each of the regressors in order to ensure the beta-values reflected relative fit and were directly comparable.

3.1.3 Experiment 1 - Results

Letter familiarization task

While overall accuracy on the familiarization task was quite high (mean = 92%), four stimuli had accuracies below 70% (shown crossed with red lines in Figure 13). The distribution of accuracies reveals the vast majority of stimuli were highly recognizable with accuracies greater than 90%. The four stimuli that fell below 70% were removed from further analyses due to concerns that they may be either unrecognized or misidentified. It is important to note that, besides the four outlier stimuli, the novel grid font was highly recognizable.

Survey results

Participants were asked if the rotated character stimuli looked familiar and if so, to give examples of what they were. Of the 44 participants, only 7 identified them as being multiple alphabetic letters[13]. Three additional participants recognized the letter T and failed to correctly identify anything else. A majority of responses were statements indicating that the rotated stimuli were not familiar (23 participants) and the remaining 11 participants provided non-alphanumeric examples (e.g., pencil, house, fish). These results demonstrate that rotating the gridfont rendered the stimuli unrecognizable for a majority of participants.

Correlation analysis results

Nine pRSMs were correlated with the group Upright oRSM. The correlations are shown on the graph below (a. in Figure 15). Significance was evaluated by a permutation analysis involving 10,000 iterations. The actual correlation for each pRSM was ranked against the null distribution of pseudo-correlations constructed for each pRSM. Of the 9 pRSMs tested, the Allograph (r=0.67), Pixel-Overlap (r=0.65), Letter Identity (r=0.59), Motor Feature Overlap (r=0.27), and Letter Case Identity (r=0.21) were determined to be significant (i.e., the actual correlation was in the top 5 percent of the Monte-Carlo distribution) and for 4 of those 5 pRSMs the actual correlation was the top ranked correlation in the null distribution (indicated in Figure 15 with a double asterisk). The Alphanumeric (r=0.09), Letter Name Confusability (r= -0.05), Phonetic Feature Overlap (r= -0.13) and C/V Identity (r= -0.18) pRSMs failed to reach the 5% significance threshold.

The 5 pRSMs that were significantly correlated with the Upright oRSM were then correlated with the Rotated oRSM. The correlations with the Rotated oRSM served as an

---

[13] The data from these 7 will be included the main analyses but will be evaluated in an additional analysis directed at comparing the similarity structures of participants who recognized the rotated gridfont with those who did not. Furthermore, all of the analyses were run removing these 7 participants and the results were substantively the same (i.e., no insignificant results became significant or vice versa).

estimate of the correlation between the visual similarities of the stimulus shapes without the contribution of letter recognition. Therefore, any influence that recognition had on visual similarity judgments would be revealed by a difference in a pRSM's correlation with theU versus Rotated oRSM. The bar graph in Figure 15 (b) shows the correlation for the Upright and the Rotated oRSM and the difference (r_{diff} = upright r – rotated r) was evaluated for significance using the label-scramble permutation analysis described in the method section. Of the 5 pRSMs tested, significant r_{diff} values were obtained for: Allograph ($r_{diff} = 0.28$; $p_{rank}=0.001$), Letter Identity ($r_{diff} = 0.29$; $p_{rank}=0.001$), Letter Case Identity ($r_{diff} = 0.19$; $p_{rank}=0.001$), and Motor-Feature Overlap ($r_{diff} = 0.06$; $p_{rank}=0.047$). Only the Pixel Overlap pRSM difference score was not significant ($r_{diff} = 0.02$; $p_{rank}=0.33$).

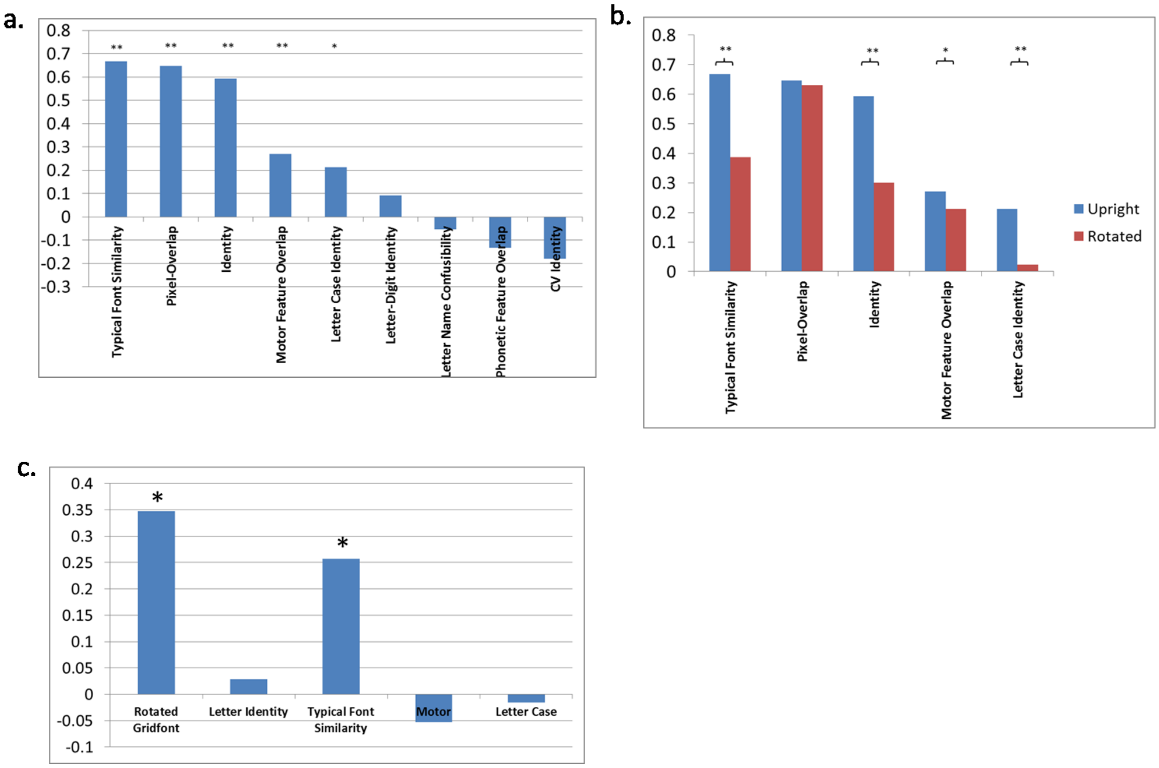

Figure 15. Bar graphs depicting results from Experiment 1. In all graphs, * indicates significance at a p_{rank}<0.5 while ** indicates a top ranked value. (a) Depicts the r values from correlations between 9 pRSMs and the upright similarity judgment oRSM. (b) Depicts correlation comparisons between the 5 significant pRSMs from (a) with the upright oRSM (in blue) and with the rotated oRSM (in red). (c) Depicts the beta weights from a regression analysis where the significant pRSMs from (b) acted as predictors of the Upright oRSM. The Rotated oRSM was included as well under the label Rotated Gridfont.

The regression analysis provided a strong test of the unique contribution of each of the representational types. Results from the regression analysis revealed that the overall model is significant (adjusted $R^2 = 0.79$; f(235, 5) = 219.9; p<0.0001). Regressors whose betas were significant in a one-tailed t-test were the Rotated oRSM ($\beta = 0.35$; t(285) = 19.1; p<0.0001) and the Allograph pRSM ($\beta = 0.26$; t(285) = 7.5; p<0.0001). The other regressors failed to reach significance (see Figure 15, c).

3.1.4 Experiment 1 Discussion

In Experiment 1, I obtained visual similarity judgments for pairs alphanumeric characters presented in 3 fonts: an atypical gridfont, the atypical gridfont rotated, and a typical font which served as a proxy for the representational similarity of allograph representations. Predicted similarity values (pRSMs) for ALI, allograph, letter-case, and motoric production code representations were significantly more correlated with the upright gridfont similarity judgments the those of the rotated gridfont letters suggesting that while keeping low-level visual similarity constant, correctly identifying the letters in the upright condition introduced a similarity bias from these four types of letter representations. An additional regression analysis demonstrated that of these four pRSMs, only the Allograph pRSM uniquely accounted for the variance when the stimulus shape similarity is accounted for with the inclusion of the Rotated oRSM. This result provides strong evidence for the influence of the visual similarity of allograph representations on similarity judgments of the upright gridfont letters/digits.

3.2 Experiment 2 - Physical same-different judgments of upright and rotated letters and digits presented in an atypical gridfont.

That stored allographs both were accessed and influenced visual similarity judgments was quite apparent from the results in Experiment 1 though what was less clear was the nature of this influence. For example, instead of an unconscious bias on these visual judgments, it could be that participants misread the instructions indicating that the similarity judgments were to be based strictly on visual criterion. If they just judged letter similarity more generally, it would be less surprising that stored letter knowledge would make a contribution. Furthermore, since visual similarity was never explained to the participants, different participants could be using different criteria when mentally computing visual similarity. In the experiment that follows, I collected reaction times of same-different judgments to various letter pairs. In this experiment, two letter-images were shown and the participant decided whether the two stimulus-images were visually identical or not. The amount of time it took to make this same-different decision was recorded for each letter pair. The set of all such RTs for the different responses was used to calculate an RT based oRSM. Since the same-different decisions were based on the visual identity, if a participant misunderstood the directions, it would be easy to spot since they would systematically respond incorrectly when the letter pair consists of font or case variants of the same letter identity. Additionally, since the finding of allograph bias was a novel result from a novel method, convergence across multiple types of tasks would serve to strengthen confidence in the result.

3.2.1 Methods

Participants

100 participants were recruited from Amazon's Mechanical Turk (AMT). Workers (participants from AMT) were instructed not to participate in any experiment if they had a history of reading or spelling disabilities. Furthermore, workers were instructed not to participate if they were literate in any other written script besides the Roman alphabet. Neither of these conditions was verified. Workers were only recruited from the US and had to have participated in at least 1000 HITs (tasks on AMT) with an approval rating of at least 95%. The participants were split into two groups based on the type of stimuli shown. 50 participants were shown the upright gridfont and were paid

$1.00 for their participation. The other 50 participants were shown the rotated gridfont and paid $0.80 for their participation.

Stimuli and design

Upright Gridfont Group

Experimental stimuli were composed of a subset of the upright grid font stimuli used in Experiment 1 (Figure 13). The stimulus familiarization portion consisted of 38 trials, displaying each stimulus twice. The visual same-different decision portion consisted of 15 practice trials and 285 experimental trials. The 285 experimental trials consisted of every possible different-stimulus pair within the set of 19 stimuli (171 trials or 60% of total) and 6 repetitions of each of the 19 possible same pairs (114 trials or 40% of total). The 15 practice trials were randomly selected from the set of possible experimental trials. Stimulus position (left or right) was randomized for each trial and trial order was randomized for each worker.

Rotated Gridfont Group

Experimental stimuli and design were identical to the Upright Gridfont Group except for three variations. Like the Rotated Gridfont Group in Experiment 1, each letter stimulus was flipped around its vertical axis and rotated 90°ccw in order to make it difficult to recognize. Next, there was no familiarization portion of the experiment and the stimuli were referred to as shapes instead of letters. Finally, at the end of the experiment, a survey was presented asking if any of the shapes were recognized and if so provide a few examples as to what they were.

Like the Upright Gridfont Group, the experiment consisted of 15 practice trials and 285 experimental trials (40% same, 60% different). The different trials consisted of every possible different-stimulus pair within the set of 19 rotated stimuli (171 trials) and the same trials consisted of 6 repetitions of each of the 19 same pairs (114 trials). The 15 practice trials were randomly selected from the set of possible experimental trials. Stimulus position (left or right) was randomized for each trial and trial order was randomized for each worker.

Procedure

Qualified workers on AMT found the experiment by clicking on a link found on the AMT website titled "Visual Letter Same-or-Different Judgments (May be completed only once per worker)". Workers were not allowed to view or begin the experimental tasks until they both agreed to the consent form and accepted the HIT. This experiment consisted of two tasks.

The first task both familiarized the workers with, and tested the legibility of, each stimulus. Workers were instructed to indicate the identity of the character by pressing the appropriate key on their keyboard. They were also told responses were not case-sensitive. A stimulus character would appear within the display frame. Once a response was given (correct or incorrect), the correct answer appeared on the screen in Arial font (e.g., "lower-case g"). Workers began the next trial by pressing spacebar. Each character stimulus appeared twice. Responses and reaction times were recorded but only responses were analyzed further.

The second task gathered visual same or different judgments for simultaneously presented letter stimuli. Participants were told through written instruction that they would see two letter shapes and a dot on the center of the screen and to decide whether the two letter shapes are visually identical or not. Pressing **s** on the keyboard indicated a "same" response and **d** indicated a "different" response. They were instructed to respond with their first impression as quickly as possible. A countdown of the number of remaining trials remained visible throughout the task. Once a trial began, a fixation dot appeared in isolation for either 400ms or 800ms (143 and 142 trials respectively, randomly assigned) followed by a pair of stimuli. The keyboard response triggered a hyperlink to appear which was clicked to begin the next trial, allowing for self-pacing. Responses and reaction times (from stimulus onset to keyboard response) were recorded.

The procedure was identical for the Upright Gridfont Group and the Rotated Gridfont Group except for the Rotated Gridfont Group there was no familiarization portion of the experiment and there was a survey added on at the end.

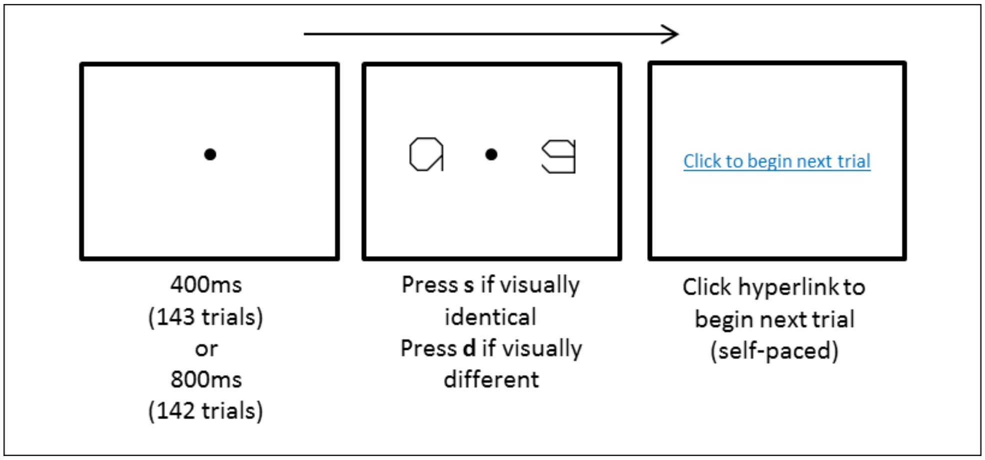

Figure 16. The time course of a trial in the same-different decision paradigm.

3.2.2 Experiment 2 Analyses and results

Letter familiarization task

Overall accuracy on the familiarization task was very high (mean = 98%). All of the letter stimuli used in this experiment were highly recognizable with accuracies greater than 90% (Range: 91%-100%).

Visual same-different decision task - Upright Gridfont Group

For the same-different judgment portion of the experiment, 50 participant Reaction Time Similarity Matrices (participant oRSMs) and 1 group reaction time Similarity Matrix (group oRSM) were constructed out of the reaction times to Different trials. The values in each participant oRSM were reflected across the matrix diagonal and only the upper triangle of the similarity matrix was analyzed. The diagonal consisted of the RTs for the "same" responses and were removed. Finally, to remove outliers and to normalize across participant specific reaction times, each participant's RTs were z-normalized and RTs that fell outside 2.5 standard deviations (above or below) were removed. Response times from incorrect responses were also removed.

Outlier participants were removed using the same Similarity-to-Sample procedure described in Experiment 1. The 50 similarity to sample values were considerably lower than the similarity judgment experiments suggesting greater cross-participant variability in this task. Outliers were defined as participants whose similarity to sample value fell 1.5 standard deviations below the mean similarity to sample value (0.0658). Four participant oRSMs were found to be outliers in this manner and removed from further analysis. The mean similarity to sample was increased to 0.08 after it was recomputed with the remaining 46 participant oRSMs.

The group oRSM was computed by taking, for each stimulus pair, the mean of the 46 participant z values and placing the mean value in the corresponding cell in the group oRSM. The group oRSM was then z normalized. In further analyses it will be referred to as the **Upright oRSM.**

Visual same-different decision task - Rotated Gridfont Group

50 participant oRSMs and 1 group oRSM (rotated oRSM) were constructed in the identical manner to the Upright Gridfont Group. 3 outlier participants were identified and removed increasing the mean similarity to sample value from 0.0645 to 0.0728.

Like the Upright Gridfont Group, an oRSM for the Rotated Gridfont Group was computed by taking, for each stimulus pair, the mean of the remaining 47 participant similarity z values and placing the mean value in the corresponding cell in the oRSM. The Rotated oRSM was then z normalized.

Survey results

Participants were asked if the rotated character stimuli looked familiar and if so, to give examples. Of the 47 participants, only 13 identified them as being multiple alphabetic letters[14]. Three additional participants recognized the letter T and failed to correctly identify anything else. A majority of responses were statements indicating that

---

[14] Like Experiment 1, participants who could identify the rotated gridfont stimuli were not removed before forming the Rotated oRSM although they were analyzed in a separate analysis reported below in this chapter. Furthermore, the analyses in this experiment were rerun after removing these participants and the results were not substantively different.

the rotated stimuli were not familiar (20 participants) and the remaining 11 participants provided non-alphanumeric examples (e.g. cross, angles, house). These results demonstrate that rotating the gridfont used in 2.a. rendered the stimuli unrecognizable for a majority of participants.

Correlation and regression results

Analyses were identical to those in Experiment 1 with the only differences being that, instead of visual similarity judgments, similarity measures consisted of both reaction times and number of erroneous responses for different letter pairs. The logic is that more similar stimuli will require more time to correctly respond "different" and will more likely generate errors. The same pRSMs examined in Experiment 1 were tested in this experiment with the exception of the letter-digit pRSMs as the stimulus set in this experiment only consisted of letters. The remaining pRSMs tested were those used in Experiment 1: Allograph, Pixel-Overlap, Letter Identity, Letter-Case, Consonant or Vowel Status, Motor Feature Overlap, Phonetic Feature Overlap, and Letter-Name Confusability.

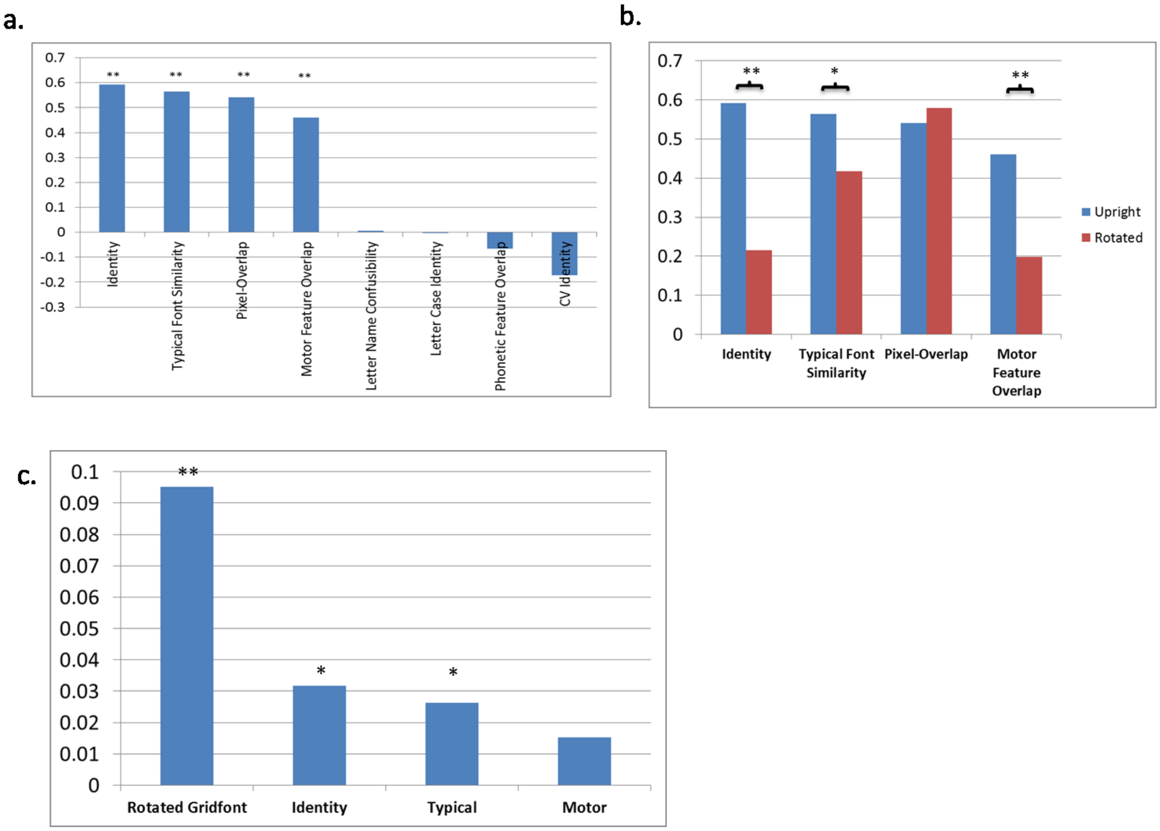

Figure 17. Bar graphs depicting results from the RT analysis in Experiment 2. In all graphs, * indicates significance at a $p_{rank}<0.5$ while ** indicates a top ranked value. (a) Depicts the r values from correlations between 9 pRSMs and the upright similarity judgment oRSM. (b) Depicts correlation comparisons between the 5 significant pRSMs from (a) with the upright oRSM (in blue) and with the rotated oRSM (in red). (c) Depicts the beta weights from a regression analysis where the significant pRSMs from (b) acted as predictors of the Upright oRSM. The Rotated oRSM was included as well under the label Rotated Gridfont.

First, each of the pRSMs was correlated with the Upright oRSM for both the RTs and Errors. Significance of the correlations was assessed using the permutation analysis described and used in Experiment 1. The analysis indicated that the following pRSMs were significantly correlated with both the RT-based and Error-Based oRSMs: Pixel-overlap (RT: $r = 0.54$; $p=0.0001$, Error: $r = 0.30$; $p = 0.0007$), Allograph (RT: $r = 0.56$; $p=0.0001$, Error: $r = 0.47$; $p = 0.0001$), Letter Identity (RT: $r = 0.59$; $p=0.0001$, Error: $r = 0.53$; $p = 0.0001$) and Motor-Feature Overlap (RT: $r = 0.46$; $p = 0.0001$, Error: $r = 0.43$; p

= 0.0001). None of the other pRSMs reached significance when correlated with either the RT-based or the Error-based oRSMs.

To determine whether the above significant correlations could be fully explained by the visual similarity of the character shapes, the significant pRSMs were correlated with both the RT-based and Error-based oRSMs generated from the rotated gridfont stimuli from Experiment 1). As a reminder, the rotated gridfont stimuli were completely matched in terms of pixelwise similarity to the upright gridfont stimuli but the rotation rendered them much more difficult to recognize. Like Experiment 1, the difference between the pRSM correlations with the Upright and Rotated oRSMs was interpreted as a value measuring the bias introduced in virtue of recognition ($r_{diff} = r_{upright} – r_{rotated}$). Significance of the difference value was assessed via a permutation analysis described in Experiment 1. Of the four tested pRSMs, 3 were significant for both the RT-based and Error-based oRSMs. They were Allograph (RT: $r_{diff} = 0.15$; p=0.044, Error: $r_{diff} = 0.30$; p = 0.0053), Letter Identity (RT: $r_{diff} = 0.38$; p=0.0001, Error: $r_{diff} = 0.37$; p = 0.0002) and Motor-Feature Overlap (RT: $r_{diff} = 0.26$; p = 0.0011, Error: $r_{diff} = 0.28$; p = 0.0067). The difference value for Pixel-Overlap failed to reach significance for both the RT-based and Error-based oRSMs (RT: $r_{diff} = -0.04$; p = 0.69, Error: $r_{diff} = 0.15$; p = 0.11).

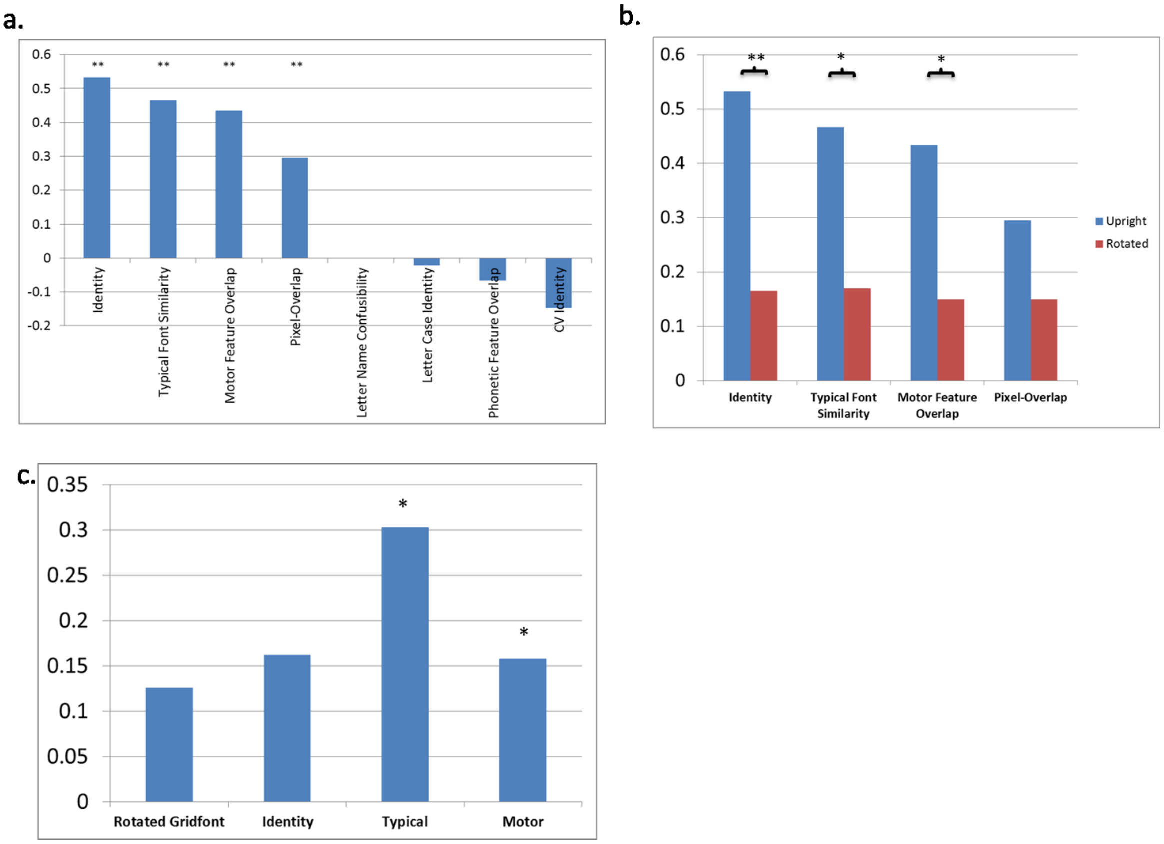

Figure 18. Bar graphs depicting results from the error analysis in Experiment 2. In all graphs, * indicates significance at a p_{rank}<0.5 while ** indicates a top ranked value. (a) Depicts the r values from correlations between 9 pRSMs and the upright similarity judgment oRSM. (b) Depicts correlation comparisons between the 5 significant pRSMs from (a) with the upright oRSM (in blue) and with the rotated oRSM (in red). (c) Depicts the beta weights from a regression analysis where the significant pRSMs from (b) acted as predictors of the Upright oRSM. The Rotated oRSM was included as well under the label Rotated Gridfont.

Finally, the 3 pRSMs with significant difference values were entered into 2 regression analyses. In one regression analysis the Y value consisted of the RT-based oRSM from the upright gridfont letters. The regressors consisted of the RT-based oRSM from the rotated gridfont letters, the Letter Identity, Allograph, and Motor-Feature Overlap pRSMs and a constant. The other regression was identical except the oRSM consisted of error counts instead of RTs. Results from the RT regression analysis revealed that the overall model was significant (adjusted $R^2 = 0.54$; f(159, 4) = 48.3;

$p<0.0001$). Regressors whose betas were significant in a one-tailed t-test were the Rotated RT-based oRSM ($\beta = 0.095$; $t(159) = 8.84$; $p<0.0001$), the Allograph pRSM ($\beta = 0.026$; $t(159) = 1.67$; $p<0.05$) and Letter Identity ($\beta = 0.031$; $t(159) = 2.49$; $p<0.01$). Results from the Error-based regression analysis reveal that the overall model is significant (adjusted $R^2 = 0.26$; $f(159, 4) = 13.7$; $p<0.0001$). Regressors whose betas were significant in a one-tailed t-test were the Allograph pRSM ($\beta = 0.30$; $t(159) = 2.49$; $p<0.01$) and the Motoric Feature pRSM ($\beta = 0.16$; $t(159) = 1.67$; $p<0.05$). The beta values for both the Rotated error-based oRSM and the Letter Identity pRSM were marginally nonsignificant ($p=0.065$ in both instances).

3.2.3 Experiment 2 discussion

Experiment 2 was designed to provide converging evidence regarding the results from Experiment 1 while addressing some concerns about the open-endedness of visual similarity judgments as a similarity metric. Therefore, using a subset of the stimuli from Experiment 1 and the same logic and design, we obtained similarity measures by using the reaction times and errors in a task where participants were presented with two stimuli and asked to judge if they were physically identical or not. Since the task was well defined (stimuli were either physically identical or not) and considerations about stimulus similarity were not explicitly brought to the attention of the participant, interference effects from stored letter representations could be thought to arise less consciously and more automatically.

Results were remarkably similar across Experiments 1 and 2, with Allograph, Letter Identity, and Motor Feature Overlap significantly influencing similarity judgments, RTs, and errors. The only major difference between the two experiments was the fact that the Letter-Case pRSM significantly influenced visual similarity judgments but not RTs or errors from the same-different decision task. One possibility is that Letter-Case results from the same-different decision experiment were not sensitive enough to reveal this effect; another is that it is related to task differences. Previous research has found that split-half reliability measures were considerably higher for letter similarity judgment values than "different" response RTs in a same-different decision task (Podgorny & Garner, 1979). Consistent with this, mean Similarity-to-Sample values, which measured how consistent each participant's responses were to one another, were much higher in the similarity judgment experiment (Upright: 0.39; Rotated 0.42) vs. the RTs in the same-different decision experiment (Upright: 0.08; Rotated 0.07). One drawback to this explanation is that if noise was the issue, the effect size should best predict whether a result will replicate and while the r_{diff} for the Letter-Case pRSM was larger than the r_{diff} for the Motor Feature Overlap pRSM in Experiment 1, the effect from the Motor Feature Overlap replicated across experiments while the Letter-Case result did not.

Finally, the pattern of results so far has consistently revealed that for multiple measures of visual similarity, characters presented in the atypical gridfont were influenced by the visual similarity of the characters in a more typical font—providing support for the role of allographic representations. One possible issue arises from the assumption that the similarity measures of the upright and rotated gridfont characters were completely matched at the level of the computed stimulus shape representations. It is possible that the rotation of the stimuli changes the visual similarity of the computed shapes and therefore, the Rotated oRSM is not a perfect control. Furthermore, since the typical font similarity judgments were obtained from upright letters, the concern arises that the allograph effect was driven by the fact that both the upright gridfont and the upright typical font share the same orientation. I examined this possibility in two ways. First, I took advantage of the fact that some participants were able to correctly identify the letters presented in the rotated grid font. I was then able to correlate the Allograph pRSM with the Rotated oRSMs from the participants who recognized the letters and compare it with the oRSMs from the participants who did not recognize the letters. Since both the participants who recognized the rotated letters and those who did not saw the exact same stimuli, any differences would be in virtue of accessing the stored letter representations and not orientation effects. Next, I ran a third experiment that directly compared the influence of rotating a set of pseudo-letters on visual similarity judgments. Both of these are explained in more detail below.

3.3 Recognizers vs. Nonrecognizers for the rotated characters

Participants in the Rotated Gridfont groups in Experiments 1 and 2 provided visual similarity judgments or made visual same-different decisions—respectively—for pairs of difficult-to-recognize rotated characters. After each experiment, a survey was presented to determine which participants correctly recognized (at least some of) the rotated characters. Participants were classified into three groups based on their survey responses: nonrecognizers, recognizers, and ambiguous[15]. One potential avenue of evidence comes from comparing the oRSM-pRSM correlations of the recognizers to those of the nonrecognizers. Since the visual stimuli for both groups were the same pairs of rotated characters (i.e. completely visually matched), the most apparent source for any

---

[15] While these groups reflect the explicit degree of recognition for each participant, the rotated stimuli could have been identified implicitly.

differences in correlation values would be biases introduced when the rotated characters were recognized. In other words, recognizers may have activated and engaged recognition-dependent representations like Allographs and ALIs that the nonrecognizers did not and therefore these letter representations may have influenced the errors, RTs, or visual similarity judgments of the Recognizers to a greater extent than the Nonrecognizers.

For each of the pRSMs, a Recognizer Bias Value (RBV) was computed in the following manner: z-scored participant oRSMs were classified as Recognizers, Nonrecognizers, or Ambiguous based on survey responses (Ambiguous oRSMs were discarded). Group Recognizer and Nonrecognizer oRSMs were formed by computing the mean z-values (or sum for error counts) for each letter-pair for the Recognizers and Nonrecognizers separately. The oRSMs from each of these groups were then correlated (Pearson) with each pRSM. The change in r from the Recognizer oRSM-pRSM correlation to the Nonrecognizer oRSM-pRSM correlation (Recognizer r - Nonrecognizer r) was the Recognizer Bias Value.

Significance was assessed via a permutation analysis wherein the participant oRSMs (not including the Ambiguous oRSMs) were randomly assigned as either Recognizers or Nonrecognizers, keeping the ratio of participants in each category the same. For example, in Experiment 1 there were 7 Recognizers and 34 Nonrecognizers and the random participant reassignment kept this ratio constant. Pseudo-Group oRSMs were formed for each group by either taking the mean or sum (for error counts) across participants and Pseudo-Recognition Bias Values were computed for each pRSM by correlating the Pseudo-Group oRSMs with each pRSMs and subtracting the Pseudo-

Nonrecognizer r from the Pseudo-Recognizer r. A distribution of 10,000 Pseudo-Recognition Bias Values was formed for each oRSM type (similarity judgments, same-different RTs, and same-different Errors) by performing 10,000 random reassignments. The p-value was computed by taking the percentile of the real Recognition Bias Value within the permutation distribution and subtracting that percentile from 1 and p-values less than 0.05 were considered significant.

The Recognition Bias Values for the 9 pRSMs derived from the Visual Similarity Judgment experiment revealed a pattern of results that was remarkably consistent with the results from previous analyses. Specifically, in the Visually Similarity Judgment experiment, Recognizers had significant greater correlations than Nonrecognizers for the following pRSMs: Allograph (RBV = 0.03; p=0.024), Motor Feature Overlap (RBV = 0.07; p=0.015), and Letter Case Identity (RBV = 0.08; p=0.039). The Letter Identity pRSM was marginally significant (RBV = 0.03; p=0.065). None of the other pRSMs reached significance. When examining the RBV values from the RTs and errors from same-different decision experiment, the pattern was much less consistent with previous analyses. The only pRSM to reach significance was the Letter Case Identity pRSM (RBV = 0.11; p=0.043).

For the visual similarity judgments at least, the fact that the Allograph pRSM was more correlated with the oRSMs derived from the Recognizers than the Nonrecognizers suggests that accessing allograph representations influenced the visual similarity judgments for the rotated gridfont characters. This influence could not be explained by orientation effects because both the Recognizers and Nonrecognizers viewed the rotated grid-font letters.

3.4 Experiment 3: The visual similarity of upright and rotated pseudoletters

Experiment 3 specifically tested an alternative interpretation of the finding that the visual similarity judgments for the stimuli presented in a typical font was more correlated with the Upright oRSM than the Rotated oRSM. While the explanation put forward was that this difference was due to the influence of stored allograph representations on the similarity measures, an alternative interpretation of these results was that it occurred because both the typical font and the upright gridfont were upright letters and, the rotated gridfont letters—even though the pixel-wise similarity is comparable to the upright gridfont letters—nonetheless had a different visual similarity structure. It should be noted that in order for this explanation to account for the observed representational interference effects, the visual change from rotating the stimuli must be large enough to completely account for the observed differences in correlation between the rotated upright grid-font letters. While comparing Recognizers with Nonrecognizers provided evidence for the influence of stored letter representations using behavioral measures of similarity that were not explainable by this alternative account, the effect sizes in this analysis were quite small and the significant results were inconsistent across task (similarity judgments vs. same-different decision RTs and accuracies). Therefore, Experiment 3 directly tests this possibility by examining if/how much rotation influences the similarity judgments of pixel-wise matched shapes.

To test this possibility, similarity judgments from a set of pseudoletters, along with judgments from the same pseudoletters rotated were obtained. Since the stimuli were meaningless in both orientations, and since the stimulus pairs were pixel-wise matched across changes in orientation, any differences in visual similarity should be due to the rotation itself.

3.4.1 Methods

Participants

40 participants were recruited from AMT. Workers were only recruited from the US and had to have participated in at least 1000 HITs (tasks on AMT) with an approval rating of at least 95%. Participants were paid $0.35 for their participation.

Stimuli and design

Experimental stimuli and design was similar to Experiment 1. The major difference was the stimulus set used (see Figure 19). Specifically, the stimuli were constructed using the same gridfont constraints as the upright gridfont (see description of gridfont stimuli in Exp. 1, Figure 12). However, unlike the upright gridfont from Exp.1, the shapes created were not real alphanumeric characters. Six "upright" pseudoletters were created and then six "rotated" pseudoletters were created by flipping the "upright" pseudoletters about the vertical axis and rotating them 90°ccw.

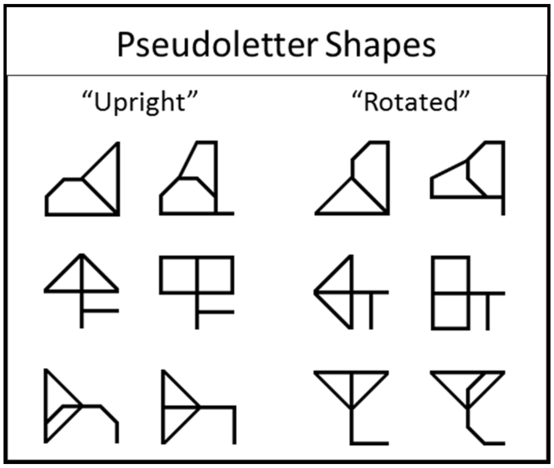

Figure 19. The 6 "Upright" pseudoletter shapes used in experiment 3 along with their rotated counter parts. The rotated pseudoletters were flipped about the vertical axis and rotated 90°ccw.

The similarity judgment portion consisted of 6 practice trials and 2 runs of 30 experimental trials. Each run consisted of every possible different pairing within the 6 “upright” stimuli (15 trials) and the 6 “rotated” stimuli (15 trials). There were no pairs containing a mix of “upright” and “rotated” pseudoletters. Once the first run ended, the second run began without the participants’ knowledge. The 6 practice trials were randomly selected from the set of possible different-stimulus pairs. Stimulus position (left or right) was randomized for each trial and the trial order was randomized for each run. Ultimately, each stimulus pair had two similarity judgments per participant—one from each run.

Procedure

The procedure was identical to experiment 1 except there was no familiarization portion. Briefly, participants were instructed to indicate how visually similar the two pseudoletter stimuli were on a scale of 1 through 5. Once the task began, a pair consisting of the pseudoletter stimuli was shown. A keyboard response immediately triggered the appearance of the next stimulus pair. Responses and reaction times were recorded but only responses were analyzed further.

3.4.2 Experiment 3 - Analysis and results

Visual Similarity Judgment Task

For the similarity judgment portion of the experiment, 40 participant oRSMs and 1 group oRSM were constructed in the identical manner to Experiment 1. Additionally, 2 outlier participants were identified and removed following the same procedure described in Experiment 1 increasing the mean similarity to sample value from 0.48 to 0.54.

The group oRSM was then split twice; first by run and then by pseudoletter orientation—whether the judgments were for “upright” or “rotated” pseudoletters—forming 4 oRSMs. As figure 20 shows, the oRSMs from run 1 were combined and correlated with the combined oRSMs from run 2 so that judgments of the “upright” pseudoletters in run 1 were correlated with judgments of the “upright” pseudoletters in run 2, and likewise for the “rotated” pseudoletters. This correlation measured the reliability of the judgments. In the second correlation, the “upright” pseudoletters in run 1 were correlated with the matched “rotated” pseudoletters in run 2 and vice versa. The difference between the former reliability correlation and the latter orientation-switch correlation was interpreted as the size of the orientation effect. Significance of the difference was assessed by forming a distribution of 10,000 r difference values by randomly permuting the “upright” and “rotated” labels in run 2 and recomputing both the reliability r and the switch r values using the permuted labels, and then taking the difference of these correlation values. The p value was computed by obtaining the percentile of the real r difference within the random distribution and subtracting that percentile decimal from 1. A p value less the 0.05 was considered significant.

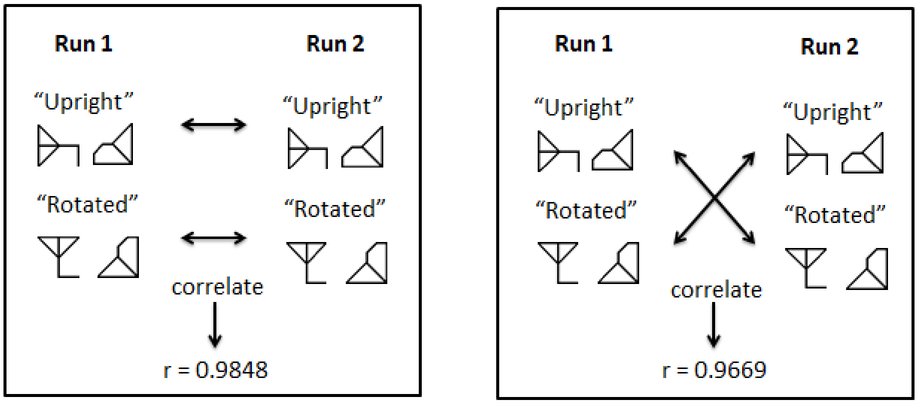

Figure 20. The logic and results from experiment 3. The left most figure depicts the reliability correlation where the similarity judgments from run 1 were correlated with the similarity judgments of the same letter pairs in run 2. The switch correlation (right) involved correlating the similarity judgments from run 1 with the matched pairs at a different orientation in run 2.

As Figure 20 shows, the reliability correlation, where "upright" pseudoletter judgment values from run 1 were correlated with the "upright" values from run 2 and likewise for the "rotated" pseudoletters, was $r = 0.9848$. The switch correlation, where the "upright" judgments from run 1 were correlated with the "rotated" judgments from run 2 and vice versa the "rotated" judgments from run 1, was $r = 0.9669$. The correlation difference value was 0.0179 which was significant ($p < 0.05$).

3.4.3 Experiment 3 - Discussion

In experiment 3 we tested an alternative explanation to the finding that the allograph pRSM was more correlated with the Upright oRSM than with the Rotated oRSM. The alternative explanation posited that the larger correlation between the Allograph pRSM and the Upright oRSM occurred by virtue of the fact that the letter stimuli were upright when generating both RSMs unlike the Rotated oRSM. We set out to quantify the effect of orientation on visual similarity judgments and found that it led to a significant difference of $r_{diff} = 0.0179$. While this difference was significant, compared to the size of correlation difference for the Allograph pRSM observed in experiment 1, ($r_{diff} = 0.29$), this minor rotation effect would not come close to explaining the difference by itself. This experiment, along with the results from the Recognizer vs. Nonrecognizer analyses presents a strong case that the upright and rotated r differences were due to the influence of stored letter representations, particularly allographs, and not an artifact of using rotated stimuli as the visual control.

3.5 General discussion

3.5.1 Stored allographs

The most consistent result across multiple experiments and analyses was that, across multiple empirical measures of visual similarity, the behavioral measures of visual similarity of an atypical gridfont were biased towards the visual similarity of a more typical font. This effect, I propose, is best explained by referring to models of letter processing that posit font-invariant stored allograph representations. Specifically, this account proposes that when two letters a represented in an atypical gridfont, the stored allographs are accessed and—whether it be via feedback to lower-level stimulus shape representations (Lupyan et al., 2010) or via downstream response competition (Chen & Proctor, 2012)—the allograph representations biased the similarity judgments to be closer to the similarity of the stored allograph representations.

pRSM	Similarity Judgments	Same-Diff Decisions—RT	Same-Diff Decisions—Errors	Recognizors vs. Nonrecognizors
Pixel-Overlap				
Typical Font Similarity (Allograph)	XX	XX	XX	X
Letter Identity (ALI)	X	XX	XX	
Letter-Case Identity (Case marker)	X			X
Consonant-Vowel Identity (CV marker)				
Letter-Digit Identity (Character Category)				
Motoric Feature Overlap (Motoric production code)	X	XX	XX	X
Phonetic Feature Overlap (Letter Name)				
Letter Name Confusability (Letter Name)				

Figure 21. A summary of the results for each pRSM tested and for each analysis employed, from the set of experiments presented in this chapter. **X** indicates that the difference in r values (upright – rotated or Recognizors – Nonrecognizors) were significant for that pRSM. **XX** indicates that the regression beta value for that pRSM was significant in a regression analysis. The Recognizors vs. Nonrecognizors analysis did not include a regression so **XX** is impossible.

3.5.2 Motoric production codes

Along with allograph representations, a pRSM derived from a set of motoric production stroke features consistently influenced the RTs and errors in the physical same-different decision task presented in Experiment 2. Specifically, stimulus pairs that had highly overlapping motoric production features were slower to respond different and more error prone than stimulus pairs that had a smaller degree of motoric feature overlap. This effect held even after accounting for visual similarity in a regression analysis. These results suggest that motor production codes were accessed regardless of whether they will be used or not and this access influences the similarity measures.

3.5.3 Abstract letter identities

In these experiments, we add to previous evidence of ALIs by demonstrating that letter identity appears to influence multiple behavioral measures of visual similarity. Specifically, when letters share the same identity, similarity measures were also increased relative to a visually matched control. While this has previously been demonstrated using visual same-different letter decisions (Carrasco et al., 1988; Chen & Proctor, 2012; Lupyan et al., 2010; Wiley et al., submitted), this is the first experiment that has also examined explicit visual similarity judgments. Furthermore, while other experiments have controlled for pairwise visual similarity (Lupyan et al., 2010; Chen & Procter, 2012), this is one of the first to do it with a large set of alphanumeric stimuli (see also Wiley et al., submitted). Finally, this is one of very few studies to also attempt to account for many types of letter representations within the same experiment and with the same participants (see also Rothlein & Rapp, 2014; Wiley et al., submitted).

It is worth noting that the regression analysis in the similarity judgment task did not reveal a significant effect of ALIs. This suggests that the significant ALI result from the correlation analysis may be confounded by the other pRSMs—namely the Stimulus Shape and the Allograph pRSMs. While this finding complicates the relationship between ALI representations and their influence on similarity judgments, the larger question regarding the existence of ALI representations should not be called into question. Even if ALIs do not influence similarity judgments, we provided evidence that they influence same-different decision RTs and accuracies. The same-different task results in conjunction with the wealth of converging evidence from other experiments suggests that the lack of ALI influence on similarity judgments is, at most, task specific.

3.5.4 Identity independent case markers

While less consistent than the aforementioned letter representations, the result from the visual similarity judgment experiment suggests that identity independent case-markers may additionally contribute to visual similarity judgments. It should be noted that overall size of the uppercase letters and lowercase letters were matched in the gridfont so any case effects would be based on the stored letter representations, rather than stimulus size differences. An alternative interpretation for this effect was that it is nonetheless a relative size effect and that the stored allograph representations contain relative size information. Specifically, it could be that even though the presented gridfont characters were matched in size across case, the size information was reintroduced at the level of allograph representations and that this size information was contributing to visual similarity judgments. One would need to compare upper and lower case letters that were typically matched in size in order to rule out this possibility (e.g., **t** and **T**). However, a more parsimonious account is that abstract case markers were automatically activated and that these case markers influenced visual similarity judgments.

3.5.5 Other letter representations

While this research revealed a number of letter representations that influenced measures of visual similarity, a number of tested possible representations failed to produce any influence. Specifically, whether the character was a consonant or vowel, or letter or digit did not appear to influence visual similarity responses. Additionally, two measures of letter name similarity that were used to assess the influence of phonological letter name on visual similarity judgments failed to reveal any influence. There is some evidence that letter names are activated when letters are visually presented, even in contexts where the letter names are not required for the task at hand (Rothlein & Rapp,

2014) but perhaps these letter representations were activated too late to influence response times and similarity judgments.

An important consequence of the failure to find influence of letter name representations using this methodology is that they cannot be used to explain the influences of other proposed letter representations. Specifically, because letter name representations are also case-invariant letter representations name codes have been used to explain letter identity effects (Miller & Vaknin, 2012; Posner, Boies, Eichelman, & Taylor, 1969). In other words, both ALI representations and letter name representations predict interference for cross-case identity-matched letter pairs (e.g., **b** and **B**) since the both share the same name and the same identity. The finding that letter names do not influence similarity judgments or RTs and errors, argues against this alternative explanation for the ALI effects.

3.6 Conclusions

The research in this chapter has provided strong evidence in favor of models of letter processing that include allograph and abstract letter identity representations. Furthermore, motoric production features and letter case influence visual similarity judgments as well. The neural correlates of these various representational types, with a particular focus on allograph representations, will be explored in the following chapter.

Chapter 4 - Letter representations along the ventral visual stream: Form and identity

Frequently viewed visual stimuli, like faces and scenes, are widely believed to have category-selective neural circuits within the ventral visual stream (see Kanwisher, McDermott, & Chun, 1997 for faces; Epstein & Kanwisher, 1998 for scenes; Downing, Jiang, Shuman, & Kanwisher, 2001 for body parts; for alternative accounts see Behrmann & Plaut, 2013; Gauthier, Skudlarski, Gore, & Anderson, 2000; Gauthier, Tarr, et al., 2000). Embedded within this cortical milieu are neural substrates that are preferentially responsive to words and letterstrings (Cohen et al., 2000; Dehaene & Cohen, 2011) as well as isolated letters (Flowers et al., 2004; James, James, Jobard, Wong, & Gauthier, 2005; Pernet, Celsis, & Démonet, 2005; Turkeltaub, Flowers, Lyon, & Eden, 2008). While there is currently some debate about the evolutionary origins of the neural selectivity of these face and scene regions (e.g., Behrmann & Plaut, 2013; Gauthier, Tarr, Anderson, Skudlarski, & Gore, 1999), there is little doubt that letters and words, being a recent cultural invention and learned relatively late in development, must co-opt neural circuitry that was not specifically designated by evolution for letter and word processing. Despite its learned origins, the fact that words and letters are preferentially processed in the same neural regions so consistently across the literate population suggests these regions have intrinsic properties that make them particularly suited for letter and word recognition—though what these properties are remains an open question. Determining how the representational content of letters is transformed as the orthographic information is processed along the ventral stream will both serve to evaluate current models of visual letter recognition and potentially provide a clue to the nature of the organization of the ventral stream that leads to these apparent specializations.

One of the major challenges of single letter identification is dealing with the large degree of shape variability in letters of different fonts. These are challenges faced by both letter and object recognition more generally. Accordingly, neurally grounded models of letter recognition are largely inspired by models of visual object processing (Grainger et al., 2008; Riesenhuber & Poggio, 1999). According to these models of object recognition, object shapes are computed via the conjunction of increasingly complex visual features that are stored in progressively anterior and lateral retinotopic regions within the ventral stream (Connor, Brincat, & Pasupathy, 2007)—from lines and bars in V1, to T-junctions and crosses in V2v and V3v to entire shapes in V4. Furthermore, as the features get more complex, they become increasingly invariant to spatial properties like retinotopic position, size and orientation (Connor et al., 2007; Dicarlo, Zoccolan, & Rust, 2012). Based largely on this literature, proposals like the Local Combination Detector or LCD model (Dehaene et al., 2005) specify the representational content of brain areas responsible for processing letters in a posterior to anterior gradient along the ventral stream. The most posterior regions store simple visual features and shape complexity and invariance to position and size increase the more anteriorly the representation is encoded (see also Purcell, Shea, & Rapp, 2014) culminating in abstract graphemic representations of multiple letters and short words. These representations correspond, more or less, to those posited in the cognitive model of letter processing presented in Figure 2. Specifically, bilateral V1 is thought to represent low-level lines and bars, veridically representing the retinotopic image and bilateral V2 is thought to represent local contours.

These low-level domain-general visual features (involved in visual processing of all objects, not only letters) go on to activate letter shapes in V4. What is unclear, in the LCD model at least, is if these shape representations correspond to font-specific computed stimulus shape representations or stored, font invariant, allograph representations.

Outside of the domain of letter processing, a number of studies have investigated how the representation of object shape changes across different regions along the ventro-temporal cortex (Kriegeskorte et al., 2008; Op de Beeck, Torfs, & Wagemans, 2008). Op de Beeck et al., (2008) found that the representation of visually presented novel shapes was sensitive to the shape's envelope in retinotopic cortex (V1-V4) while regions lateral (LO) and ventral and anterior (pF) were more sensitive to the subjective visually similarity of the shapes. Similarly, Kriegeskorte et al., (2008) presented a large set of different visual objects, body parts, and faces and found that early visual cortex was highly sensitive to the pixel-wise similarity of the images whereas LO and pF were more sensitive to semantic information like object animacy. Following a similar logic, the experiment presented in this chapter investigated the letter representations encoded in early, retinotopic visual cortex and compared these representations to those encoded in lateral/anterior ventral visual regions.

Whereas the intent of the experiments in the previous chapter was to provide evidence for the existence of stored letter representations in visual letter processing (e.g., allographs, ALIs, letter names C/V status etc.), the goal of this experiment was to localize their neural substrates. To do this, Representational Similarity Analysis (RSA) (Kriegeskorte et al., 2008) was used to interpret the multi-voxel neural signal evoked by single letter stimuli. As discussed in Chapter 2, RSA involves testing the pairwise similarity structure of a multi-voxel pattern in response to a set of stimuli. In Experiment 4 reported in this Chapter, we presented a set of letter and digit stimuli and obtained the multi-voxel similarity structure for the retinotopic regions: V1, V2v, V3v, and V4 as well as other cortical regions that were active in response to letter and digit stimuli. Crucially, we wanted to identify the transition from font-specific stimulus shape representations to font-invariant allograph representations. In order to reduce the correlation in predicted similarity structure between these two types of letter representations, the novel gridfont from the Experiments 1 and 2 in Chapter 3 was used. The logic of the experiment reported in this chapter is as follows: If a neural region encodes allograph representations, we would predict that the neural response patterns to viewing the **upright gridfont** would be correlated with the visual similarity of the **unseen** typical font (the Allograph pRSM). This is because while the neural substrates encoding the font-specific computed stimulus-shape representation would capture the specific visual patterns of the upright gridfont (estimated without the influence of stored letter representations by using the **rotated gridfont** similarity judgments) the neural substrates encoding allographs would abstract away from those specific patterns and be more strongly correlated with visual similarity judgments from a more visually typical font. In the experiment that follows, the observed representational similarity matrices (oRSMs) derived from retinotopic and other ventral visual areas obtained by viewing single upright gridfont letters and digits were compared against predicted similarity matrices (pRSMs) for stimulus shape and allograph letter representations (amongst others). To preview the results: we found that retinotopic cortex, particularly in the right hemisphere, encoded font-specific stimulus shape representations while regions anterior and lateral to the retinotopic cortex in the left middle occipital gyrus and the left fusiform gyrus encoded font-invariant allograph representations.

4.1 Methods

Participants

12 participants (6 women) were recruited from the Johns Hopkins University student population. Participants were right handed, had no history reading or learning disabilities, and were reporting only being able to read letters from the Roman alphabet. Each participant provided written consent and was compensated in accordance with the requirements of The Johns Hopkins Institutional Review Board. One participant was excluded from all analyses due to excessive head motion.

Procedures

Participants performed two experimental tasks within a 2 hour scan session. The first task was a symbol detection task (Rothlein & Rapp, 2014) and the second was a passive viewing Retinotopic Localizer. Both tasks were presented and responses were recorded using E-Prime 2.0 Software (Psychology Software Tools, Pittsburgh, PA).

Symbol detection task

In the symbol detection task, participants viewed 37 alphanumeric characters presented in isolation. Importantly, the alphanumeric characters were presented in the novel and atypical gridfont from Experiment 1 (see Figure 13). Of the 37 characters, 28 were font and case variants of 6 letter identities, 5 were digits and 4 were non-letter, nondigit alphanumeric symbols. Participants were asked to press two buttons—one in each hand—whenever they observed a non-letter symbol. The experimental procedure consisted of 3 trial types: (1) Letter/digit trials, which were comprised of a 200ms fixation dot, 300ms letter stimulus, and 3500ms of a blank white screen; (2) Symbol trials, which was the same as letter trials except a non-letter symbol was shown instead of a letter stimulus and participants were expected to respond; (3) Blank trials, which consisted of a 200ms fixation and 3700ms of a blank white screen. Each trial lasted 4000ms. The trials were grouped into blocks that contained 33 letter trials (one for each letter or digit stimulus), 4 symbol (response) trials, and 10 blank trials (~20% of trials). Runs contained 2 blocks and the entire experiment consisted of 6 runs resulting in each letter and digit stimulus being shown 12 times (total run time approx. 40min). Trial order was randomized within each block.

Retinotopic localizer: meridian mapping

In the retinotopic localizer scan, participants passively viewed a shape composed of two wedges aligned so their apices met at a fixation dot in the center of the display. The shape was filled in with a checkerboard texture. The black and white squares in the checkerboard texture alternated at a frequency of 4 Hz, creating a flickering effect. There were 3 conditions presented in a block design: (1) a vertical block where the two wedges were oriented along the vertical axis; (2) a horizontal block where the two wedges were oriented along the horizontal axis and (3) a fixation block where only a fixation dot was shown. A run consisted of 21 blocks and each block was 12 seconds long making for a scan that was 4 minutes and 15 seconds. Of the 21 blocks, 11 were fixation blocks, 5 were vertical blocks and 5 were horizontal blocks. The presentation order alternated between vertical and horizontal blocks with fixation blocks separating them.

Imaging parameters

MRI data were acquired using a 3.0-T Phillips Intera Scanner. Whole-brain T2-weighted gradient-echo EPIs were acquired with a 32 channel SENSE (Invivio) parallel imaging head coil in ascending 3 x 3 mm slices with 1mm gap. TR = 2 s for the Symbol Detection Task and Retinotopic Localizer. Echo time = 30ms, flip angle = 65º, field of view = 240 x 240mm, matrix = 128 x 128mm. Structural images were acquired using an MR-Rage T1-weighted sequence yielding images with 1mm isotropic voxels (repetition time = 8.036ms, echo time = 3.8ms, flip angle = 8º.

4.1.1 fMRI data processing

Data from both the symbol detection task and the retinotopic localizer were preprocessed identically using Brain Voyager Q.X. software (Maastricht, Netherlands). Functional images were corrected for slice time (ascending) and motion (trilinear 3D motion correction with sinc interpolation. Additionally, a temporal high-pass filter removed components occurring fewer than three cycles per run (high-pass GLM-Fourier 3 Cosines) and linear trend removal for correcting scanner drift. Images were resampled to $3mm^3$ voxels.

The data from the symbol detection task was analyzed in an MVPA-RSA design that was VOI based. This required the following: (1) generating the participant and stimulus-specific activation patterns used to generate oRSMs within the VOIs, (2) identifying the relevant VOIs and (3) generating the oRSMs and pRSMs for the analysis.

(1) Activation patterns for the VOI analysis

For each participant, a GLM analysis was carried out based on data from the event-related design using 37 experimental regressors: one for each letter or digit stimulus (33) and one for each symbol (4). Additionally, 1 linear trend regressor, 6 head-motion parameter time-course regressors, 6 fourier-based non-linear trend regressors (up to three cycles per run for sine and cosine) and 1 confound regressor representing run number were included. The experimental regressors were created by convolving a boxcar function corresponding to the 200ms duration of appearance of each experimental condition with a Boynton hemodynamic response function. The duration of the boxcar function for the 4 symbol regressors lasted the entire 4000ms trial duration to ensure inclusion of the expected motor response. For the experimental trials, the 200ms corresponding to the fixation appearance and the 3500ms of blank screen following the stimulus disappearance were not modelled along with the entire 4000ms duration of blank trials. These time periods served as the implicit baseline. Each regressor (both experimental and confound) was z-normalized and then fit against the fMRI time-course signal expressed as percent signal change. The resulting beta-maps were converted to t-maps—one map for each of the 33 experimental conditions (letter or digit stimuli). These participant-specific t-maps (in native ACPC space) were used as the activation values for the MVPA-RSA. MVPA-RSA was carried out using in house code run in MATLAB (Math Works) and NeuroElf (http://NeuroElf.net/) was used to integrate Brain Voyager and MATLAB.

(2) Identification of functionally-localized Alphanumeric VOIs (see Figure 22)

VOIs were generated from both the symbol detection and the retinotopic mapping experiments. For the symbol detection experiment, a group univariate activation map was created in order to identify Alphanumeric VOIs that corresponded to comparable functional neural regions across participants. fMRI data from the symbol detection task was smoothed 6mm FWHM and normalized to Talairach space. A GLM was then constructed in a similar manner as for the MVPA-RSA GLM with the only difference being that the GLM was a group GLM containing data from each participant. Participants were treated as random variables in a RFX GLM. The results of a contrast consisting of all letters and digits > baseline was thresholded at an uncorrected $p<0.05$ with a cluster-size threshold of 30 voxels. The surviving clusters were then expanded by 5mm in each direction and converted back to native ACPC space for each participant.

Data from the Retinotopic Localizer were analyzed in native ACPC space in order to localize V1, V2v, V3v, and V4 for each participant. A GLM analysis was carried out using 2 experimental regressors: one for vertical and one for horizontal flashing checkerboards. Additionally, 1 linear trend regressor, 6 head-motion parameter time-course regressors, 6 Fourier-based non-linear trend regressors (up to three cycles per run for sine and cosine) and 1 confound regressor representing run number were included. The experimental regressors were created by convolving a boxcar function corresponding to duration of appearance of each experimental condition with a 2-gamma hemodynamic response function. Periods where only the fixation dot was present were not modeled and served as the implicit baseline. Each regressor (both experimental and confound) was z-normalized and then fit against the fMRI time-course signal expressed as percent signal change. The contrast of Vertical Checkerboards > Horizontal Checkerboards was run for each participant creating a Meridian Map. The participant's anatomical MP-RAGE scan was then inflated using Brain Voyager's built in software and the Meridian Map was overlaid on the inflated brain. Retinotopic VOIs were created manually by drawing in regions that correspond to retinotopic functional subdivisions (Brain Voyager QX, Maastricht, Netherlands). These drawn maps were created for each participant except one who did not have well defined retinotopic regions. This participant's data were not used in the RSA analysis of the Retinotopic VOIs but was used in the Alphanumeric VOIs. The Retinotopic VOIs were converted to uninflated ACPC space for further analyses. Specifically, 5 VOIs were created where 4 corresponded to bilateral V1, V2v, V3v and V4 and 1corresponded to **Bilateral Retinotopic Cortex** that was defined for each individual by combining the voxels from each from the retinotopically defined areas (V1-V4).

(3) Generation of oRSMs and pRSMs.

An oRSM was constructed for each VOI in the following manner. Within a VOI, a vector of t-values was created for each letter or digit by taking the t-values associated with each letter or digit stimuli and vectorizing them. In other words, for a given stimulus type (e.g. **H)**, a vector was created were each value in the vector corresponded to the activation t-value at a given voxel in response to **H.** The set of t-values in the vector correspond to the set of voxels within a VOI. For each VOI, these vectors were created for each stimulus type. An oRSM was constructed by computing a pairwise (Pearson) correlation for each possible vector pairing and placing the r value in the corresponding cell within a matrix. The matrix contained a row and column dedicated to each stimulus and each cell corresponded to the correlation of the t-values from the set of voxels for the row stimulus and the t-values from the same voxels for the column stimulus. Each matrix was triangular (due to symmetry across the diagonal) and the cells in the diagonal were excluded. To prevent including duplicated values in the analyses (which would artificially inflate the degrees of freedom), only the values in the upper triangle were analyzed.

A group oRSM was constructed for each VOI in the following manner. First, the values from each participant's oRSM were z normalized to have a mean of 0 and a standard deviation of 1. The group oRSM was composed of the mean z value across participants within each cell. The group oRSMs was then z-normalized to have a mean of 0 and a standard deviation of 1. This group oRSM served as the estimate of the representational similarity structure within any give VOI.

Ten pRSMs were constructed to test if the similarity structure for a given oRSM was consistent with a predicted (idealized) RSM for a particular type of representation. Three pRSMs were particularly important for this study. They were the **Stimulus Shape pRSM** which predicted the similarity structure at the level the font-specific stimulus shape representation. The similarity values consisted of pairwise visual similarity judgments for the gridfont letters rotated so they were difficult to recognize while maintaining the same pixelwise image similarity structure (see chapter 3 for more detail). The **Allograph pRSM** consisted of pairwise visual similarity judgments for letters presented in a typical Calibri-based font. These similarity judgments served as an estimate of the similarity structure at the level of Allograph representations. It is important to note that the typical font was never shown to participants in the scanner but instead they only saw a visually distinct atypical gridfont. Finally, an **ALI pRSM** was constructed by assigning a value of 1 to any letter pairs that share the same identity and a value of 0 to any character pairs that do not. In addition to these three pRSMs, other pRSMs estimated motoric feature representations, letter-name representations (estimated via phonetic feature overlap and letter name confusability matrix, case marker representations, consonant-vowel marker representations, and letter or digit identity representations. All of the pRSMs only included predictions for the letter stimuli (excluding digits) except for the letter or digit identity pRSM which necessarily included letters and digits.

4.1.2 Sensitivity, selectivity, and feature comparison analyses

The RSA –VOI-based analyses consisted of three phases: sensitivity, selectivity, and feature comparison analyses.

Sensitivity analysis

The goal of the sensitivity analysis was to determine, for a given VOI, whether the observed similarity structure was consisted with one or more of the similarity structures predicted for various types of representations. For each VOI, the sensitivity consisted of a Pearson correlation between the oRSM derived from that VOI and each of the 10 pRSMs.

Significance for each of the aforementioned correlations was established using a permutation Monte-Carlo analysis. This analysis was carried out by creating 10000 Pseudo-oRSMs in the following manner: the rows and columns of the original oRSM were scrambled forming Pseudo-oRSMs. Importantly, the rows and the columns were scrambled identically (e.g., if the **a** column swaps places with the **d** column, then the **a** row would swap places with the **d** row). For each pRSM a distribution of 10000 random correlations were computed by taking the correlation of the Pseudo-oRSM and a pRSM. If the actual correlation between the pRSM and oRSM fell within the top 5% of correlation values, the correlation was labeled significant. Reported one-tailed p values were computed by subtracting the percentile rank of the r value from 1.

Selectivity analysis

The goal of the selectivity analysis was to determine the relative contribution of each pRSM in accounting for the similarity structure (oRSM) from a given VOI. For each VOI, the group oRSM was evaluated in a regression analysis that contained 3 regressors corresponding to the **Stimulus Shape**, **Allograph**, and **Letter Identity pRSMs** as well as a constant. The other pRSMs were excluded because the results of the Sensitivity Analysis did not find any of them to be significant in any of the VOIs. In order to compute standardized regression coefficients, each of the group oRSMs and the pRSMs was z normalized to a mean of 0 and a standard deviation of 1. The regression analysis was carried out using MATLAB's REGSTAT function. A t-value was computed for each β coefficient and was evaluated for statistical significance assuming a two-tailed p value.

Feature comparison analysis

Following on the findings that show differences in the content of visual representations from early retinotopic cortex to pF and LO along the ventral stream (Kriegeskorte et al., 2008; Op de Beeck et al., 2008), we examined how letter representations changed from early, retinotopic cortex to Alphanumeric VOIs located in regions similar to LO and pF. In order to test for a difference between stimulus shape and allograph representations across two VOIs, two-way ANOVA analyses were performed with representation (stimulus shape or allograph) and VOI as factors. To do this a regression analysis was run for each participant predicting oRSM from the bilateral Retinotopic VOI and each of the left hemisphere Alphanumeric VOIs. Each regression model included the Allograph, Stimulus Shape and ALI pRSMs as regressors. The dependent variable consisted of participant-specific β coefficients for the Allograph pRSM regressor and the Stimulus Shape pRSM regressor in a model that also included an ALI pRSM regressor and a constant. Participant specific oRSMs were obtained for each VOI and the participant specific β coefficients were obtained by using the aforementioned regressors to predict each participant specific oRSM in multiple regression models (one for each participant for each VOI). The resulting set of β coefficients for the Stimulus Shape and the Allograph pRSMs where entered into the two-way ANOVA analysis. The interaction term indicated a difference in the representational content across the two VOIs.

4.2 Results

VOIs

The Group RFX GLM identifying Alphanumeric VOIs yielded three clusters (for coordinates of the peak voxels as well as statistics and cluster sizes, see table 1): a cluster in the left middle occipital gyrus, a cluster in the left fusiform gyrus bordering the occipito-temporal sulcus, and a cluster in the right fusiform gyrus encompassing regions in the right middle occipital gyrus as well. To generate the Alphanumeric VOIs, each of these clusters was inflated 5mm in all directions and the coordinates of each of the voxels within the cluster were transformed into each participant's ACPC space. Table 2 below provides a summary of the both the Alphanumeric VOIs and the Retinotopic VOIs.

Table 1. Clusters used for alphanumeric VOIs. Peak voxel coordinates, statistics and cluster sizes from the group activation map comparing letter and digit stimuli greater than implicit baseline. The results reported below are in Talairach space and are reported prior to the 5mm expansion for the participant VOIs.

Anatomical Label	Peak X	Peak Y	Peak Z	T(10)	p	# of voxels
Left Middle Occipital Gyrus	-42	-73	-7	7.14	<0.00005	173
Left Mid. Fusiform Gyrus	-41	-63	-19	4.47	<0.005	20
Right Fusiform Gyrus	31	-79	-16	8.31	<0.00001	130

Table 2. Properties of the VOIs used to generate the oRSMs. The Alphanumeric VOIs were derived from the clusters reported in Table 1 by inflating each of these clusters by 5mm in all directions and converting the cluster coordinates to each participants ACPC space. For each VOI, the average number of functional (3x3x3mm) voxels across participants along with the range. Additionally the average center of mass for each VOI is reported.

		# of voxels: average	# of voxels: min	# of voxels: max	Center of mass (TAL: X, Y, Z)
Alphanumeric VOIs	Left Middle Occipital Gyrus	717	445	882	(-35, -81, -10)
	Left Mid. Fusiform	326	218	376	(-44, -64, -18)
	Right Fusiform	1241	1062	1313	(36, -65, -16)
Retinotopic VOIs	Bilateral Retinotopic Cortex	1516	1245	1721	(-2, -84, -12)
	V1	596	470	689	(-2, -90, -8)
	V2v	326	266	393	(-1, -86, -16)
	V3v	294	251	341	(-3, -82,-16)
	V4	224	159	266	(-2, -78, -18)

Sensitivity analysis

For each VOI, each of the 10 pRSMs was correlated (Pearson) with the VOI's oRSMs (one from each VOI). The magnitude of the correlation was a measure of how consistent the similarity structure of a VOI's neural responses was with the similarity structure of the type of representation a given pRSM is estimating. Complete results from the sensitivity analysis can be seen on Table 3. The only pRSMs with significant results were those estimating the representational similarity of Stimulus Shape, Allograph, and Letter Identity representations. None of the other 7 pRSMs had any significant results so they will not be discussed further.

Table 3. Results from the sensitivity analysis. Reported values are correlation r values. * indicates $p<0.05$ and ** indicates $p<0.001$.

		Stimulus Shape	**Allograph**	**Letter Identity**
Alphanumeric VOIs	Left Middle Occipital Gyrus	0.073	0.194*	0.07
	Left Mid. Fusiform	0.079	0.205**	0.095*
	Right Fusiform	0.049	0.129*	0.081*
Retinotopic VOIs	Bilateral Retinotopic Cortex	0.183*	0.169*	0.099*
	V1	0.147*	0.19*	0.111*
	V2v	0.144*	0.122*	0.058
	V3v	0.221**	0.087	0.061
	V4	0.108	0.139*	0.087*

Stimulus Shape pRSM

As can be seen on Table 3, all of the Retinotopic VOIs except V4 were significantly sensitive to the Stimulus Shape pRSM while none of the Alphanumeric

VOIs were significantly sensitive to the Stimulus Shape pRSM. The largest correlation with the Stimulus Shape pRSM was localized to V3v ($r = 0.221$, $p<0.001$). It is worth noting that the bilateral retinotopic cortex as a whole was sensitive to the Stimulus Shape pRSM ($r = 0.183$, $p<0.05$).

Allograph pRSM

Unlike the Stimulus Shape pRSM, all of the Alphanumeric VOIs were sensitive to the Allograph pRSM. Specifically the left middle occipital gyrus ($r = 0.194$, $p<0.05$), the left mid. fusiform gyrus ($r = 0.205$, $p<0.001$) and the right fusiform gyrus ($r = 0.129$, $p<0.05$). Additionally, most of the Retinotopic VOIs were sensitive to the Allograph pRSM as well. This included the bilateral retinotopic cortex as a whole ($r = 0.169$, $p<0.05$). The only non-significant VOI was V3v.

Abstract Letter Identity pRSM

Bilateral retinotopic cortex as a whole was sensitive to the Letter Identity pRSM ($r = 0.099$, $p<0.05$). Within the Retinotopic VOIs, both V1 and V4 were sensitive to Letter Identity ($r = 0.111$, $p<0.05$; $r = 0.087$, $p<0.05$ respectively). For the Alphanumeric VOIs, both the left and right fusiform VOIs were sensitive to the Letter Identity pRSM ($r = 0.089$, $p<0.05$; $r = 0.081$, $p<0.05$ respectively) while the left middle occipital gyrus was not.

Table 4. Results from the regression analysis across multiple VOIs. β coefficients are standardized beta-weights. * indicates $p<0.05$ and ** indicates $p<0.001$.

		Regression model statistics			β coefficients		
		R^2 (Adj.)	F(287, 3)	p	Stimulus Shape	Allograph	Letter Identity
Alphanumeric VOIs	Left Middle Occipital Gyrus	0.037	4.74	0.003*	-0.019	0.138**	-0.068
	Left Mid. Fusiform	0.04	5.01	0.002*	-0.011	0.128*	-0.038
	Right Fusiform	0.004	1.39	0.247	0.003	0.044	0.002
Retinotopic VOIs	Bilateral Retinotopic Cortex	0.035	4.54	0.004*	0.075*	0.046	0.009
	V1	0.033	4.31	0.005*	0.061	0.063	0.028
	V2v	0.019	2.83	0.039*	0.067	0.078	-0.041
	V3v	0.031	4.11	0.007*	0.112*	0	-0.005
	V4	0.011	2.07	0.104	0.03	0.053	0.003

Selectivity analysis

Selectivity was measured by running multiple linear regression analyses, one for each VOI, in order to determine the unique contribution of the Stimulus Shape, Allograph and ALI pRSM regressors at each VOI. As Table 4 shows, the regression model was not significant for 2 of the 8 VOIs—namely, V4 and the right fusiform VOI.

Two VOIs had significant β coefficients for the Stimulus Shape pRSM. These were specifically the bilateral retinotopic cortex VOI ($\beta = 0.075$, $p<0.05$) and V3v ($\beta = 0.112$, $p<0.05$). Likewise, only two VOIs had significant β coefficients for the Allograph pRSM. Notably, both Left Alphanumeric VOIs—the left middle occipital gyrus and the left mid. fusiform gyrus—had significant Allograph β coefficients ($\beta = 0.138$, $p<0.001$; $\beta = 0.128$, $p<0.05$ respectively).

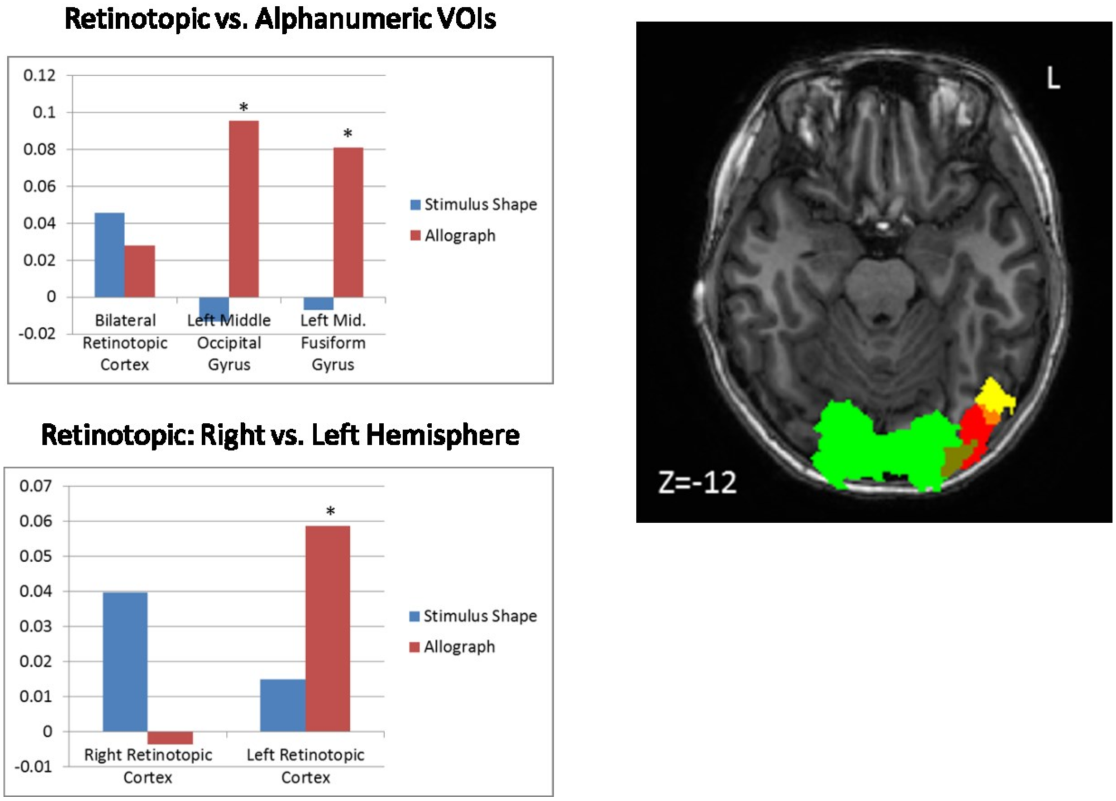

Figure 22. Bar graphs depicting the mean β coefficients across participants for a regression model that included Stimulus Shape, Allograph and Letter Identity pRSMs as regressors. Top left shows the mean β coefficients from the regression analysis at 3 VOIs. The interaction between the Stimulus Shape and Allograph pRSM and VOI for bilateral retinotopic cortex and the left MOG as well as left mid. fus. were significant. Bottom Left is a bar graph depicting the results from the regression analysis comparing the left and right retinotopic cortex. The interaction is marginal at $p<0.1$. * indicates $p<0.05$. Top Right depicts the retinotopic VOI (green), the left MOG (red) and the left fusiform VOI (yellow).

Feature comparison analysis

Three two-way ANOVAs were run to test the differences in β coefficients for the Stimulus Shape pRSM and the Allograph pRSM across two VOIs. Of particular interest was the interaction between VOI and pRSM. This interaction term was interpreted as a transition of neural encoding of one type of representation (e.g., font-specific stimulus shape) to another (e.g., font-invariant allograph). The first two ANOVAs compared the β coefficients from bilateral retinotopic cortex with those from (1) the left middle occipital gyrus and (2) the left mid. fusiform gyrus. A third ANOVA (3) compared the β coefficients from the left retinotopic cortex with those from the right retinotopic cortex.

The ANOVA analyses (1) and (2) compared the β coefficients for the Stimulus Shape and Allograph pRSMs across bilateral retinotopic cortex and (1) left MOG and (2) left fusiform. While there was no significant main effects for VOI ($f(41, 1) = 0.03$, $p = 0.857$; $f(41, 1) = 0$, $p = 0.996$ respectively) or pRSM ($f(41, 1) = 3.82$, $p = 0.058$; $f(41, 1) = 2.44$, $p = 0.126$ respectively), the interaction between VOI and pRSM was significant for both ($f(41, 1) = 7.37$, $p < 0.01$; $f(41, 1) = 5.57$, $p < 0.05$ respectively). ANOVA (3) comparing the same pRSMs across the left and right retinotopic cortex had no significant main effects (VOI: $f(41, 1) = 0.55$, $p = 0.464$; pRSM: $f(41, 1) = 0$, $p = 0.998$) or interaction ($f(41, 1) = 2.96$, $p = 0.094$) although this interaction could be considered marginally significant.

4.3 Discussion

The results from the experiments in Chapter 3 provided strong evidence that even when participants viewed letters and digits presented in a visually atypical gridfont, behavioral responses—such as pairwise visual similarity judgments or physical same-different RTs and errors—were strongly influenced by font-invariant allograph representations. A major goal of this experiment was to identify the neural substrates that encode font-invariant allograph representations as opposed to the computed, font-specific, stimulus shape representation. To this end, Representational Similarity Analysis was used to investigate the representational content of letter stimuli presented in an atypical gridfont across a set of Retinotopic VOIs as well as a set of Alphanumeric VOIs.

Of particular interest was the finding that the similarity structure of the neural responses to the presented atypical gridfont indicated the encoding of stimulus shape representations in retinotopic cortex and the encoding the stored (not-presented) font-invariant allograph shape representations in lateral and anterior ventral visual clusters—specifically in the left hemisphere.

4.3.1 Stimulus shape vs. allograph representations

The RSA sensitivity analysis revealed that, with a few exceptions, Retinotopic VOIs were sensitive to both Stimulus Shape and Allograph pRSMs. Alphanumeric VOIs, on the other hand, were only sensitive to allograph representations. A regression analysis revealed that the Stimulus Shape pRSM best explained the oRSM from the bilateral retinotopic cortex VOI while the Allograph pRSM best explained the oRSMs from Alphanumeric VOIs in the left middle occipital gyrus and the left mid. fusiform gyrus. Significant interactions from 2 two-way ANOVAs between the bilateral retinotopic cortex and each of the two left hemisphere Alphanumeric VOIs demonstrated a change between the representations of the atypical gridfont's stimulus shapes in retinotopic cortex to the representatiosn of font-invariant allographs in the left middle occiptal gyrus and left mid. fusiform gyrus. While previous research has already identified neural substrates that encode abstract letter identities (e.g., Rothlein & Rapp, 2014), no fMRI study has specifically sought out to uncover neural regions that encode allograph representations as being distinct from either stimulus letter shape representations or ALI representations. For example, researchers have used priming and MVPA to investigate font-invariance before (Gauthier, Tarr, et al., 2000; Qiao et al., 2010), but these researchers did not ensure that the priming or MVPA effects were not being driven by the fact that two fonts of lower case **a** also share the same ALI. Therefore, to my knowledge, this is the first study that localized neural substrates of allograph representations. It is worth noting that the position of the left MOG VOI (TAL: -35, -81, -10) that ostensibly encodes allographs is quite close to the Left LO which is a neural region thought to be important for representing object shapes more generally (Kim, Biederman, Lescroart, & Hayworth, 2009; Kourtzi & Connor, 2011) and reflects perceived similarity instead of the physical similarity of viewed objects (Drucker & Aguirre, 2009; Kourtzi & Kanwisher, 2001; Op de Beeck, Torfs, & Wagemans, 2008).

Another interesting finding was the tendency of the right hemisphere retinotopic VOIs to represent the font-specific stimulus shape and the left retinotopic VOIs to represent allographs. When collapsing across V1, V2v, V3v, and V4, an ANOVA analysis comparing the Stimulus Shape and Allograph pRSMs across right and left retinotopic VOIs revealed a marginally significant interaction term, suggesting a possible bias towards font-specific stimulus shape representations in the right retinotopic cortex and font-invariant allograph representations in left retinotopic cortex. This is consistent with theories that posit that visual processing in the right hemisphere is more exemplar-based with the goal of faithfully representing the visuospatial features of the stimulus being viewed while left hemisphere visual processing is more abstract and categorical with the goal of rapid identification (Marsolek, 1995; Marsolek, 1999).

4.3.2 Stored letter representations in V1 and V2

One unanticipated result was finding evidence for both stored allograph and letter identity representational content within V1. While unexpected, there are previous findings showing letter and word-specific brain activation in V1 and V2. In one study by

Szwed et al., (2011) visually degraded word stimuli were compared with gestalt matched pseudo-words, line drawings of objects, and scrambled versions of these line drawings. In left V1, the overall activity was greatest for the word stimuli. This was not the case in right V1. Furthermore in a later study (Szwed et al., 2014) this effect was replicated and compared with Chinese literates viewing the more complex Chinese characters. Szwed et al. (2014) found this character specific activation in left V1 for French, while Chinese emerged around V3a and V4. Importantly this effect was not found in V3v-V4 for the French reader.

Our results build upon Szwed et al. (2011 & 2014) by clarifying the nature of the activation in V1 and V2. Specifically, these regions appear to be representing both allographs and ALIs. One possible interpretation of these findings is that frequent exposure to letter and word stimuli caused the neural pathways to develop special letter specific features in early visual cortex. An alternative view is that these activation patterns are a consequence of feedback from higher level processing regions to early visual cortex. It should be noted that both Szwed et al. (2011) and the present study used letter stimuli that were somewhat atypical. This could necessitate stronger than normal feedback in order to maximize the accuracy with which the signal is interpreted. This interpretation helps deal with the fact that researchers who used typical font stimuli failed to find such an effect (e.g., Vinckier et al., 2007). If letter identity information is fed back to early visual areas, a paradox emerges: if regions receiving input from V1 expect visual or shape information, how could identity information benefit processing of the signal? While this research does not answer this question, it does offer clues by revealing the representational content of the low-level visual activations.

4.4 Conclusions

The experiment presented in this Chapter set out to map representations involved in letter processing from the font-specific stimulus shape of an atypical gridfont letter to that letter's font-invariant allograph representation. Using Representational Similarity Analysis to uncover the representational content of VOIs within retinotopic cortex and Alphanumeric VOIs in the left and right ventral occipital and temporal lobes, the results provided evidence that Retinotopic cortex, particularly in the right hemisphere, encoded computed stimulus shape representations of letters and the Alphanumeric VOIs and certain left hemisphere retinotopic regions encoded stored font-invariant allograph representation. This is the first fMRI study to specifically investigate the transition from font-specific to font-invariant spatial representations of letters and furthermore, it is one of the first studies that used the similarity structure of typical exemplars to explain the neural signal evoked by atypical exemplars in order to reach conclusions about stored shape representations. The methods and logic used in this experiment could be applied to many different categories of objects.

While the experiment in this chapter primarily focused on representations of the shape of the letter, the sensitivity analyses revealed neural regions sensitive to case-invariant Letter Identity representations in retinotopic cortex and along the left and right ventral stream. The experiment in the next chapter explores the neural representation Letter Identity even further by determining how the sensory modality of stimulus presentation (visual or auditory) relates to neural representation.

Chapter 5 - Are abstract letter identity representations amodal as well?

Information about the world is constantly arriving via our various sensory organs. The brain must process and integrate this information across the multiple sensory modalities in order properly interact with the local environment. Investigating and theorizing how the brain integrates this information requires us to make fundamental assumptions about how the brain works. On one view, sensory modalities and motor control circuits are the organizing structures of the brain (Stein & Meredith, 1993). Brain regions can be easily divided into being visual, auditory, olfactory, motor, somatosensory and so on. Processing in these regions is modality specific and multisensory integration occurs at multi-modal association areas. These association areas directly map representations from one modality to another. For example, in the task of orally naming a viewed letter, the visual letter's form is processed and recognized in visual cortex and then that visual representation is linked to the phonological/articulatory representations in auditory/motor cortex used for orally naming the viewed letter. An alternative view posits that the brain is organized by the representational content of objects and the types of processing they require (Pascual-Leone & Hamilton, 2001). For example, the ventral visual stream might not be specific to processing visual information but the neural circuitry might be innately tuned to represent shape information, regardless of whether the stimulus comes from visual, tactile, or even auditory modalities (e.g., Pascual-Leone & Hamilton, 2001; Striem-Amit, Cohen, Dehaene, & Amedi, 2012). In this view, letters are processed in the ventral stream because rapid shape processing for identification is essential to reading and the neural circuits in the ventral stream are designed to represent shape information—even for braille readers who decipher shape through touch (Büchel, Price, & Friston, 1998). The experiment in this study investigated how the representations involved in processing visually and aurally presented letters (letter names) interacted by identifying neural substrates that were activated by visually or aurally presented letter names. RSA-MVPA was then used to investigate the representational content of these letter-responsive regions. Of particular interest was investigating amodal identity representations.

Saying that a particular mental representation is modality specific, cross-modal or amodal requires further clarification. Because the term modality can refer to subtly different phenomenon, I have highlighted three common usages: input modality, content modality, and cortical modality. Most straightforwardly, **input modality** refers to the sensory organ that initially transduces the stimulus. For example, if a letter is presented visually, then any neural representation of that letter is also visual. Another use, which I will refer to as **content modality**, refers to the representational content of a stimulus within a brain region. For example, while both visual and auditory inputs can activate the representation of /eI/, phonological information is generally associated with auditory and motor modalities while visual information is generally associated with visuospatial features. Modality also refers to cortical regions affiliated with a particular sensory modality. I will refer to this usage as **cortical modality**. For example, the calcarine sulcus is thought to primarily process visual input and Heschl's gyrus is thought to process auditory input.

The terms **cross-modal** and **multi-modal** refer to the relationship between the input modality of a stimulus and the internal (neural) representations of that stimulus. A neural representation can be multi-modal in the sense that multiple input modalities can access the same representation. For example, the neural representation of the letter name /eI/ could be **multi-modal** in this sense if both hearing the letter name /eI/ and seeing a visually presented stimulus **A** accesses the same phonological name representation /eI/. In this paper, **cross-modal** simply refers to particular multi-modal effects. In this example, the multi-modal representation /eI/ will demonstrate cross-modal activation in that it is activated in response to visually and aurally presented letters. In this experiment, we compared the similarity of cross-modal activation patterns (the similarity of activation patterns across visual and auditory presentations) to determine whether a neural representation was multi-modal and importantly, the content of that representation.

The question of whether a representation is multi-modal or not is orthogonal to the question of the content modality of that representation. Representational content can be **modality specific** or **abstract**. A representation is **modality specific** if the information represented is highly associated with one or more sensorimotor modality. In the example of the letter name representation /eI/ described above, while the representation is multi-modal because it demonstrates cross-modal activation, the content of the representation /eI/ is associated with the auditory, sensory and articulatory motor systems so the content modality is **modality specific**. A representation is generally thought to be **abstract** if the content of the representation is not associated with any modality. Letter identity representations are thought to be **abstract** because even though the input modality may often be visual, the same representation can be activated despite large visuospatial changes to the stimulus (e.g., **r** and **R** activate the same ALI representation). I wish to further define **amodal** representations as abstract representations (meaning the representational content is not associated with any modality) that are also multi-modal (meaning multiple input modalities activate the same abstract representation). For example, ALI representation would be amodal if the same representation is activated in response, not only to lower and upper case letters that share the same identity, but the letter name associated with that identity as well (e.g., **a**, **A**, and /eI/ would activate the same amodal ALI representation).

As can be seen in Figure 2, the representations in the domain of letter processing are multi-modal. A seen letter can go on to trigger knowledge of the motor codes used to produce that letter or it could go on to trigger the name of the letter or the sound that is commonly associated with the letter. That all this information is accessible from a visual stimulus is not surprising. Understanding how these modality specific representations connect with one another, on the other hand, is an active domain of study. The framework we present in Figure 2 hypothesizes that the ALI representations not only abstract away from visual information, but they represent a letter's identity regardless of the modality of presentation or production as well—rendering ALIs amodal. Furthermore, it is these amodal ALI representations that serve as a conduit between all the modality-specific representations in addition to lexical processes. On this view, seeing the letters **a** and **A** and hearing /eI/ should activate the same amodal ALI representation. Furthermore, in order to produce the name /eI/ from viewing the shape **a**, the ALI representation [A] must mediate the connection.

Previous neuroimaging research has investigated the neural response to letters presented to different modalities. In one study, researchers presented participants with single letters visually and aurally while recording the resulting neural activity in a MEG scanner (Raij, Uutela, & Hari, 2000). They identified regions activated for just visual letters in occipital and ventral occipito-temporal cortex while the regions sensitive to aurally presented letters were in the anterior superior temporal sulcus (STS). The researchers then identified neural substrates activated by both visually and aurally presented letters in the left and right posterior STS (pSTS). To determine if the visual and auditory letter signals were multimodal (i.e., activated the same neural representation) they found that the neural signals were not additive when visual and aural letters were presented simultaneously. Raij et al. (2000) interpreted this nonlinearity as demonstrating that visual and aurally presented letters accessed shared representations in the left and right posterior STS (although the interaction in the left was 70ms earlier than in the right). These findings were replicated in an fMRI study that also suggested multi-modal effects can even be seen in primary sensory areas (van Atteveldt, Formisano, Goebel, & Blomert, 2004). While both of these studies suggest neural signals from different input modalities interact at multimodal convergence zones in the pSTS (also referred to as heteromodal convergence zones or association areas), these results do not determine the content of the representations at the point of these interactions. In other words, what is the content of the representation these modalities share? Do letters from both input modality activate the same phonological letter name representation? Do they activate the same abstract identity representation? MVPA-RSA can be used to investigate the content of these representations.

MVPA has been used to more directly test the nature of multimodal interactions in other contexts. For example, a study by Man et al. (2012) trained a classifier on the multi-voxel patterns of neural responses to visual and auditory clips of the same event.

They found that the activation patterns in pSTS trained in one modality could classify the patterns of the same events presented to the other modality regardless of whether it was visual to auditory or vice-versa. While this study directly demonstrated that visually and aurally presented stimuli share the same representational content in pSTS, it does not elucidate the nature of the shared representational content. Other studies have used MVPA RSA to determine that semantic/conceptual properties of the stimuli that appear to be driving the interactions, at least in terms of broad object categories (e.g. clothes, mammals, and tools) (Bonner, Peelle, Cook, & Grossman, 2013; Fairhall & Caramazza, 2013). For example, Fairhall & Caramazza (2013) identified a set of brain regions whose responses to visually presented objects and corresponding aurally presented object names were similar to one another. This was evidence for multi-modal representations within these brain regions. Importantly, they determined that the similarity structures within two of these brain regions (specifically the posterior middle temporal gyrus and posterior cingulate) were consistent with representing abstract semantic category information of the stimuli regardless of the input modality. Fairhall and Caramazza concluded that these two neural regions represented the semantic category of the presented stimuli in an abstract and amodal manner. Following a similar logic, we used MVPA-RSA with letters to localize cortical regions that represented the amodal identity of letters consistent with the ALI representation in the letter processing model presented in Chapter 1. Furthermore we set out to investigate the representational content of modality specific and cross-modal activation patterns.

5.1 Methods

Participants (identical to Experiment 4 in Chapter 4)

12 participants (6 female) were recruited from the Johns Hopkins University student population. Participants were right handed, had no history reading or learning disabilities, and were only able to read letters from the Roman alphabet. Each participant provided written consent and was compensated in accordance with The Johns Hopkins Institutional Review Board. One participant was excluded from all analyses due to excessive head motion.

Procedures

Participants performed three experimental tasks within a 2 hour scan session. The first was an auditory name detection task, the second was a visual symbol detection task and the third was a passive viewing Retinotopic Localizer (the data from the latter two tasks were also analyzed in Chapter 4). All tasks were presented and responses were recorded using E-Prime 2.0 Software (Psychology Software Tools, Pittsburgh, PA).

Auditory name detection task:

Stimuli consisted of 7 spoken letter-names (a, d, e, g, h, r, t) and 5 digit names (2, 4, 5, 7, 8) recorded by a female speaker. Additionally, two single syllable male names served as targets (“Dave” and “Jim”). The letter and number names corresponded to the 7 letter and 5 digit identities of the gridfont stimuli from Chapters 3 and 4. Additionally, Iterated Ripple Noise or “Ripples” (Yost, 1996) were presented as a baseline. Appropriately calibrated ripple noise has been used successfully to simulate appropriate "spectro-temporal response fields" of speech in humans without producing any perceptible speech sounds (Ley et al., 2012).

Participants listened to 7 letter names and 5 number names resulting in 12 total names. Additionally, 2 target monosyllabic male-names were presented. Participants were asked to press two buttons—one in each hand—whenever they heard the male name. The experimental procedure consisted of 3 trial types: (1) Name trials, which were comprised of a 300ms fixation dot, and up to 3700ms for the auditory presentation of a letter or digit name while the monitor displayed a blank white screen; (2) male-name trials, which were the same as name trials except a male name was presented instead of a letter or digit name and participants were expected to respond; (3) Ripple trials, which consisted of a fixation dot and then a brief ripple noise and the remainder of the trial which was a blank white screen. The ripple durations were matched against the length of the letter, digit, and male name durations. Each trial lasted 4000ms. In sum, there were 12 name trials, 2 male name trials, and 3 ripple trials per block for a total of 17 trials per block. Each run consisted of 4 blocks and there were 3 runs in total making for 12 repetitions of each condition.

The Visual Symbol Detection task and the Retinotopic Localizer data was the same data that was analyzed in Experiment 4 (see Chapter 4 a description of the task).

5.1.2 Imaging parameters (identical to Experiment 4 in Chapter 4)

MRI data were acquired using a 3.0-T Phillips Intera Scanner. Whole-brain T2-weighted gradient-echo EPIs were acquired with a 32 channel SENSE (Invivio) parallel imaging head coil in 30 ascending 3 x 3 mm slices with 1 mm gap. TR = 2 s for the

Symbol Detection Task and Retinotopic Localizer. Echo time = 30ms, flip angle = 65º, field of view = 240 x 240mm, matrix = 128 x 128mm. Structural images were acquired using an MR-Rage T1-weighted sequence yielding images with 1mm isotropic voxels (repetition time = 8.036ms, echo time = 3.8ms, flip angle = 8 º

5.1.3 fMRI data processing

Data from the Auditory Name Detection task, the Symbol Detection task and the Retinotopic Localizer were preprocessed identically using Brain Voyager Q.X. software (Maastricht, Netherlands). Functional images were corrected for slice time (ascending) and motion (trilinear 3D motion correction with sinc interpolation. Additionally, a temporal high-pass filter removed components occurring fewer than three cycles per run (high-pass GLM-Fourier 3 Cosines) and linear trend removal for correcting scanner drift. Images were resampled to $3mm^3$ voxels.

The data from the auditory name and symbol detection tasks were analyzed in an MVPA-RSA design that was VOI based. This required the following: (1) generating the participant and stimulus-specific activation patterns used to generate oRSMs within the VOIs, (2) identifying the relevant VOIs and (3) generating the oRSMs and pRSMs for the analysis.

(1) Activation patterns for the VOI analysis.

Two event-related GLMs were carried out: one included 37 experimental regressors for the visual symbol detection task and the other included 15 regressors for the auditory name detection task. The regressor set for the visual symbol detection task included one for each letter or digit stimulus (33) and one for each symbol (4) while the auditory name detection task had one for each letter or digit name (12), one for the ripple noise and 1 for each male name (2). Additionally, both GLMs had 1 linear trend regressor, 6 head-motion parameter time-course regressors, 6 fourier-based non-linear trend regressors (up to three cycles per run for sine and cosine) and 1 confound regressor representing run number. The experimental regressors were created by convolving a boxcar function corresponding to the duration of appearance of each experimental condition with a Boynton hemodynamic response function. The duration of the boxcar function for the 4 symbol regressors from the visual symbol detection task and the 2 male name regressors from the auditory name detection task lasted the entire 4000ms trial duration to ensure inclusion of the expected motor response. For the experimental trials, the 200ms corresponding to the fixation appearance and the 3500ms of blank screen following the stimulus disappearance were not modelled. The entire 4000ms duration of blank trials was not modelled as well. These time periods served as the implicit baseline. Each regressor (both experimental and confound) was z-normalized and then fit against the fMRI time-course signal expressed as percent signal change. The resulting beta-maps were converted to t-maps—one map for each of the 33 experimental conditions (letter or digit stimuli) for the symbol detection task and one map for each of the 12 letter and digit name stimuli. These t-maps (in native ACPC space) were used as the activation estimates for the MVPA-RSA analyses. MVPA-RSA was carried out using in house code run in MATLAB (Math Works). NeuroElf (http://NeuroElf.net/) was used to integrate Brain Voyager and MATLAB.

(2) Identification of functionally-based VOIs

VOIs were constructed for both the Symbol and Spoken Name Detection tasks in order to identify Visual Alphanumeric VOIs from the former task and Auditory Alphanumeric Name VOIs. The Visual Alphanumeric VOIs were the same Alphanumeric VOIs analyzed in Chapter 4.

Prior to running the group RFX GLM analysis, fMRI data from the symbol and spoken name detection tasks were smoothed 6mm FWHM and normalized to Talairach space. Two GLMs were then constructed in a similar manner as described in analysis (1). The only distinction was that the GLMs were group GLMs containing data from each participant. Participants were treated as random variables in these RFX GLMs and a contrast of activation levels for letter and digits > baseline for the symbol detection task and all letter and digit names > ripple sound for the spoken name detection task were carried out with results thresholded at an uncorrected $p<0.05$ with a clustersize threshold of 30 voxels (clusters reported in Table 5). The surviving clusters were then expanded by 5mm in each direction and converted back to native ACPC space for each participant (Table 6).

Data and analysis from the Retinotopic Meridian Map Localizer corresponded to the data analysis reported in Chapter 4

(3) Generation of oRSMs and pRSMs

An oRSM was constructed for each VOI in the same manner as described in Chapter 4. For each VOI, three types of oRSMs were created. (1) Visual oRSMs corresponded to the activation patterns generated in response to the visually presented letters and digits from the Symbol Detection Task. (2) Auditory oRSMs corresponded to the pairwise correlation of activation patterns in response to the aurally presented letter and digit names from the Auditory Name Detection Task. (3) Cross-modal oRSMs were oRSMs created by taking the activation pattern evoked by a visually presented letter or digit and correlating that pattern with the pattern evoked by an aurally presented letter or digit name. The correlation value reflects the similarity of the multi-voxel patterns in response to a visual stimulus and an auditory stimulus.

Three group oRSMs were constructed for each VOI in the following manner. First, the values from each participant's oRSMs were z normalized to have a mean of 0 and a standard deviation of 1. The group oRSMs corresponded to the mean z value across participants within each cell. Like the participant oRSMs, the group oRSMs were z-normalized to have a mean of 0 and a standard deviation of 1. These group oRSMs served as the estimate of the representational similarity structure within any give VOI for the Visual and Auditory stimuli and for the Cross-modal similarity between the two. Digit stimuli were excluded from the Visual oRSMs but were included in the Auditory and Cross-modal oRSMs because these oRSMs were composed of considerably fewer stimuli and removing digits would have greatly reduced the power (number of data points) for the correlation and regression analyses.

Multiple pRSMs were constructed to test if the similarity structure for a given oRSM was consistent with a predicted (idealized) RSM for that particular type of representation (see Appendix 1 for examples of each pRSM). Four sets of pRSMs were constructed corresponding to the content-modality of the representation that the pRSM was predicting. When possible, multiple versions of each pRSM were constructed for each content modality—one that predicts the similarity structure from the visual input modality, one that predicts the similarity structure from the auditory input modality, and one tests for multi-modal representations but comparing the cross-modal similarity between stimuli presented to the visual and auditory input modalities.

Visual content pRSMs

The Pixel-overlap pRSM and a Stimulus Shape pRSMs (both described in Chapters 3 and 4) were constructed for testing the Visual oRSMs. Because these pRSMs represent font-specific visual information that is unlikely to be represented by the auditory stimuli, Auditory or Cross-modal oRSMs were not constructed for the Pixel-overlap or Stimulus Shape pRSMs. The Allograph pRSM, composed of pairwise visual similarity judgments for letters presented in a typical Calibri-based font, was constructed for testing the Visual, Auditory, and Cross-modal oRSMs. The Visual Allograph pRSM was described in Chapter 4. The Auditory Allograph pRSMs consisted of 2 pRSMs also based on the typical font similarity matrix. Since letter names do not have case, 2 separate visual pRSMs were created—one for each case. For example, the Lowercase Auditory Allograph pRSM placed the lower case visual similarity for a and e in the cell that predicted the response to the names /eI/ and /i:/ while the uppercase Auditory Allograph pRSM placed the visual similarity for A and E in that cell. Similarly, 2 Cross-modal Allograph pRSMs were constructed: one assuming the heard letter names activated uppercase allographs and another assuming the names activated lowercase allographs.

Motor content pRSMs

A pRSM which estimated motoric production representations by measuring the overlap of a proposed set of motor features (Rapp & Caramazza, 1997) was constructed (see Chapter 3 for more details.) This pRSM was adapted to the Auditory and Cross-modal oRSMs in the same manner as the Allograph pRSM—namely, two pRSMs were constructed for both the Auditory and the Cross-modal oRSMs. One pRSM assumed the auditory name activated a lowercase motor code and the other assumed the name activated an uppercase motor code.

Auditory content pRSMs

There were pRSMs used for representing the similarity of letter names. The Phonetic Feature Overlap pRSM involved estimating name similarity by computing the amount of phonetic feature overlap of each alphanumeric name with every other name (see Chapter 3 for more details). The Letter Name Confusability pRSM consisted of an empirically derived alphanumeric-name confusability matrix (Hull, 1973). Both of these pRSMs were straightforwardly adapted to the Visual, Auditory and Cross-modal oRSMs

Identity content pRSMs

A letter identity pRSM was constructed for the Visual oRSMs by assigning a value of 1 to any letter pairs that shared the same identity and a value of 0 to any letter pairs that did not. A Letter and Digit Identity pRSM was adapted to fit the Cross-modal oRSM. It predicted that the pattern of activation between a seen letter and heard letter name should be more similar if they corresponded to the same identity than if they did not (see figure 23).

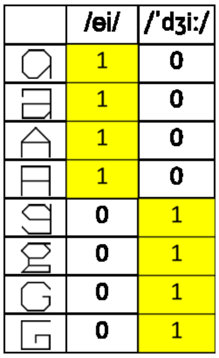

	/ei/	/ˈdʒiː/
	1	0
	1	0
	1	0
	1	0
	0	1
	0	1
	0	1
	0	1

Figure 23. An Amodal ALI pRSM. This pRSM predicts that the patterns of activation for visually presented letters and aurally presented letter names will be more similar if they share the same identity.

5.1.4 ALI localizer and Selectivity analyses

Searchlight ALI localizer

In order to identify amodal letter identity representations, neural substrates of ALI representations were identified in a searchlight analysis. These neural substrates could then be tested for cross-modal identity representations. A replication of the regression-based searchlight analysis reported in Rothlein and Rapp (2014) was performed on the MVPA-RSA data from the visual symbol detection task in this experiment. Described in Chapter 2, the searchlight analysis was carried out within the same searchspace from Rothlein and Rapp. A 7 voxel sphere generated an oRSM for each searchlight region in the searchspace. Each of the searchlight oRSMs were fit to a regression model where 4 pRSMs served as regressors: an Abstract Letter Identity pRSM, a Visual Similarity pRSM which was identical to the Stimulus Shape pRSM, a Letter Name pRSM which was derived from the Letter Name Confusability pRSM. Finally a Motor Feature Overlap pRSM was adapted from the Motor Feature Overlap pRSM described in Chapter 3 was included as a regressor. Both the Letter Name and the Motoric pRSM were binarized so the only values in the pRSMs were 0 and 1. This was done by computing the average value within each pRSM and assigning all cells with values greater than the average value a 1 and all other cells a 0. The searchlight analysis yielded 4 beta-maps where the beta values associated with each pRSM were assigned to the central voxels in the searchlight. These participant beta-maps were spatially smoothed (6mm or 2 FWHM) and then normalized to Talairached space. A t-test was then run at each voxel testing to see if the beta values across the 11 participants associated with each pRSM were greater than 0. This generated 4 Group Feature Regression Maps which were thresholded by applying a voxelwise uncorrected threshold of $p<0.10$.

Selectivity analysis

For each VOI, each type of oRSM was evaluated in a regression analysis for a total of 3 regression analyses per VOI. The Visual oRSM regression model contained the following 5 regressors: the Stimulus Shape, Allograph, Identity, Motoric and Phonetic Feature Overlap pRSMs. The Auditory oRSM regression model contained the following 6 regressors: Uppercase Visual Similarity, Lowercase Visual Similarity, Uppercase Motoric Similarity, Lowercase Motoric Similarity, Phonetic Feature Overlap and Letter Name Confusability pRSMs. The Cross-modal oRSM regression model contained the following 6 regressors: Amodal Identity, Phonetic Feature Overlap, Uppercase Visual Similarity, Lowercase Visual Similarity, Uppercase Motoric Similarity, and Lowercase Motoric Similarity pRSMs. In order to compute standardized regression coefficients, each of the group oRSMs and the pRSMs were z normalized to have a mean of 0 and a standard deviation of 1. The regression analysis was carried out using MATLAB's REGSTAT function. A t-value was computed for each β coefficient and was evaluated for statistical significance assuming a two-tailed p value.

5.2 Results

VOIs

Eight clusters—3 from the Visual Alphanumeric contrast and 3 from the Auditory Alphanumeric Name contrast (aurally presented names > ripple noise baseline)—were identified (for coordinates and other details see Table 5 and Table 6): for the visual contrast, a cluster in the Left Middle Occipital Gyrus, a cluster in the Left Fusiform Gyrus bordering the Occipito-temporal Sulcus, and a cluster in the Right Posterior Fusiform Gyrus. For the auditory contrast, clusters in both the right and left Superior Temporal Sulcus (STS) were identified along with a cluster in the Left Anterior STS region. Additionally, clusters in the anterior cingulate and the right central sulcus were identified in the Alphanumeric Name contrast. These 8 clusters were then enlarged by 5mm in all directions and converted in to each participant's native space to demarcate functionally relevant VOIs. In addition, Retinotopic cortex was defined using meridian mapping. An overview of these VOIs consisting of voxels can be found on Table 6 and Figure 24.

Table 5. Properties of the clusters that were expanded to become the VOIs.

	Anatomical Label	**Peak X**	**Peak Y**	**Peak Z**	**T(10)**	**p**	**# of voxels**
Visual (Letters + Digits) > Fixation Baseline	Left Middle Occipital Gyrus	-42	-73	-7	7.14	<0.00005	173
	Left Fusiform Gyrus	-41	-63	-19	4.47	<0.005	20
	Right Fusiform Gyrus	31	-79	-16	8.31	<0.00001	130
Auditory (Letters + Digits) > Ripple	Left Superior Temporal Sulcus	-60	-25	4	5.61	p<0.0005	113
	Bilateral Anterior Cingulate	6	-7	58	6.71	p<0.0001	210
	Right Superior Temporal Sulcus	49	1	2	8.18	p<0.00001	221

Table 6. Properties of the VOIs used to generate the oRSMs. For each VOI, the average number of functional (3x3x3mm) voxels across participants along with the range. Additionally the average center of mass for each VOI is reported.

		# of voxels: average	# of voxels: min	# of voxels: max	Center of mass (TAL: X, Y, Z)
Retinotopic Cortex	Bilateral Ventral V1-V4	1147	991	1251	(-2, -84, -12)
Visual Alphanumeric VOIs	Left Middle Occipital Gyrus (L. MOG)	732	445	889	(-36, -82, -11)
	Left Fusiform Gyrus	330	218	376	(-46, -66, -19)
	Right Fusiform Gyrus	1244	1062	1313	(35, -66, -17)
Auditory Alphanumeric Name VOIs	Left Superior Temporal Sulcus	794	662	862	(-57, -25, 2)
	Left Anterior Superior Temporal Sulcus	338	253	402	(-50, 5, -4)
	Bilateral Cingulate	1310	1229	1396	(-2, -3, 45)
	Right Superior Temporal Sulcus	1508	1259	1601	(50, -14, -1)
	Right Central Sulcus	697	632	736	(41, -20, 42)

VOI analysis: Visual oRSMs (Table 5)

Multiple pRSMs were tested against oRSMs generated from correlating the activation patterns generated from visually presented letters and digits. Within the retinotopic cortex, the regression analysis—with all the visual pRSMs as regressors—revealed that only the beta value of the Stimulus Shape pRSM was significant ($\beta = 0.066$; $p<0.05$).

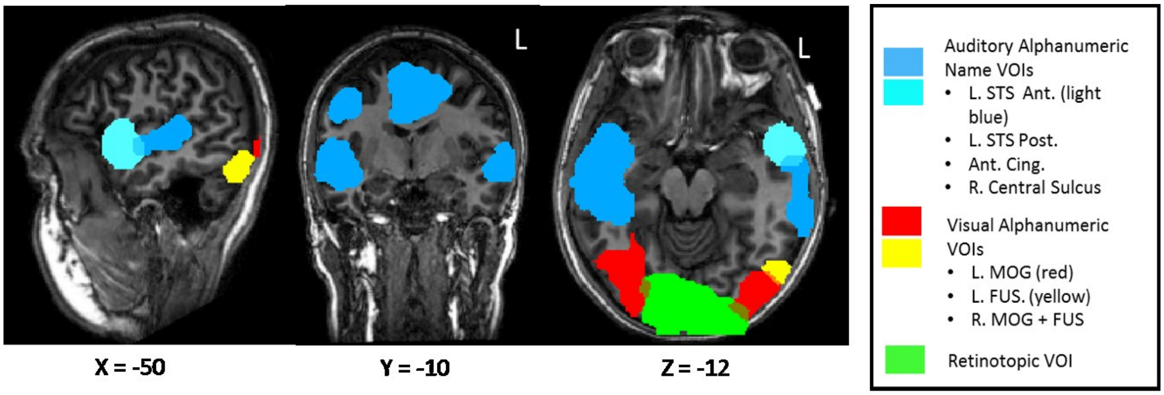

Figure 24. Image depicting the neurotopgraphy of the VOIs. Both red and yellow indicate VOIs that were responsive to visually presented letters and digits. Both light and dark blue VOIs indicate Auditory Alphanumeric Name VOIs. The different colors allow the cluster boundaries to be visible when the two clusters are touching. For the same reason, both red and yellow VOIs indicate Visual Alphanumeric VOIs.

Within Visual Alphanumeric VOIs defined by brain regions more active for visual letters and digits than a fixation baseline, the regression analysis revealed that only the Allograph pRSM was significant in the left MOG and the left fusiform ($\beta = 0.149$, $p<0.05$; $\beta = 0.124$, $p<0.05$ respectively).

The last set of VOIs was defined as regions that were sensitive to aurally presented letter and digit names compared to a Ripple noise. In the context of other pRSMs in a regression analysis, the beta value of the Stimulus Shape pRSM was significant in the left STS ($\beta = 0.061$, $p<0.05$). Additionally, the Letter Identity pRSM was significant in the bilateral cingulate VOI ($\beta = 0.077$; $p<0.05$). Finally, the regression revealed the Motor Feature Overlap pRSM to be significant in the right central sulcus ($\beta = 0.049$, $p<0.05$).

Table 7. Results from the regression analyses for the oRSMs derived from visually presented letters and digits. Reported values are correlation r values. * indicates p<0.05 and ** indicates p<0.001.

		Visual oRSMs							
		Regression model statistics			β weights				
		R²	F(285, 5)	p	Stimulus Shape	Allograph	Letter Identity	Motor Feature Overlap	Phonetic Feature Overlap
Retinotopic Cortex	Bilateral Ventral V1-V4	0.042	3.573	0.004	0.066*	0.09	-0.028	-0.042	0.039
Visual Alphanumeric VOIs	Left Middle Occipital Gyrus (L. MOG)	0.036	3.157	0.009	-0.021	0.149*	-0.091	-0.002	0.032
	Left Fusiform Gyrus	0.035	3.115	0.009	-0.004	0.124*	-0.048	0.009	0.017
	Right Fusiform Gyrus	0.007	1.429	0.214	0.01	0.042	-0.004	0.021	0.019
Auditory Alphanumeric Name VOIs	Left Superior Temporal Sulcus	0.006	1.357	0.24	0.061*	-0.063	0.059	0.009	0.017
	Left Anterior Superior Temporal Sulcus	-0.004	0.78	0.565	0.008	0.037	-0.03	0.028	0.034
	Bilateral Cingulate	0.016	1.967	0.084	0.015	-0.055	0.077*	-0.001	0.012
	Right Superior Temporal Sulcus	-0.003	0.854	0.513	0.011	0.007	0.008	0.01	0.033
	Right Central Sulcus	0.001	1.048	0.39	0.002	-0.038	0.046	0.049*	-0.007

Auditory oRSMs

Auditory oRSMs were generated from correlating the activation patterns in response to aurally presented letter and digit names. None of the beta values from the regression analyses in which all the auditory pRSMs served as regressors for the auditory oRSM were significant. Within Alphanumeric VOIs, the β coefficient for the Lowercase Motoric Feature pRSM in the regression analysis in the left fusiform was significant (β = 0.1, p<0.05).

From the Auditory Alphanumeric Name VOIs, the regression analysis revealed that the L. STS had significant beta values for the Phonetic pRSM (β = 0.214, p<0.001), the Uppercase Visual pRSM ($\beta = 0.185$, $p<0.05$), as well as the Lowercase Motoric pRSM ($\beta = 0.146$, $p<0.05$). The anterior left STS VOI was only significant for the Lowercase Motoric pRSM ($\beta = 0.232$, $p<0.001$). In the bilateral cingulate, the Lowercase Visual pRSM was significant in the regression analysis ($\beta = 0.112$, $p<0.05$). The right STS VOI had significant beta values for the Uppercase Visual Similarity pRSM ($\beta = 0.169$, $p<0.05$) and the Lowercase Motoric pRSM ($\beta = 0.126$, $p<0.05$). Finally the central sulcus VOI had significant beta values for the Lowercase Motoric Similarity pRSM ($\beta = 0.095$, $p<0.05$).

Table 8. Results from the regression analysis for the oRSMs derived from aurally presented letter and digit names. Reported values are correlation r values. * indicates p<0.05 and ** indicates p<0.001.

		Auditory oRSMs								
		Regression model statistics			β weights					
		R^2	F(59,6)	p	Phonetic Feature Overlap	Letter Name Similarity	Visual Similarity: Uppercase	Visual Similarity Lowercase	Motor Similarity Uppercase	Motor Similarity Lowercase
Retinotopic Cortex	Bilateral Ventral V1-V4	0.065	1.756	0.124	0.041	-0.001	-0.008	0.076	-0.022	0.066
Visual Alphanumeric VOIs	Left Middle Occipital Gyrus (L. MOG)	-0.01	0.865	0.526	-0.019	0.009	0.033	0	0.019	0.057
	Left Fusiform Gyrus	0.028	1.313	0.266	0.047	-0.011	0.056	-0.045	-0.008	0.1*
	Right Fusiform Gyrus	-0.03	0.686	0.662	-0.007	-0.013	0.017	0.023	-0.003	0.019
Auditory Alphanumeric Name VOIs	Left Superior Temporal Sulcus	0.412	8.584	<0.001	0.214**	0.018	0.185*	0.012	-0.109	0.146*
	Left Anterior Superior Temporal Sulcus	0.296	5.559	<0.001	-0.022	-0.003	0.12	0.071	-0.055	0.232**
	Bilateral Cingulate	0.301	5.674	<0.001	0.018	0.028	0.042	0.112*	-0.029	0.044
	Right Superior Temporal Sulcus	0.242	4.465	0.001	0.096	0.029	0.169*	-0.02	-0.014	0.126*
	Right Central Sulcus	0.115	2.414	0.037	-0.093	-0.031	0.001	-0.043	-0.012	0.095*

Cross-modal oRSMs

Cross-modal oRSMs were generated by correlating the activation patterns in response to aurally presented letter names with the patterns in response to seen letters. Cross-modal oRSM-pRSM regression analyses tested if the representational content at a particular VOI was the same regardless of the sensory modality of the stimulus. Regression analyses revealed the Retinotopic and the left fusiform VOIs to be significant for Identity ($\beta = 0.058$; $p<0.05$) and ($\beta = 0.058$; $p<0.05$) respectively. Additionally, the left anterior STS was significant for Lowercase Visual Similarity ($\beta = 0.058$; $p<0.05$).

Table 9. Results from the regression analysis for the oRSMs derived from the activation patterns in response to aurally presented letter and digit names correlated with the activation patterns in response to visually presented letters and digits. Reported values are correlation r values. * indicates $p<0.05$ and

		Cross-modal oRSMs								
		Regression model statistics			β weights					
		R^2	F(341, 6)	p	Identity	Phonetic Feature Overlap	Visual Similarity: Uppercase	Visual Similarity Lowercase	Motor Similarity Uppercase	Motor Similarity Lowercase
Retinotopic Cortex	Bilateral Ventral V1-V4	0.027	2.608	0.017	0.058*	-0.062	-0.059	0.018	-0.044	0.017
Visual Alphnumeric VOIs	Left Middle Occipital Gyrus (L. MOG)	0.009	1.517	0.171	0.029	-0.03	-0.035	-0.009	-0.026	0.028
	Left Fusiform Gyrus	-0.001	0.921	0.48	0.058*	-0.018	-0.032	0.004	-0.026	-0.01
	Right Fusiform Gyrus	-0.005	0.705	0.646	-0.002	-0.012	-0.001	0.013	-0.022	0.017
Auditory Alphanumeric Name VOIs	Left Superior Temporal Sulcus	-0.009	0.495	0.812	0.003	0.027	-0.007	0.016	-0.01	-0.001
	Left Anterior Superior Temporal Sulcus	0.017	2.019	0.063	0.019	-0.007	0.016	0.058*	-0.072	-0.006
	Bilateral Cingulate	-0.004	0.76	0.602	-0.021	-0.007	0.03	0.018	0.012	0.004
	Right Superior Temporal Sulcus	-0.01	0.405	0.876	-0.01	0	0.016	-0.021	0.01	0.011
	Right Central Sulcus	0.008	1.483	0.183	0.001	0.007	-0.03	-0.036	0.011	0.008

ALI VOI Analysis[16]

A regression searchlight was run in order to identify voxels that selectively represent ALIs. The group ALI t-map was thresholded at an uncorrected voxelwise threshold of $p<0.10$ (identical to Rothlein and Rapp, 2014). This revealed an insignificant cluster largely overlapping with the regression ALI searchlight cluster reported in Rothlein and Rapp (2014) (Figure 25 in orange; peak voxel TAL: -32, -59, -13.) The cluster from the present experiment was 89 voxels with a peak at TAL: -29, -67, -7 ($t(10) =6.5$). This peak voxel was significant after applying an FDR familywise correction for multiple comparisons of $q <0.05$ (depicted as yellow voxels in Figure 25).

---

[16] An additional, more precise, replication of Rothlein and Rapp (2014) was performed. Like Rothlein and Rapp (2014), the stimulus activation values consisted of beta-weights instead of t-values generated from the beta values. Additionally, like Rothlein and Rapp (2014) the activation values were mean normalized so that at each voxel the mean beta value computed over all the alphanumeric stimuli in that voxel is subtracted from each voxel to ensure that every mean-normalized voxel has a mean of 0. Of the four pRSMs tested—ALI, Visual Similarity, Letter Name Similarity, and Motoric Similarity—only the ALI pRSM had a significant cluster after applying an uncorrected voxelwise threshold of $p<0.10$ and a clustersize corrected threshold of $p<0.05$. This cluster consisted of 505 voxels with a center of gravity at TAL: -12, -76, -13. The statistical peak voxel of this cluster was located at TAL: -26, -65, -6 ($t(10) = 5.87$) which was quite close to the peak of the ALI cluster reported in Rothlein and Rapp (TAL: -32, -59, -13).

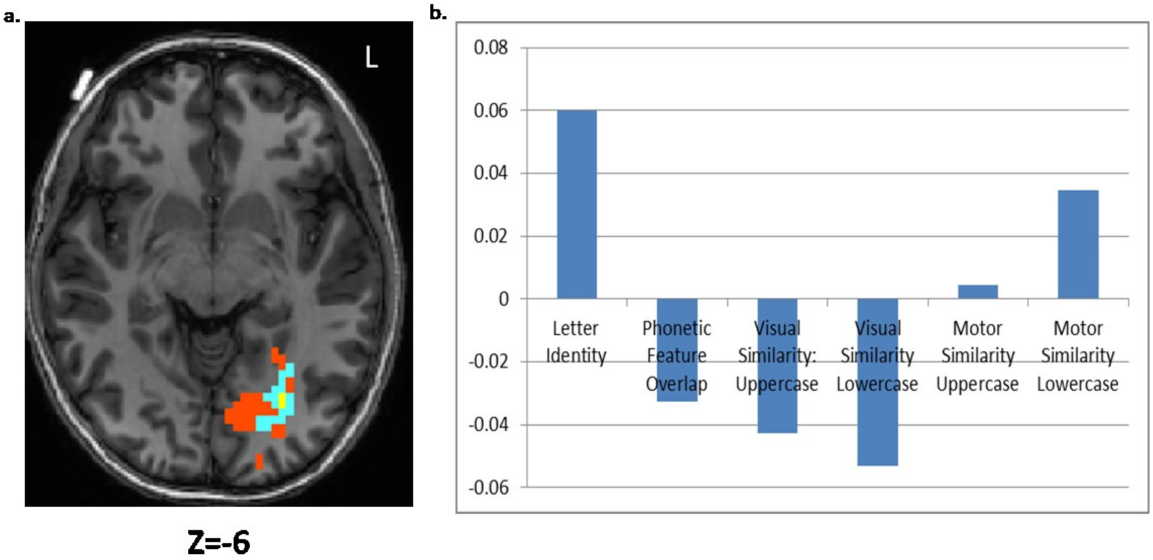

Figure 25. (a) Results from searchlight analysis replicating the Rothlein and Rapp (2014) ALI cluster using the regression searchlight analysis. The orange voxels indicate the voxels from the significant ALI cluster reported in Rothlein and Rapp (2014). The blue voxels indicate the ALI VOI identified in the present experiment. The yellow voxels indicate the FDR corrected ($q<0.05$) significant voxels from the ALI VOI. (b) The β coefficients for each of the cross-modal pRSM regressors in a regression analysis predicting the cross-modal oRSM derived from the ALI searchlight cluster (light blue in (a)). Evidence for amodal letter identity representations comes from the marginally significant ($p = 0.057$) cross-modal identity pRSM.

This ALI cluster was used as a VOI to generate a Cross-modal oRSM which was tested with the cross-modal regression analysis. This revealed a significant model with an Adjusted $R^2 = 0.021$ ($f(341, 6) = 2.22$, $p<0.05$). Importantly, the identity pRSM was marginally significant ($\beta = 0.061$, $p=0.057$). The β coefficients for the other pRSMs are displayed in Figure 25 although none approached significance.

5.3 Discussion

This chapter set out to investigate the relationship between ALI representations and stimulus modality—specifically, whether case-invariant ALI representations are amodal as well. Amodal means that the same ALI representation was accessed regardless of whether the letter stimulus was presented visually or aurally. More broadly, we set out to investigate how the input modality of the letter stimulus interacts with every type of letter representation.

5.3.1 Expected modality-specific results

Expected modality specific results consist of instances where the modality-specific representational content is aligned with both the cortical modality as well as the input modality. In Chapter 4, we found that the activation patterns in response to visually presented letters in the visual cortical region bilateral retinotopic cortex (ventral V1-V4), were sensitive and selective to the Visual pRSMs (stimulus shape and allograph). This result is consistent with countless studies that have used RSA with visually presented stimuli to uncover visuospatial representations in low-level visual cortex (Connolly et al., 2012; Kriegeskorte et al., 2008; Mur et al., 2013; Op de Beeck et al., 2008).

Within the Auditory Alphanumeric Name VOIs, the Auditory oRSMs derived from aurally presented letter names were sensitive to pRSMs representing auditory/articulatory content—specifically, the Phonetic Overlap pRSM in the left STS. These results were expected served as confirmation that the pRSMs were capable of picking up on the representational content of the visual and aurally presented alphanumeric stimuli.

5.3.2 Cross-modal results

The results of this experiment have demonstrated that, even without instruction, presenting a letter or digit in one input modality can activate representations often associated with other modalities. For example, the activation pattern for visually presented letters in left STS reflected letter name similarity and not visual similarity. This suggests that the neural from the visual input modality goes on to activate phonological letter name representations in left STS. This is consistent with the finding from Rothlein and Rapp (2014) that showed the left posterior STS was sensitive to letter name similarity. Additionally, the oRSMs formed from aurally presented letter names in retinotopic cortex were sensitive to visual pRSMs suggesting the representational content of the auditory signal activates visuospatial representations when travelling from left STS to retinotopic cortex. Interestingly and unexpectedly, many Auditory VOIs were sensitive to visual and motor representational content, even when the stimuli were aurally presented letter-names. To my knowledge this finding has little precedent and merits further investigation. These results could possibly be explained as feedback processes from visual and motoric cortical areas.

Regression Analysis		Representational Content			
		Visual	Motor	Auditory	Identity
Retinotopic	Ventral V1-V4	V			CM
Visual Cortex	Left MOG	V			
	Left Fusiform	V	A		CM
	Right Fusiform				
Auditory Cortex	Left STS	V + A	A	A	
	Left Ant. STS	CM	A		
	Bilat. Cing.	A			V
	Right STS	A	A		
	Right Central Sulc.		V + A		

Figure 26. Summary of all the significant results from the regression analyses. The VOIs are divided by whether they were derived from retinotopic meridian mapping (green), univariate activation in response to visual letters and digits (red) and univariate activation in response to auditory letters and digits (blue). Each of these VOIs was tested with pRSMs which examine if the similarity structure of a particular VOI is consistent with that VOI encoding the representational content the pRSM was based on. Visual content included the pixel-overlap, rotated gridfont and typical font similarity judgments as well as either upper or lowercase visual similarity for auditory and cross-modal pRSMs. Within each cell, a **V** indicates that oRSM-pRSM beta value, derived from the visually presented letters and digits, was significant. The **A** indicated the same thing as the **V** except the oRSM and pRSM were based on the aurally presented letter and digit names instead. The **CM** indicates the oRSM and pRSM based on how similar the activations were between aurally and visually presented letters and digits.

5.3.3 Amodal letter identity representations

I proposed that a brain area encodes amodal ALI representations if it meets two criteria. First, the brain area must represent abstract letter identities (and therefore abstract representational content); and second, these ALI representations must be multimodal (i.e., similar patterns of activation are produced for letters that share the same identity despite being presented in different modalities). For example, a brain area that encodes amodal ALIs would produce a similar pattern of activation **a**, **A** and /ei/ while the patterns for **E** and /di/ would be different.

The experiment presented in this chapter sought out amodal ALIs within VOIs defined as either Retinotopic, responsive to Visual Alphanumeric stimuli, responsive to Auditory Alphanumeric Name stimuli, and selective to ALI representations. Three VOIs were shown to respond similarly to alphanumeric stimuli that share the same identity across visually and auditory input modalities. Crucially, the ALI localizer VOI, which was selected in virtue of selectively representing the abstract letter identity of visually presented letters, was shown to represent ALIs amodally. The two other VOIs were the Bilateral Retinotopic VOI and the Visual Alphanumeric VOI in the left fusiform gyrus.

Consistent with previous research, the left ventral temporal and occipital cortex appears to represent letter stimuli from different input modalities. This region has been shown to be active in response to braille reading (Büchel et al., 1998) and even auditory information that conveys shape information (Striem-Amit et al., 2012). The present findings suggest that this ventral occipital region may not only represent shape information multi-modally, but may represent ALI information multi-modally (amodal ALI representations).

5.4 Conclusions

In the experiment described in this chapter, visually and aurally alphanumeric stimuli were presented to participants in an fMRI scanner to see the effect of different input modalities on the representational content of alphanumeric representations. Of particular interest was determining whether ALI representations (previously defined as case-invariant letter representations) were invariant to input modality as well. While previous research has found that neural signals evoked by auditory and visual stimuli that share the same identity are similar (Man et al., 2012), the representational content that drives this similarity has rarely been investigated (but see Fairhall & Caramazza, 2013). Results from this experiment found an ALI cluster within the left medial ventral visual cortex that represented ALIs amodally. The finding from this cortical region supports the notion that ALI representations are amodal as well, acting as an intermediary between the various modality specific representations.

Chapter 6 – Summary and conclusions

The research in this dissertation used novel behavioral experimental tasks and integrated them with fMRI data in order to further examine the set of representations that are involved in letter identification and processing. Additionally, fMRI studies helped to lay out the neurotopography of these representations. Two of the most important contributions were novel behavioral and neuroimaging evidence for font-invariant allograph representations and neuroimaging evidence for amodal as well as case-invariant ALI representations.

The behavioral experiments examined visual similarity judgments as well as RTs and errors from a same-different decision task with visually presented pairs of letters. These experiments took advantage of the fact that both the visual similarity judgments and same-different decision RTs and errors were influenced by multiple types of letter representations above and beyond font-specific computed stimulus shape representations. By using a difficult-to-recognize rotated gridfont stimuli as a baseline, I found that when participants judged the visual similarity of identifiable upright gridfont stimuli (or made physical same-different decisions about them), their responses were biased towards the similarity structure of stored, font-invariant allographs (estimated by the visual similarity of a more typical font) as well as by abstract letter identity, case similarity and motor production feature similarity. This was interpreted as providing evidence that these stored letter representations were accessed in behavioral tasks that did not require them for accurate performance. While evidence for ALIs has previously come from multiple methodologies, evidence for stored allographs has been largely limited to cognitive neuropsychological case studies of individuals with developmental or acquired dyslexia

(Brunsdon et al., 2006; Schubert & McCloskey, 2014). Therefore, demonstrating the influence of stored allograph representations in behavioral measures with neurotypical individuals provided a novel source of evidence for allograph representations (see also Walker & Hinkley, 2003).

In addition to the behavioral evidence, neural evidence of stored allographs was obtained by presenting the upright gridfont in an fMRI scanner and computing the pair-wise similarity of the multi-voxel activation patterns triggered by each gridfont letter/digit stimulus. By examining the neural/observed representational similarity structures derived from retinotopically defined cortical regions as well as regions that were generally responsive to alphanumeric stimuli, I found that the retinotopic regions, particularly in the right hemisphere, were selective to the font-specific computed stimulus shape similarity (as estimated by the similarity judgments of the rotated gridfont) while the left Alphanumeric VOIs were selective to the font-invariant allograph representations (estimated by the similarity judgments to the typical letter font). This finding both provides a novel source of evidence for allograph representations and identifies the neural substrates of allograph representations and, in doing so, furthers our understanding of how letters and words are processed in the brain.

A final experiment set out to expand upon the work by Rothlein and Rapp (2014) concerning the identification of neural substrates that selectively encode ALI representations. Specifically the question addressed was: In addition to abstracting away from visual form entirely, do ALI representation also abstract away from input modality as well? (Are ALI representations amodal?) This question was investigated by examining if visually and aurally presented alphanumeric stimuli that share the same identity activate the same identity representation. By identifying voxels involved in ALI representation (replicating the findings from Rothlein and Rapp, 2014) and comparing the multi-voxel pattern of visually and aurally presented stimuli within the ALI cluster, I found evidence that ALI representations identified in that posterior left fusiform cluster were also amodal.

While elucidating the representations that mediate letter identification and multimodal letter processing is an important endeavor, the methods and experimental logic described in this experiment can be applied to domains beyond letter and word processing. For example, I presented evidence for allograph representations by demonstrating that the similarity of atypical exemplars is influenced by the visual similarity of typical exemplars. Do other categories of objects like chairs or birds have allograph-like stored shapes representations as well? Could their neural substrates be identified by presenting a set of atypical stimuli (e.g., chairs, birds, cars) to participants in an fMRI scanner and, applying RSA analyses, see if there are regions where the similarity structure of neural responses to these atypical stimuli reflects of the visual similarity of the typical versions of the presented stimuli? Using RSA to localizing stored shape information would allow researchers to analyze neural responses in these regions to learn more about the content and format of these stored shape representations.

Within the domain of letter processing, while the experiment in Ch. 5 explored the neural responses to letters presented across different input modalities, comparing the representation in identification vs. production would be very interesting. Are the allograph representations that mediate recognition also involved in motoric letter production? Are the phonological letter name representations that mediate auditory letter recognition also involved in letter naming tasks? Exploring this efferent/afferent relationship by examining the representational content of activation patterns involved in these tasks could provide a new source of evidence in understanding the relationship between sensory and motor representations.

In sum, the findings in the set of experiments described in this dissertation support the cognitive architecture of letter and word processes presented in Figure 2. Specifically, this model posits increasingly abstract representations that serve as a conduit between modality specific representations and lexical / orthographic processing. This abstractionist account is inconsistent with grounded / episodic views of cognition that posit cognitive tasks like reading do not use abstract representations (Barsalou, 2010; Tulving, 1985). Our results demonstrate a clear progression from sensory representations that encode font-specific information to spatial representations that encode font-invariant stored shape information (allographs) to amodal identity representations that encode abstract identity regardless of the input modality.

REFERENCES

Adams, M. J. (1979). Models of Word Recognition. *Cognitive Psychology*, *11*, 133–176.

Barsalou, L. W. (2008). Grounded cognition. *Annual Review of Psychology*, *59*, 617–45.

Barsalou, L. W. (2010). Grounded Cognition: Past, Present, and Future. *Topics in Cognitive Science*, *2*(4), 716–724.

Behrmann, M., & Plaut, D. C. (2013). Distributed circuits, not circumscribed centers, mediate visual recognition. *Trends in Cognitive Sciences*, *17*(5), 210–9.

Berent, I., & Van Orden, G. C. (2000). Homophone Dominance Modulates the Phonemic-Masking Effect. *Scientific Studies of Reading*, *4*(2), 133–167.

Besner, D., Coltheart, M., & Davelaar, E. (1984). Basic processes in reading: computation of abstract letter identities. *Canadian Journal of Psychology*, *38*(1), 126–34.

Boles, D. B., & Clifford, J. E. (1989). An upper- and lowercase alphabetic similarity matrix, with derived generation similarity values. *Behavior Research Methods, Instruments, & Computers*, *21*(6), 579–586.

Bonner, M. F., Peelle, J. E., Cook, P. a, & Grossman, M. (2013). Heteromodal conceptual processing in the angular gyrus. *NeuroImage*, *71*, 175–86.

Bowers, J. S. (2000). In defense of abstractionist theories of repetition priming and word identification. *Psychonomic Bulletin & Review*, *7*(1), 83–99.

Bowers, J. S., Vigliocco, G., & Haan, R. (1998). Orthographic, phonological, and articulatory contributions to masked letter and word priming. *Journal of Experimental Psychology. Human Perception and Performance*, *24*(6), 1705–19.

Boynton, G. M., Engel, S. A., Glover, G. H., & Heeger, D. J. (1996). Linear systems analysis of functional magnetic resonance imaging in human V1. *J. Neurosci.*, *16*, 4207–4221.

Brunsdon, R., Coltheart, M., & Nickels, L. (2006). Severe developmental letter-processing impairment: A treatment case study. *Cognitive Neuropsychology*, *23*(6), 795–821.

Büchel, C., Price, C., & Friston, K. (1998). A multimodal language region in the ventral visual pathway. *Nature*, *394*(6690), 274–7.

Buchwald, A., & Rapp, B. (2006). Consonants and vowels in orthographic representations. *Cognitive Neuropsychology*, *23*(2), 308–337.

Cantlon, J. F., Pinel, P., Dehaene, S., Pelphrey, K. A., Unit, N., Yvette, F.-G., … Paris-, U. (2011). Cortical Representations of Symbols , Objects , and Faces Are Pruned Back during Early Childhood. *Cerebral Cortex*, (January), 191–199.

Caramazza, A., & Hillis, A. E. (1990). Spatial representation of words in the brain implied by studies of a unilateral neglect patient. *Nature*, *346*, 267–269.

Carrasco, M., Kinchla, R., & Figueroa, J. (1988). Visual letter-matching and the time course of visual and acoustic codes. *Acta Psychologica*, *69*, 1–17.

Carreiras, M., Gillon-Dowens, M., Vergara, M., & Perea, M. (2009). Are vowels and consonants processed differently? Event-related potential evidence with a delayed letter paradigm. *Journal of Cognitive Neuroscience*, *21*(2), 275–88.

Carreiras, M., Perea, M., Gil-lópez, C., Mallouh, R. A., & Salillas, E. (2012). Neural Correlates of Visual versus Abstract Letter Processing in Roman and Arabic Scripts, 1975–1985.

Carreiras, M., & Price, C. J. (2008). Brain activation for consonants and vowels. *Cerebral Cortex (New York, N.Y. : 1991)*, *18*(7), 1727–35.

Chanoine, V., Ferreira, C. T., Demonet, J. F., Nespoulous, J. L., & Poncet, M. (1998). Optic aphasia with pure alexia: a mild form of visual associative agnosia? A case study. *Cortex; a Journal Devoted to the Study of the Nervous System and Behavior*, *34*(3), 437–448.

Chen, J., & Proctor, R. W. (2012). Influence of category identity on letter matching: Conceptual penetration of visual processing or response competition? *Attention, Perception & Psychophysics*, 716–729.

Cohen, L., Dehaene, S., Naccache, L., Lehéricy, S., Dehaene-Lambertz, G., Hénaff, M. a, & Michel, F. (2000). The visual word form area: spatial and temporal characterization of an initial stage of reading in normal subjects and posterior split-brain patients. *Brain*, *123*, 291–307.

Coltheart, M. (1981). Disorders of reading and their implications for models of normal reading. *Visible Language*, *15*, 245–286.

Connolly, A. C., Guntupalli, J. S., Gors, J., Hanke, M., Halchenko, Y. O., Wu, Y.-C., … Haxby, J. V. (2012). The representation of biological classes in the human brain. *The Journal of Neuroscience : The Official Journal of the Society for Neuroscience*, *32*(8), 2608–18.

Connor, C. E., Brincat, S. L., & Pasupathy, A. (2007). Transformation of shape information in the ventral pathway. *Current Opinion in Neurobiology*, *17*(2), 140–7.

Courrieu, P., Farioli, F., & Grainger, J. (2004). Inverse discrimination time as a perceptual distance for alphabetic characters. *Visual Cognition*, *11*(7), 901–919.

Dalmás, J. F., & Dansilio, S. (2000). Visuographemic alexia: a new form of a peripheral acquired dyslexia. *Brain and Language*, *75*(1), 1–16.

Dehaene, S., & Cohen, L. (2011). The unique role of the visual word form area in reading. *Trends in Cognitive Sciences*, 1–9.

Dehaene, S., Cohen, L., Sigman, M., & Vinckier, F. (2005). The neural code for written words: a proposal. *Trends in Cognitive Sciences*, *9*(7), 335–41.

Dehaene, S., Jobert, A., Naccache, L., Ciuciu, P., Poline, J.-B., Le Bihan, D., & Cohen, L. (2004). Letter binding and invariant recognition of masked words: Behavioral and neuroimaging evidence. *Psychological Science : A Journal of the American Psychological Society / APS*, *15*(5), 307–13.

Dehaene, S., Naccache, L., Cohen, L., Bihan, D. L., Mangin, J. F., Poline, J. B., & Rivière, D. (2001). Cerebral mechanisms of word masking and unconscious repetition priming. *Nature Neuroscience*, *4*(7), 752–8.

Dicarlo, J. J., Zoccolan, D., & Rust, N. C. (2012). How does the brain solve visual object recognition? *Neuron*, *73*(3), 415–34.

Dockeray, F. C. (1910). The span of vision in reading and the legibility of letters. *Journal of Educational Psychology*, *1*(3), 123–131.

Downing, P. E., Jiang, Y., Shuman, M., & Kanwisher, N. (2001). A cortical area selective for visual processing of the human body. *Science (New York, N.Y.)*, *293*(5539), 2470–3.

Drucker, D. M., & Aguirre, G. K. (2009). Different spatial scales of shape similarity representation in lateral and ventral LOC. *Cerebral Cortex (New York, N.Y. : 1991)*, *19*(10), 2269–80.

Eckert, M. a, Kamdar, N. V, Chang, C. E., Beckmann, C. F., Greicius, M. D., & Menon, V. (2008). A cross-modal system linking primary auditory and visual cortices: evidence from intrinsic fMRI connectivity analysis. *Human Brain Mapping*, *29*(7), 848–57.

Edelman, S. (1998). Representation is representation of similarities. *The Behavioral and Brain Sciences*, *21*(4), 449–67.

Egeth, H., & Blecker, D. (1971). Differential effects of familiarity on judgments of sameness and difference. *Perception & Psychophysics*, *9*(4), 321–326.

Epstein, R., & Kanwisher, N. (1998). A cortical representation of the local visual environment. *Nature*, *392*(6676), 598–601.

Etzel, J. a, Zacks, J. M., & Braver, T. S. (2013). Searchlight analysis: promise, pitfalls, and potential. *NeuroImage*, *78*, 261–269.

Fairhall, S. L., & Caramazza, a. (2013). Brain Regions That Represent Amodal Conceptual Knowledge. *Journal of Neuroscience*, *33*(25), 10552–10558.

Fisher, D. F., Monty, R. A., & Glucksberg, S. (1969). Visual confusion matrices: Fact or artifact? *The Journal of Psychology*, *71*(1), 111–125.

Flowers, D. L., Jones, K., Noble, K., VanMeter, J., Zeffiro, T. a, Wood, F. B., & Eden, G. F. (2004). Attention to single letters activates left extrastriate cortex. *NeuroImage*, *21*(3), 829–39.

Friston, K., Holmes, A., Worsley, K., Poline, J.-P., Frith, C. D., & Frackowiak, R. S. J. (1995). Statistical parametric maps in functional imaging: a general linear approach. *Human Brain Mapping*, *2*, 189–210.

Gauthier, I., Skudlarski, P., Gore, J. C., & Anderson, A. W. (2000). Expertise for cars and birds recruits brain areas involved in face recognition. *Nature Neuroscience*, *3*(2), 191–7.

Gauthier, I., Tarr, M. J., Anderson, A. W., Skudlarski, P., & Gore, J. C. (1999). Activation of the middle fusiform "face area" increases with expertise in recognizing novel objects. *Nature Neuroscience*, *2*(6), 568–73.

Gauthier, I., Tarr, M. J. J., Moylan, J., Skudlarski, P., Gore, J. C., & Anderson, A. W. (2000). The fusiform "face area" is part of a network that processes faces at the individual level. *Journal of Cognitive Neuroscience*, *12*(3), 495–504.

Geyer, L. H., & Dewald, C. G. (1973). Feature lists and confusion matrices. *Perception & Psychophysics*, *14*(3), 471–482.

Gilmore, G. C., Hersh, H., Caramazza, a, & Griffin, J. (1979). Multidimensional letter similarity derived from recognition errors. *Perception & Psychophysics*, *25*(5), 425–31.

Goldinger, S. D. (1998). Echoes of echoes? An episodic theory of lexical access. *Psychological Review*, *105*(2), 251–79.

Goldstone, R. (1994). Influences of categorization on perceptual discrimination. *Journal of Experimental Psychology. General*, *123*(2), 178–200.

Grainger, J., Rey, A., & Dufau, S. (2008). Letter perception: from pixels to pandemonium. *Trends in Cognitive Sciences*, *12*(10), 381–7.

Gupta, S. M., Geyer, L. H., & Maalouf, J. A. (1983). Effect of font and medium on recognition/confusion. In *Association for Computing Machinery: CHI'83 Proceedings* (pp. 144–149).

Hannagan, T., Amedi, A., Cohen, L., Dehaene-lambertz, G., & Dehaene, S. (2015). Origins of the specialization for letters and numbers in ventral occipitotemporal cortex. *Trends in Cognitive Sciences*, 1–9.

Herrick, E. M. (1974). A Taxonomy of Alphabets and Scripts. *Visible Language*, *8*(1), 5–32.

Hillis, a E., & Caramazza, a. (1991). Deficit to stimulus-centered, letter shape representations in a case of "unilateral neglect". *Neuropsychologia*, *29*(12), 1223–40.

Hofstadter, D. R., & McGraw, G. (1995). Letter Spirit: esthetic perception and creative play in the rich microcosm of the Roman alphabet. In *Fluid Concepts and Creative Analogies. Computer models of the fundamental mechanisms of thought* (pp. 407–466). New York, NY: BasicBooks.

Hull, A. J. (1973). A letter-digit matrix of auditory confusions. *British Journal of Psychology (London, England : 1953)*, *64*(4), 579–585.

James, K. H., & Atwood, T. P. (2009). The role of sensorimotor learning in the perception of letter-like forms: tracking the causes of neural specialization for letters. *Cognitive Neuropsychology*, *26*(1), 91–110.

James, K. H., & Gauthier, I. (2006). Letter processing automatically recruits a sensory-motor brain network. *Neuropsychologia*, *44*(14), 2937–49.

James, K. H., James, T. W., Jobard, G., Wong, A. C. N., & Gauthier, I. (2005). Letter processing in the visual system: different activation patterns for single letters and strings. *Cognitive, Affective & Behavioral Neuroscience*, *5*(4), 452–66.

Kanwisher, N., McDermott, J., & Chun, M. M. (1997). The fusiform face area: a module in human extrastriate cortex specialized for face perception. *The Journal of Neuroscience : The Official Journal of the Society for Neuroscience*, *17*(11), 4302–11.

Kim, J. G., Biederman, I., Lescroart, M. D., & Hayworth, K. J. (2009). Adaptation to objects in the lateral occipital complex (LOC): shape or semantics? *Vision Research*, *49*(18), 2297–305.

Kinoshita, S., & Kaplan, L. (2008). Priming of abstract letter identities in the letter match task. *Quarterly Journal of Experimental Psychology (2006)*, *61*(12), 1873–85.

Kourtzi, Z., & Connor, C. E. (2011). Neural representations for object perception: structure, category, and adaptive coding. *Annual Review of Neuroscience*, *34*, 45–67.

Kourtzi, Z., & Kanwisher, N. (2001). Representation of perceived object shape by the human lateral occipital complex. *Science (New York, N.Y.)*, *293*(5534), 1506–9.

Kriegeskorte, N. (2011). Pattern-information analysis: from stimulus decoding to computational-model testing. *NeuroImage*, *56*(2), 411–421.

Kriegeskorte, N., Mur, M., & Bandettini, P. (2008). Representational similarity analysis - connecting the branches of systems neuroscience. *Frontiers in Systems Neuroscience*, *2*(4), 1–28.

Ley, A., Vroomen, J., Hausfeld, L., Valente, G., De Weerd, P., & Formisano, E. (2012). Learning of new sound categories shapes neural response patterns in human auditory cortex. *The Journal of Neuroscience : The Official Journal of the Society for Neuroscience*, *32*(38), 13273–80.

Longcamp, M., Anton, J.-L., Roth, M., & Velay, J.-L. (2003, August). Visual presentation of single letters activates a premotor area involved in writing. *NeuroImage*, *19*(4), 1492–1500.

Longcamp, M., Boucard, C., Gilhodes, J.-C., Anton, J.-L., Roth, M., Nazarian, B., & Velay, J.-L. (2008). Learning through hand- or typewriting influences visual recognition of new graphic shapes: behavioral and functional imaging evidence. *Journal of Cognitive Neuroscience*, *20*(5), 802–15.

Lupyan, G. (2012). Linguistically modulated perception and cognition: the label-feedback hypothesis. *Frontiers in Psychology*, *3*(March), 54.

Lupyan, G., Thompson-Schill, S. L., & Swingley, D. (2010). Conceptual penetration of visual processing. *Psychological Science*, *21*(5), 682–91.

Man, K., Kaplan, J. T., Damasio, a., & Meyer, K. (2012). Sight and Sound Converge to Form Modality-Invariant Representations in Temporoparietal Cortex. *Journal of Neuroscience*, *32*(47), 16629–16636.

Marsolek, C. (2004). Abstractionist versus exemplar-based theories of visual word priming: a subsystems resolution. *The Quarterly Journal of Experimental Psychology. A, Human Experimental Psychology*, *57*(7), 1233–59.

Marsolek, C. J. (1995). Abstract visual-form representations in the left cerebral hemisphere. *Journal of Experimental Psychology. Human Perception and Performance*, *21*(2), 375–86.

Marsolek, C. J. (1999). Dissociable neural subsystems underlie abstract and specific object recognition. *Psychological Science : A Journal of the American Psychological Society / APS*, *10*(2), 111–118.

McClelland, J. L. (1976). Preliminary Letter Identification in the Perception of Words and Nonwords. *Journal of Experimental Psychology: Human Perception and Performance*, *2*(1), 80–91.

McClelland, J. L., & Rumelhart, D. E. (1981). An interactive activation model of context effects in letter perception: I. An account of basic findings. *Psychological Review*, *88*(5), 375–407.

McCloskey, M., Badecker, W., Goodman-schulman, R. A., & Aliminosa, D. (1994). The structure of graphemic representations in spelling: Evidence from a case of acquired dysgraphia. *Cognitive Neuropsychology*, *11*(3), 341–392.

McCloskey, M., Fischer-Baum, S., & Schubert, T. (2014). Representation of letter position in single-word reading: Evidence from acquired dyslexia. *Cognitive Neuropsychology*, *30*(6), 396–428.

McFarland, C., Frey, T., & Landreth, J. (1978). The acquisition of abstract letter codes. *Journal of Experimental Child*, *25*, 437–446.

Miller, P., & Vaknin, V. (2012). The involvement of letter names in the silent processing of isolated letters: A developmental perspective. *Memory & Cognition*, *40*(8), 1276–88.

Miozzo, M., & Caramazza, A. (1998). Varieties of Pure Alexia: The Case of Failure to Access Graphemic Representations. *Cognitive Neuropsychology*, *15*, 203– 238.

Mueller, S. T., & Weidemann, C. T. (2012). Alphabetic letter identification: effects of perceivability, similarity, and bias. *Acta Psychologica*, *139*(1), 19–37.

Mur, M., Meys, M., Bodurka, J., Goebel, R., Bandettini, P. a, & Kriegeskorte, N. (2013). Human Object-Similarity Judgments Reflect and Transcend the Primate-IT Object Representation. *Frontiers in Psychology*, *4*(March), 128.

Mycroft, R., Hanley, J. R., & Kay, J. (2002). Preserved access to abstract letter identities despite abolished letter naming in a case of pure alexia. *Journal of Neurolinguistics*, *15*(2), 99–108.

Op de Beeck, H. P., Torfs, K., & Wagemans, J. (2008). Perceived shape similarity among unfamiliar objects and the organization of the human object vision pathway. *The Journal of Neuroscience : The Official Journal of the Society for Neuroscience*, *28*(40), 10111–23.

Panis, S., Vangeneugden, J., & Wagemans, J. (2008). Similarity, typicality, and category-level matching of morphed outlines of everyday objects. *Perception*, *37*, 1822–1849.

Park, J., Hebrank, A., Polk, T. A., & Park, D. C. (2011). Neural Disscociation of Number from Letter Recognition and Its Relationship to Parietal Numerical Processing. *Journal of Cognitive Neuroscience*,

Pascual-Leone, A., & Hamilton, R. (2001). The metamodal organization of the brain. *Progress in Brain Research*, *134*, 427–45.

Pernet, C., Celsis, P., & Démonet, J.-F. (2005). Selective response to letter categorization within the left fusiform gyrus. *NeuroImage*, *28*(3), 738–44.

Plaut, D. C., & Behrmann, M. (2011). Complementary neural representations for faces and words: a computational exploration. *Cognitive Neuropsychology*, *28*(3-4), 251–75.

Podgorny, P., & Garner, W. R. (1979). Reaction time as a measure of inter- and intraobject visual similarity: letters of the alphabet. *Perception*, *26*(1), 37–52.

Polk, T. a, Stallcup, M., Aguirre, G. K., Alsop, D. C., D'Esposito, M., Detre, J. a, & Farah, M. J. (2002). Neural specialization for letter recognition. *Journal of Cognitive Neuroscience*, *14*(2), 145–59.

Polk, T. A., & Farah, M. J. (1997). A simple common contexts explanation for the development of abstract letter identities. *Neural Computation*, *9*, 1277–1289.

Polk, T. A., & Farah, M. J. (2002). Functional MRI evidence for an abstract, not perceptual, word-form area. *Journal of Experimental Psychology. General*, *131*(1), 65–72.

Posner, M. I., Boies, S. J., Eichelman, W. H., & Taylor, R. L. (1969). Retention of visual and name codes of single letters. *Journal of Experimental Psychology*, *79*(1), 1–16.

Price, G. R., & Ansari, D. (2011). Symbol processing in the left angular gyrus: Evidence from passive perception of digits. *NeuroImage*, *57*(3), 1205–1211.

Purcell, J. J., Shea, J., & Rapp, B. (2014). Beyond the visual word form area: The orthography-semantics interface in spelling and reading. *Cognitive Neuropsychology*, (May), 1–29.

Qiao, E., Vinckier, F., Szwed, M., Naccache, L., Valabrègue, R., Dehaene, S., & Cohen, L. (2010). Unconsciously deciphering handwriting: subliminal invariance for handwritten words in the visual word form area. *NeuroImage*, *49*(2), 1786–99.

Raij, T., Uutela, K., & Hari, R. (2000). Audiovisual integration of letters in the human brain. *Neuron*, *28*(2), 617–25.

Rapp, B. C., & Caramazza, A. (1989). Letter Processin in Reading and Spelling: Some Dissociations. *Reading and Writing: An Interdisciplinary Journal*, *1*, 3–23.

Rapp, B., & Caramazza, A. (1997). From graphemes to abstract letter shapes: levels of representation in written spelling. *Journal of Experimental Psychology. Human Perception and Performance*, *23*(4), 1130–52.

Reich, L. N., & Bedell, H. E. (2000). Relative legibility and confusions of letter acuity targets in the peripheral and central retina. *Optometry and Vision Science : Official Publication of the American Academy of Optometry*, *77*(5), 270–5.

Riesenhuber, M., & Poggio, T. (1999). Hierarchical models of object recognition in cortex. *Nature Neuroscience*, *2*(11), 1019–25.

Rothlein, D., & Rapp, B. (2014). The similarity structure of distributed neural responses reveals the multiple representations of letters. *NeuroImage*, *89*, 331–44.

Schubert, T., & McCloskey, M. (2014). Prelexical representations and processes in reading: Evidence from acquired dyslexia. *Cognitive Neuropsychology*, *30*(6), 360–95.

Shepard, R. N. (1975). Form, formation, and transformation of internal representations. In R. L. Solso (Ed.), *Information processing and cognition: The Loyola Symposium* (pp. 87–117). Hillsdale, NJ: Earlbaum.

Shepard, R. N., & Chipman, S. (1970). Second-order isomorphism of internal representations: shapes of states. *Cognitive Psychology*, *1*, 1–17.

Shum, J., Hermes, D., Foster, B. L., Dastjerdi, M., Rangarajan, V., Winawer, J., … Parvizi, J. (2013). A brain area for visual numerals. *The Journal of Neuroscience : The Official Journal of the Society for Neuroscience*, *33*(16), 6709–15.

Simpson, I. C., Mousikou, P., Montoya, J. M., & Defior, S. (2012). A letter visual-similarity matrix for Latin-based alphabets. *Behavior Research Methods*.

Stein, B. E., & Meredith, M. A. (1993). *The merging of the senses. Cognitive neuroscience.*

Striem-Amit, E., Cohen, L., Dehaene, S., & Amedi, A. (2012). Reading with Sounds: Sensory Substitution Selectively Activates the Visual Word Form Area in the Blind. *Neuron*, *76*(3), 640–652.

Szwed, M., Dehaene, S., Kleinschmidt, A., Eger, E., Valabrègue, R., Amadon, A., & Cohen, L. (2011). Specialization for written words over objects in the visual cortex. *NeuroImage*, 1–15.

Szwed, M., Qiao, E., Jobert, A., Dehaene, S., & Cohen, L. (2014). Effects of literacy in early visual and occipitotemporal areas of Chinese and French readers. *Journal of Cognitive Neuroscience*, *26*(3), 459–75.

Tenpenny, P. L. (1995). Abstractionist versus episodic theories of repetition priming and word identification. *Psychonomic Bulletin & Review*, *2*(3), 339–363.

Tinker, M. A. (1928). The relative legibility of the letters, the digits, and of certain mathematical signs. *The Journal of General Psychology*, *1*, 472–496.

Tulving, E. (1983). *Essentials of episodic memory*. (O. U. Press, Ed.). New York.

Tulving, E. (1985). How many memory systems are there? *American Psychologist*, *40*(4), 385–398.

Turkeltaub, P. E., Flowers, D. L., Lyon, L. G., & Eden, G. F. (2008). Development of ventral stream representations for single letters. *Annals of the New York Academy of Sciences*, *1145*, 13–29.

van Atteveldt, N., Formisano, E., Goebel, R., & Blomert, L. (2004). Integration of letters and speech sounds in the human brain. *Neuron*, *43*(2), 271–82.

van Der Heijden, A. H. C., Malhas, M. S. M., & van Den Roovaart, B. P. (1984). An empirical interletter confusion matrix for continuous-line capitals. *Perception & Psychophysics*, *35*(1), 85–88.

Vinckier, F., Dehaene, S., Jobert, A., Dubus, J. P., Sigman, M., & Cohen, L. (2007). Hierarchical coding of letter strings in the ventral stream: dissecting the inner organization of the visual word-form system. *Neuron*, *55*(1), 143–56.

Walker, P., & Hinkley, L. (2003). Visual memory for shape-colour conjunctions utilizes structural descriptions of letter shape. *Visual Cognition*, *10*(8), 987–1000.

Watson, A. B., & Fitzhugh, A. E. (1989). Modelling character legibility. *Society*, 360–363.

Wilson, M. (2002). Six views of embodied cognition. *Psychonomic Bulletin & Review*, *9*(4), 625–36.

Yost, W. A. (1996). Pitch strength of iterated rippled noise. *The Journal of the Acoustical Society of America*, *100*(5), 3329.

APPENDIX

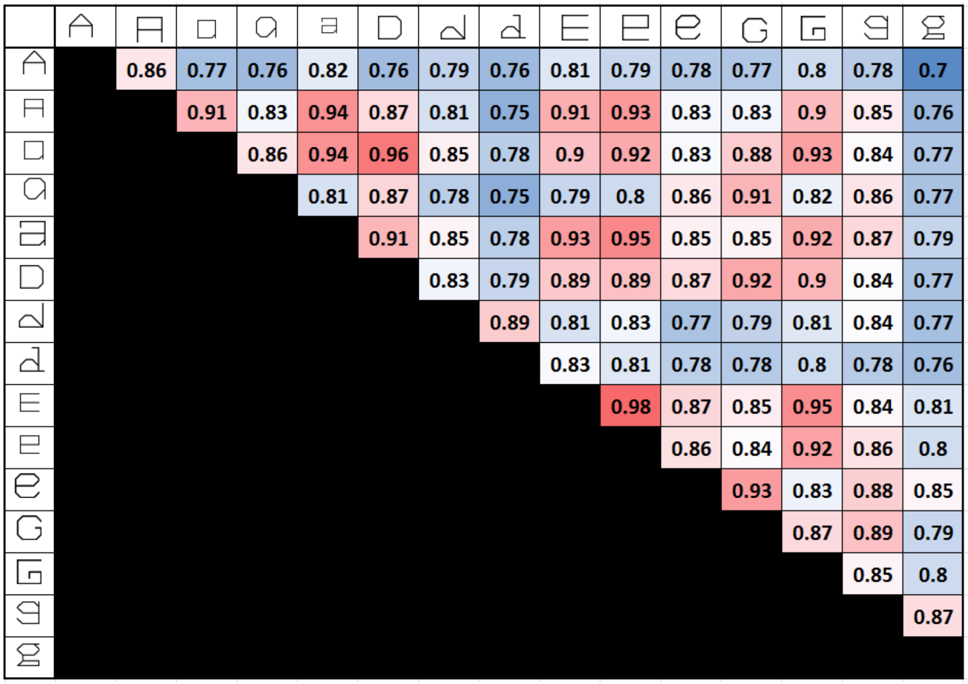

		0.86	0.77	0.76	0.82	0.76	0.79	0.76	0.81	0.79	0.78	0.77	0.8	0.78	0.7
			0.91	0.83	0.94	0.87	0.81	0.75	0.91	0.93	0.83	0.83	0.9	0.85	0.76
				0.86	0.94	0.96	0.85	0.78	0.9	0.92	0.83	0.88	0.93	0.84	0.77
					0.81	0.87	0.78	0.75	0.79	0.8	0.86	0.91	0.82	0.86	0.77
						0.91	0.85	0.78	0.93	0.95	0.85	0.85	0.92	0.87	0.79
							0.83	0.79	0.89	0.89	0.87	0.92	0.9	0.84	0.77
								0.89	0.81	0.83	0.77	0.79	0.81	0.84	0.77
									0.83	0.81	0.78	0.78	0.8	0.78	0.76
										0.98	0.87	0.85	0.95	0.84	0.81
											0.86	0.84	0.92	0.86	0.8
												0.93	0.83	0.88	0.85
													0.87	0.89	0.79
														0.85	0.8
															0.87

Appendix Figure 1. A sample of the Pixel-overlap pRSM for 15 of the 29 alphanumeric stimuli. Blacked-out cells were not included in the analysis.

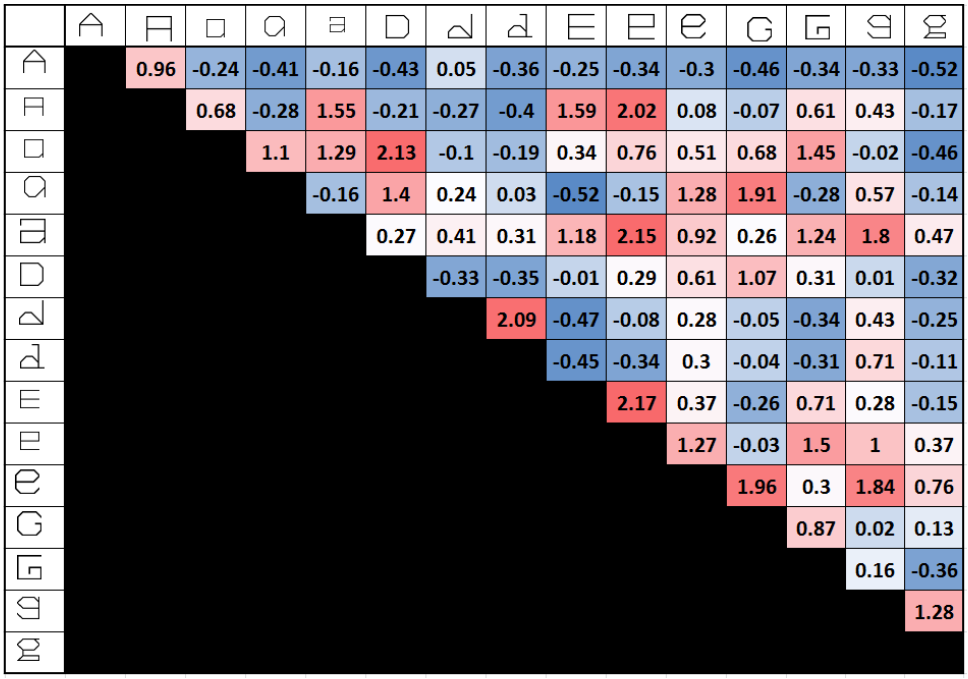

		0.96	-0.24	-0.41	-0.16	-0.43	0.05	-0.36	-0.25	-0.34	-0.3	-0.46	-0.34	-0.33	-0.52
			0.68	-0.28	1.55	-0.21	-0.27	-0.4	1.59	2.02	0.08	-0.07	0.61	0.43	-0.17
				1.1	1.29	2.13	-0.1	-0.19	0.34	0.76	0.51	0.68	1.45	-0.02	-0.46
					-0.16	1.4	0.24	0.03	-0.52	-0.15	1.28	1.91	-0.28	0.57	-0.14
						0.27	0.41	0.31	1.18	2.15	0.92	0.26	1.24	1.8	0.47
							-0.33	-0.35	-0.01	0.29	0.61	1.07	0.31	0.01	-0.32
								2.09	-0.47	-0.08	0.28	-0.05	-0.34	0.43	-0.25
									-0.45	-0.34	0.3	-0.04	-0.31	0.71	-0.11
										2.17	0.37	-0.26	0.71	0.28	-0.15
											1.27	-0.03	1.5	1	0.37
												1.96	0.3	1.84	0.76
													0.87	0.02	0.13
														0.16	-0.36
															1.28

Appendix Figure 2. A sample of the Stimulus Shape Similarity pRSM for 15 of the 29 alphanumeric stimuli. Blacked-out cells were not included in the analysis. The values in this pRSM are standardized z-scores.

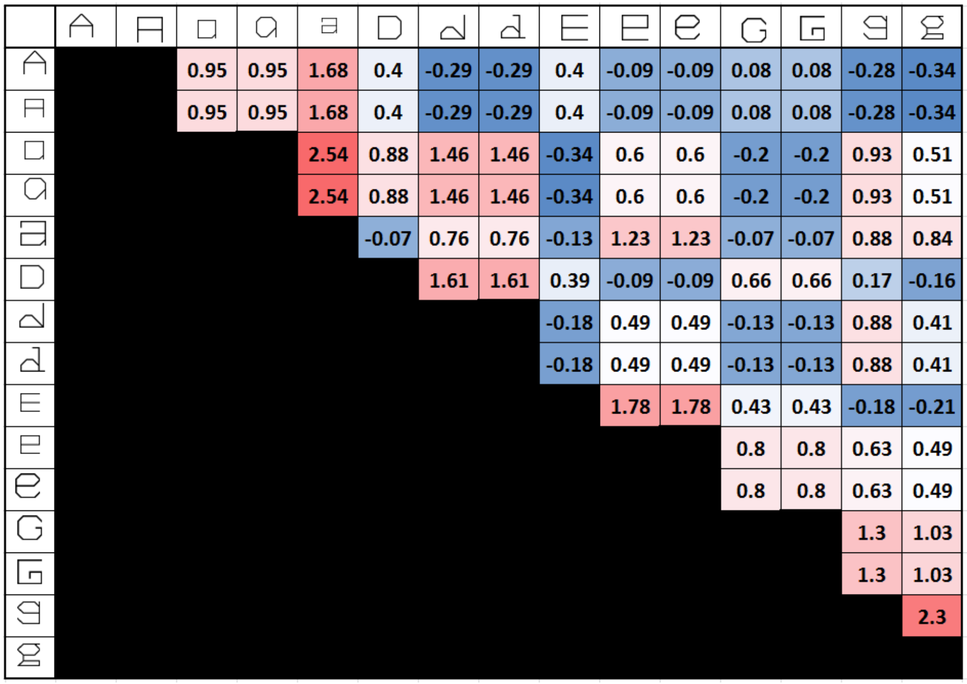

	A	A	a	a	a	D	d	d	E	E	e	G	G	g	g
A			0.95	0.95	1.68	0.4	-0.29	-0.29	0.4	-0.09	-0.09	0.08	0.08	-0.28	-0.34
A			0.95	0.95	1.68	0.4	-0.29	-0.29	0.4	-0.09	-0.09	0.08	0.08	-0.28	-0.34
a					2.54	0.88	1.46	1.46	-0.34	0.6	0.6	-0.2	-0.2	0.93	0.51
a					2.54	0.88	1.46	1.46	-0.34	0.6	0.6	-0.2	-0.2	0.93	0.51
a						-0.07	0.76	0.76	-0.13	1.23	1.23	-0.07	-0.07	0.88	0.84
D							1.61	1.61	0.39	-0.09	-0.09	0.66	0.66	0.17	-0.16
d									-0.18	0.49	0.49	-0.13	-0.13	0.88	0.41
d									-0.18	0.49	0.49	-0.13	-0.13	0.88	0.41
E										1.78	1.78	0.43	0.43	-0.18	-0.21
E												0.8	0.8	0.63	0.49
e												0.8	0.8	0.63	0.49
G														1.3	1.03
G														1.3	1.03
g															2.3
g															

Appendix Figure 3. A sample of the Allograph Similarity pRSM for 15 of the 29 alphanumeric stimuli. Blacked-out cells were not included in the analysis. The values in this pRSM are standardized z-scores.

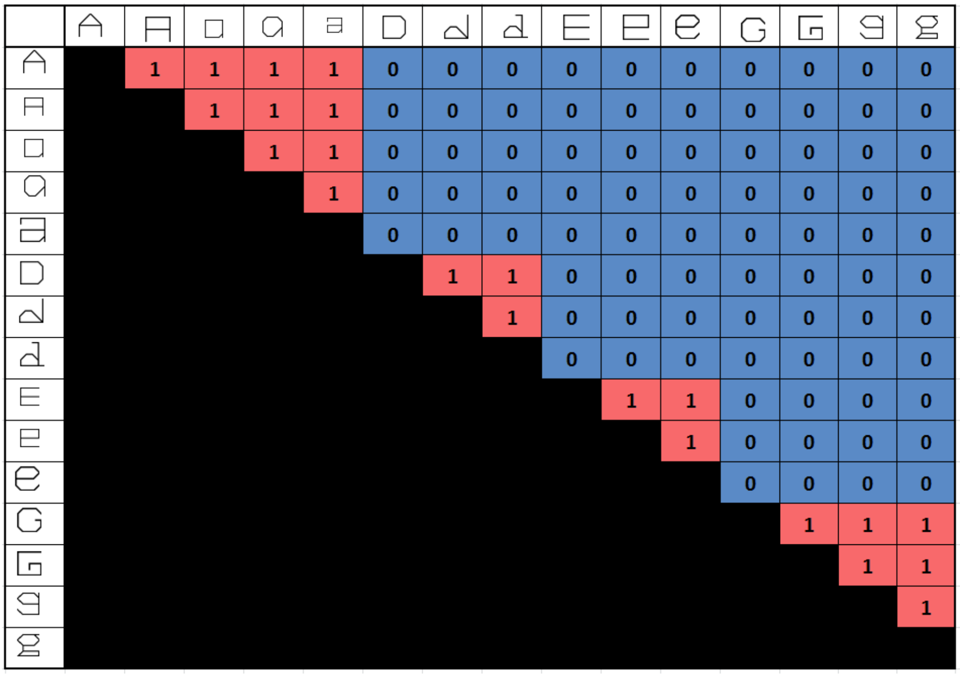

	A	A	a	a	a	D	d	d	E	E	e	G	G	g	g
A		1	1	1	1	0	0	0	0	0	0	0	0	0	0
A			1	1	1	0	0	0	0	0	0	0	0	0	0
a				1	1	0	0	0	0	0	0	0	0	0	0
a					1	0	0	0	0	0	0	0	0	0	0
a						0	0	0	0	0	0	0	0	0	0
D							1	1	0	0	0	0	0	0	0
d								1	0	0	0	0	0	0	0
d									0	0	0	0	0	0	0
E										1	1	0	0	0	0
E											1	0	0	0	0
e												0	0	0	0
G													1	1	1
G														1	1
g															1
g															

Appendix Figure 4. A sample of the Abstract Letter Identity pRSM for 15 of the 29 alphanumeric stimuli. Blacked-out cells were not included in the analysis.

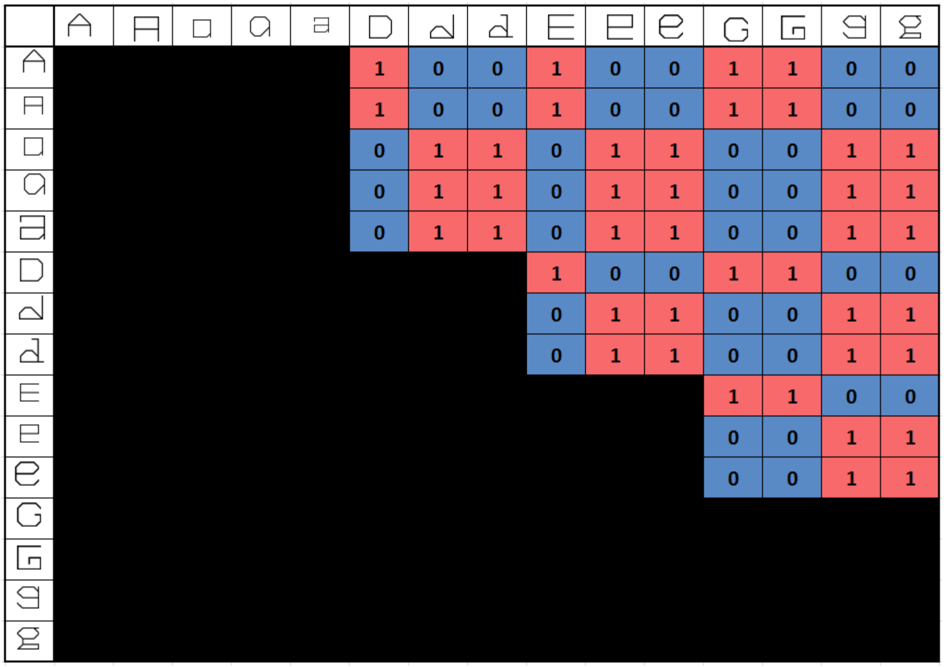

	A	A	a	a	a	D	d	d	E	E	e	G	G	g	g
A						1	0	0	1	0	0	1	1	0	0
A						1	0	0	1	0	0	1	1	0	0
a						0	1	1	0	1	1	0	0	1	1
a						0	1	1	0	1	1	0	0	1	1
a						0	1	1	0	1	1	0	0	1	1
D									1	0	0	1	1	0	0
d									0	1	1	0	0	1	1
d									0	1	1	0	0	1	1
E												1	1	0	0
E												0	0	1	1
e												0	0	1	1
G															
G															
g															
g															

Appendix Figure 5. A sample of the Case pRSM for 15 of the 29 alphanumeric stimuli. Blacked-out cells were not included in the analysis.

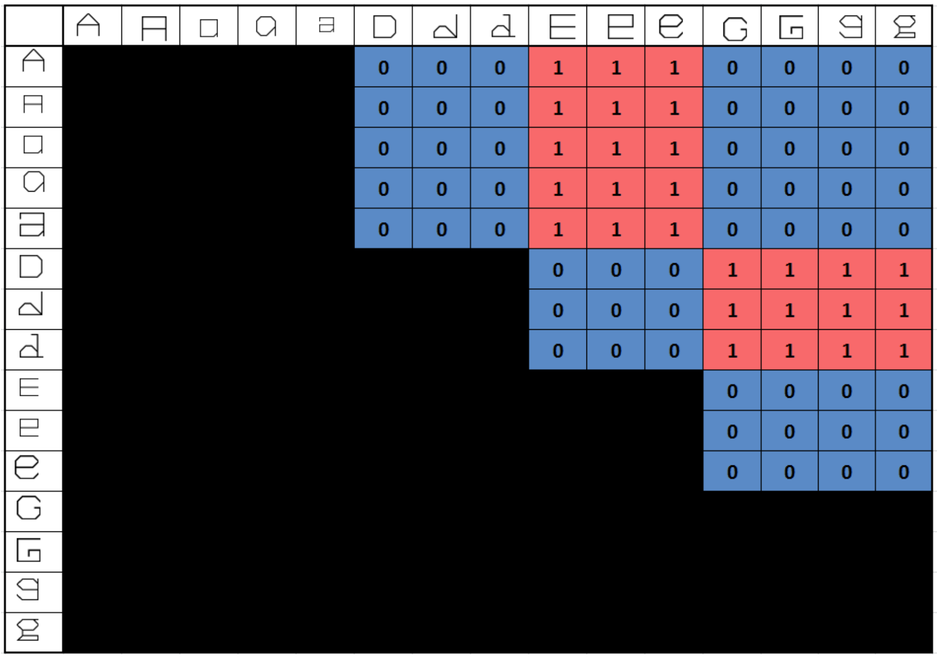

	A	A	a	a	a	D	d	d	E	E	e	G	G	g	g
A						0	0	0	1	1	1	0	0	0	0
A						0	0	0	1	1	1	0	0	0	0
a						0	0	0	1	1	1	0	0	0	0
a						0	0	0	1	1	1	0	0	0	0
a						0	0	0	1	1	1	0	0	0	0
D									0	0	0	1	1	1	1
d									0	0	0	1	1	1	1
d									0	0	0	1	1	1	1
E												0	0	0	0
E												0	0	0	0
e												0	0	0	0
G															
G															
g															
g															

Appendix Figure 6. A sample of the Consonant/Vowel pRSM for 15 of the 29 alphanumeric stimuli. Blacked-out cells were not included in the analysis.

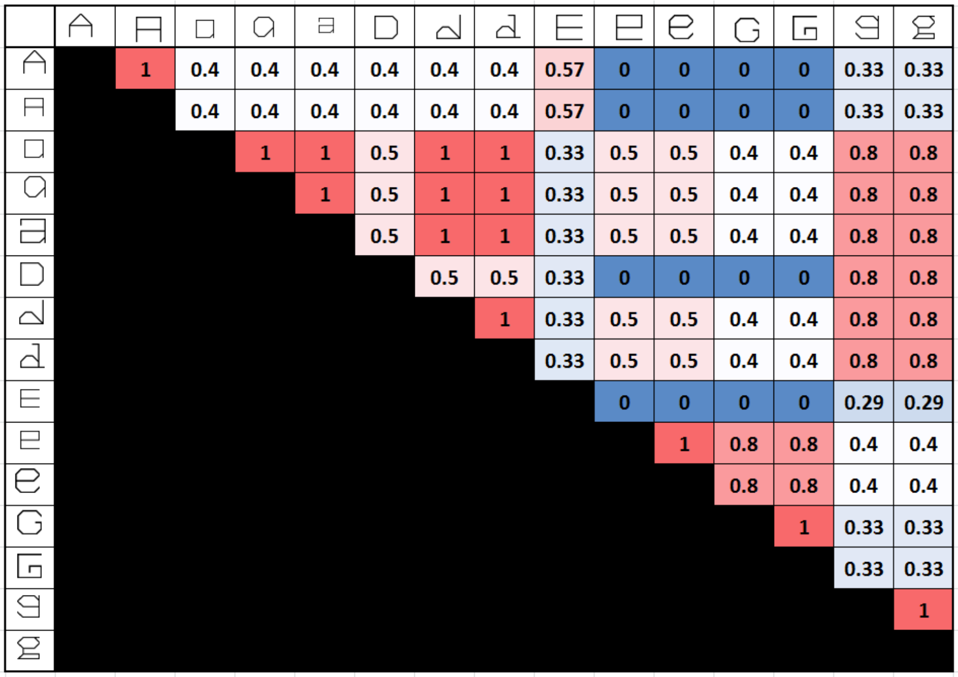

		1	0.4	0.4	0.4	0.4	0.4	0.4	0.57	0	0	0	0	0.33	0.33
			0.4	0.4	0.4	0.4	0.4	0.4	0.57	0	0	0	0	0.33	0.33
				1	1	0.5	1	1	0.33	0.5	0.5	0.4	0.4	0.8	0.8
					1	0.5	1	1	0.33	0.5	0.5	0.4	0.4	0.8	0.8
						0.5	1	1	0.33	0.5	0.5	0.4	0.4	0.8	0.8
							0.5	0.5	0.33	0	0	0	0	0.8	0.8
								1	0.33	0.5	0.5	0.4	0.4	0.8	0.8
									0.33	0.5	0.5	0.4	0.4	0.8	0.8
										0	0	0	0	0.29	0.29
											1	0.8	0.8	0.4	0.4
												0.8	0.8	0.4	0.4
													1	0.33	0.33
														0.33	0.33
															1

Appendix Figure 7. A sample of the Motor Feature Overlap pRSM for 15 of the 29 alphanumeric stimuli. Blacked-out cells were not included in the analysis.

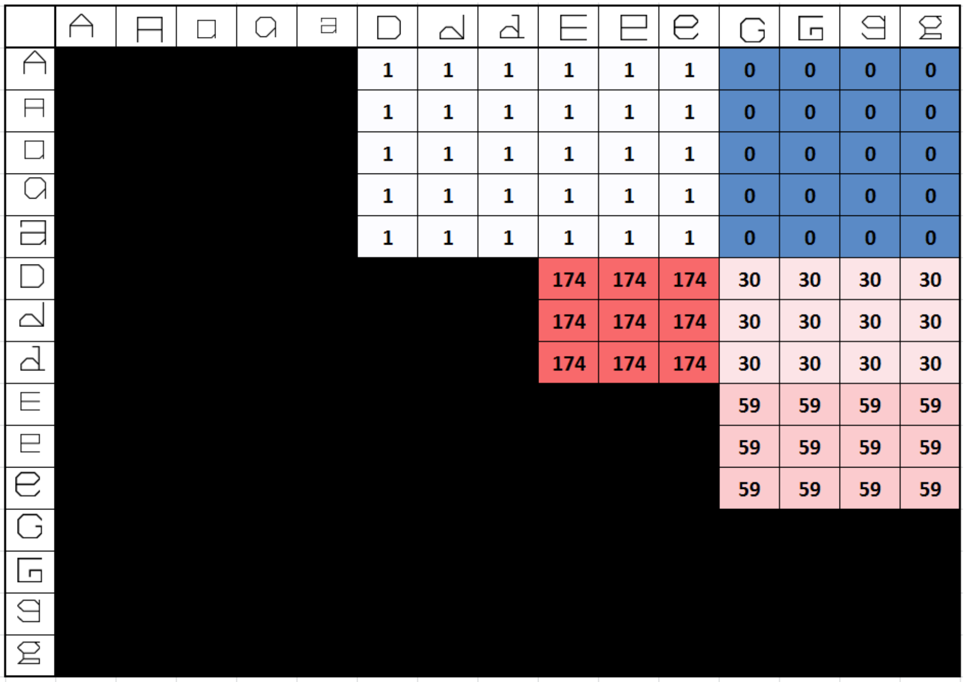

						1	1	1	1	1	1	0	0	0	0
						1	1	1	1	1	1	0	0	0	0
						1	1	1	1	1	1	0	0	0	0
						1	1	1	1	1	1	0	0	0	0
						1	1	1	1	1	1	0	0	0	0
									174	174	174	30	30	30	30
									174	174	174	30	30	30	30
									174	174	174	30	30	30	30
												59	59	59	59
												59	59	59	59
												59	59	59	59

Appendix Figure 8. A sample of the Letter Name Confusability pRSM for 15 of the 29 alphanumeric stimuli. Blacked-out cells were not included in the analysis.

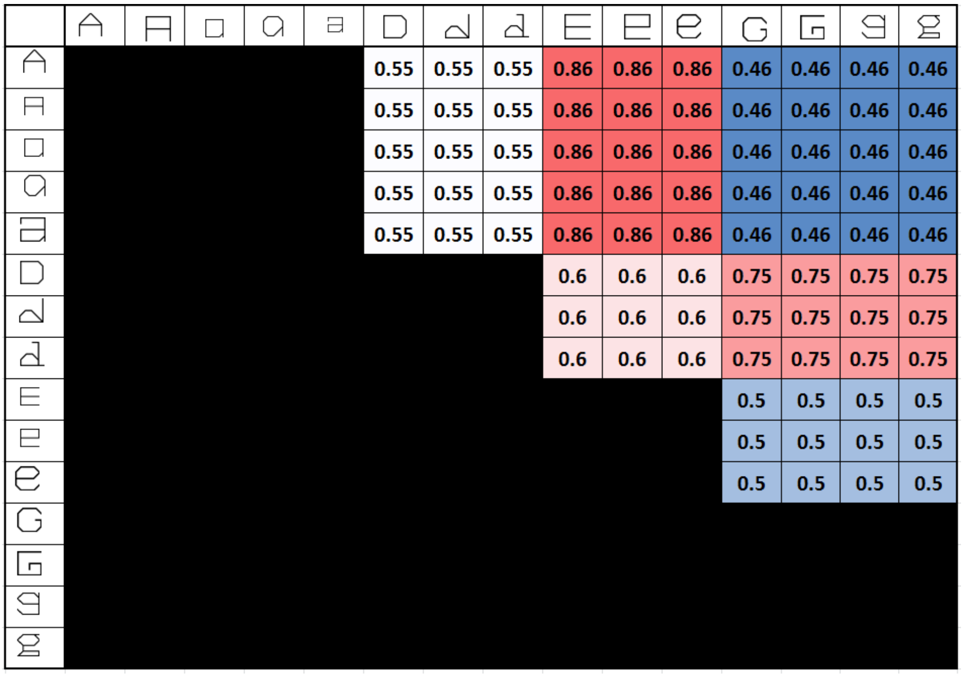

						0.55	0.55	0.55	0.86	0.86	0.86	0.46	0.46	0.46	0.46
						0.55	0.55	0.55	0.86	0.86	0.86	0.46	0.46	0.46	0.46
						0.55	0.55	0.55	0.86	0.86	0.86	0.46	0.46	0.46	0.46
						0.55	0.55	0.55	0.86	0.86	0.86	0.46	0.46	0.46	0.46
						0.55	0.55	0.55	0.86	0.86	0.86	0.46	0.46	0.46	0.46
									0.6	0.6	0.6	0.75	0.75	0.75	0.75
									0.6	0.6	0.6	0.75	0.75	0.75	0.75
									0.6	0.6	0.6	0.75	0.75	0.75	0.75
												0.5	0.5	0.5	0.5
												0.5	0.5	0.5	0.5
												0.5	0.5	0.5	0.5

Appendix Figure 9. A sample of the Phonetic Feature Overlap pRSM for 15 of the 29 alphanumeric stimuli. This pRSM was used in the Sensitivity and Correlation Analyses. Blacked-out cells were not included in the analysis.

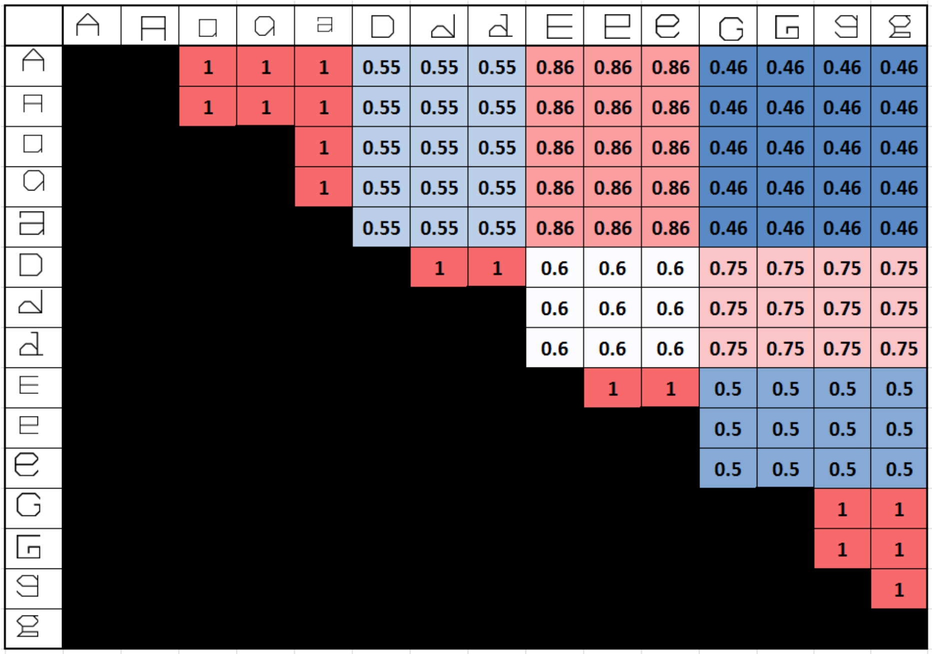

			1	1	1	0.55	0.55	0.55	0.86	0.86	0.86	0.46	0.46	0.46	0.46
			1	1	1	0.55	0.55	0.55	0.86	0.86	0.86	0.46	0.46	0.46	0.46
					1	0.55	0.55	0.55	0.86	0.86	0.86	0.46	0.46	0.46	0.46
					1	0.55	0.55	0.55	0.86	0.86	0.86	0.46	0.46	0.46	0.46
						0.55	0.55	0.55	0.86	0.86	0.86	0.46	0.46	0.46	0.46
							1	1	0.6	0.6	0.6	0.75	0.75	0.75	0.75
									0.6	0.6	0.6	0.75	0.75	0.75	0.75
									0.6	0.6	0.6	0.75	0.75	0.75	0.75
										1	1	0.5	0.5	0.5	0.5
												0.5	0.5	0.5	0.5
												0.5	0.5	0.5	0.5
														1	1
														1	1
															1

Appendix Figure 10. A sample of the Phonetic Feature Overlap pRSM for 15 of the 29 alphanumeric stimuli. This pRSM was used in the Selectivity and Regression Analyses. Blacked-out cells were not included in the analysis.

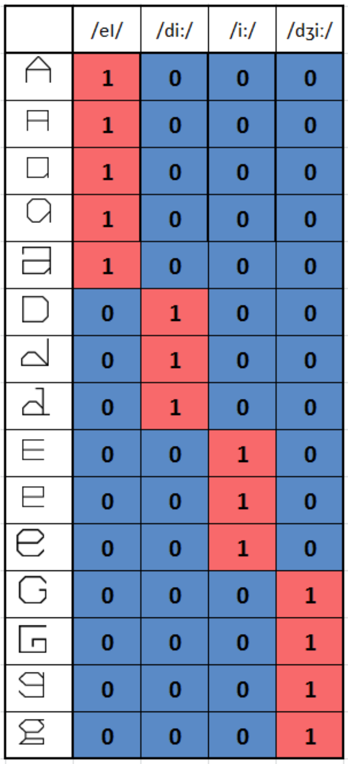

	/eI/	/di:/	/i:/	/dʒi:/
A	1	0	0	0
A	1	0	0	0
a	1	0	0	0
a	1	0	0	0
a	1	0	0	0
D	0	1	0	0
d	0	1	0	0
d	0	1	0	0
E	0	0	1	0
e	0	0	1	0
e	0	0	1	0
G	0	0	0	1
G	0	0	0	1
g	0	0	0	1
g	0	0	0	1

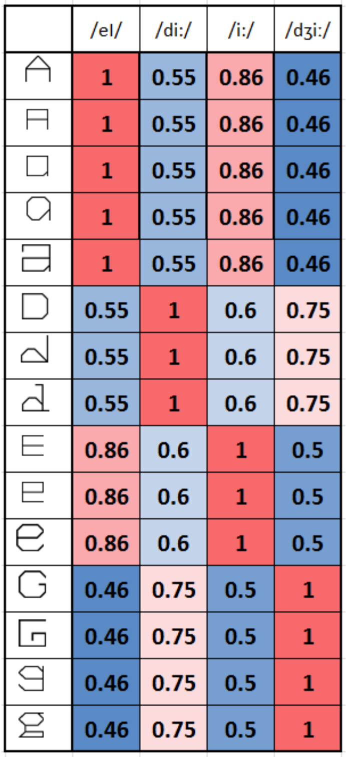

	/eI/	/di:/	/i:/	/dʒi:/
A	1	0.55	0.86	0.46
A	1	0.55	0.86	0.46
a	1	0.55	0.86	0.46
a	1	0.55	0.86	0.46
a	1	0.55	0.86	0.46
D	0.55	1	0.6	0.75
d	0.55	1	0.6	0.75
d	0.55	1	0.6	0.75
E	0.86	0.6	1	0.5
e	0.86	0.6	1	0.5
e	0.86	0.6	1	0.5
G	0.46	0.75	0.5	1
G	0.46	0.75	0.5	1
g	0.46	0.75	0.5	1
g	0.46	0.75	0.5	1

Appendix Figure 11. The image on the left depicts a sample of the Cross-modal Letter Identity pRSM. The image on the right depicts the Cross-modal Phonetic Feature Overlap pRSM for 15visual letter shapes and 4 letter names.

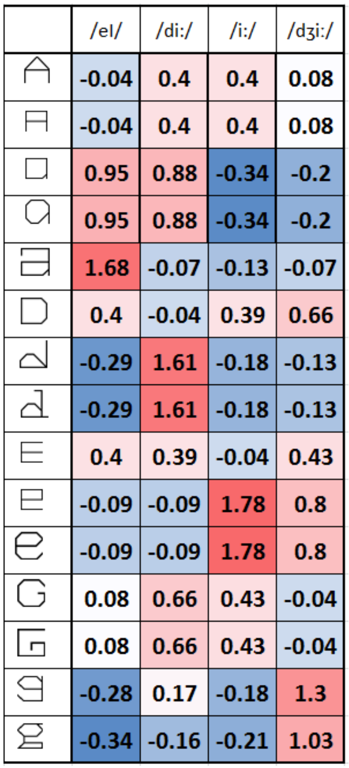

	/eI/	/di:/	/i:/	/dʒi:/
A	-0.04	0.4	0.4	0.08
A	-0.04	0.4	0.4	0.08
a	0.95	0.88	-0.34	-0.2
a	0.95	0.88	-0.34	-0.2
a	1.68	-0.07	-0.13	-0.07
D	0.4	-0.04	0.39	0.66
d	-0.29	1.61	-0.18	-0.13
d	-0.29	1.61	-0.18	-0.13
E	0.4	0.39	-0.04	0.43
e	-0.09	-0.09	1.78	0.8
e	-0.09	-0.09	1.78	0.8
G	0.08	0.66	0.43	-0.04
G	0.08	0.66	0.43	-0.04
g	-0.28	0.17	-0.18	1.3
g	-0.34	-0.16	-0.21	1.03

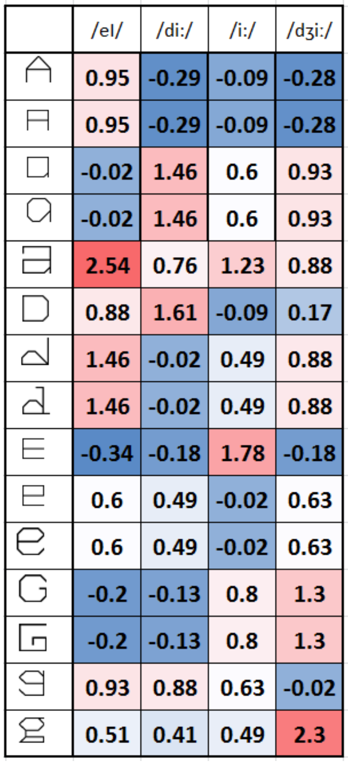

	/eI/	/di:/	/i:/	/dʒi:/
A	0.95	-0.29	-0.09	-0.28
A	0.95	-0.29	-0.09	-0.28
a	-0.02	1.46	0.6	0.93
a	-0.02	1.46	0.6	0.93
a	2.54	0.76	1.23	0.88
D	0.88	1.61	-0.09	0.17
d	1.46	-0.02	0.49	0.88
d	1.46	-0.02	0.49	0.88
E	-0.34	-0.18	1.78	-0.18
e	0.6	0.49	-0.02	0.63
e	0.6	0.49	-0.02	0.63
G	-0.2	-0.13	0.8	1.3
G	-0.2	-0.13	0.8	1.3
g	0.93	0.88	0.63	-0.02
g	0.51	0.41	0.49	2.3

Appendix Figure 12. The image on the left depicts a sample of the Cross-modal pRSM for Visually Similarity assuming the letter names activate uppercase letters. The image on the right is the same but assuming the names activate lowercase letters. The values in each pRSM are standardized z-scores.

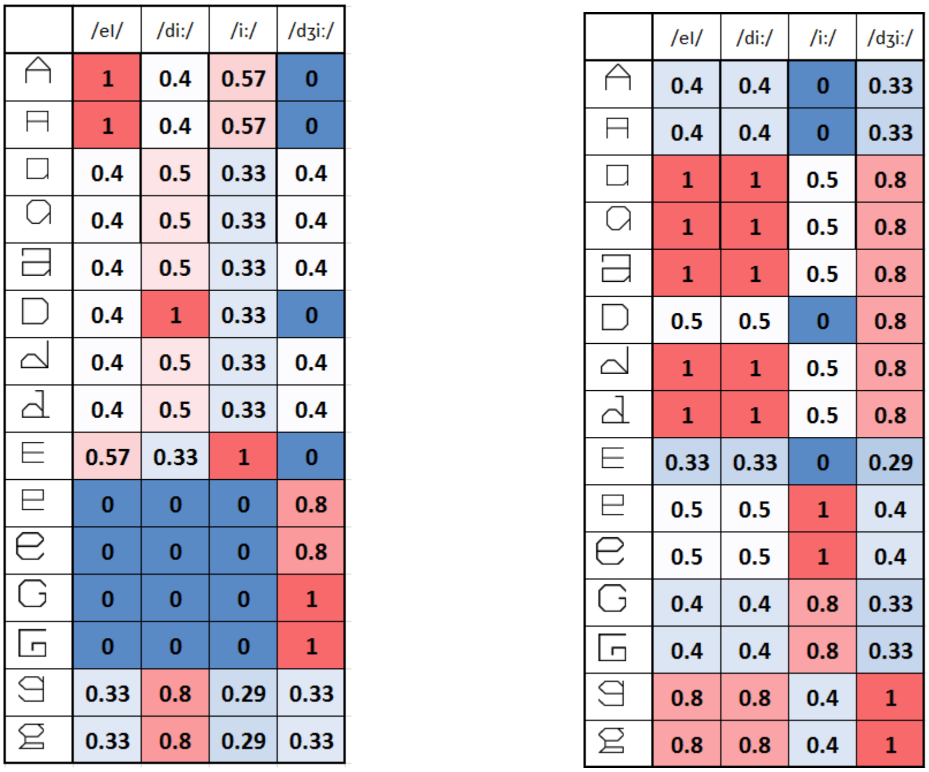

	/eI/	/di:/	/i:/	/dʒi:/
A	1	0.4	0.57	0
A	1	0.4	0.57	0
a	0.4	0.5	0.33	0.4
a	0.4	0.5	0.33	0.4
a	0.4	0.5	0.33	0.4
D	0.4	1	0.33	0
d	0.4	0.5	0.33	0.4
d	0.4	0.5	0.33	0.4
E	0.57	0.33	1	0
e	0	0	0	0.8
e	0	0	0	0.8
G	0	0	0	1
G	0	0	0	1
g	0.33	0.8	0.29	0.33
g	0.33	0.8	0.29	0.33

	/eI/	/di:/	/i:/	/dʒi:/
A	0.4	0.4	0	0.33
A	0.4	0.4	0	0.33
a	1	1	0.5	0.8
a	1	1	0.5	0.8
a	1	1	0.5	0.8
D	0.5	0.5	0	0.8
d	1	1	0.5	0.8
d	1	1	0.5	0.8
E	0.33	0.33	0	0.29
e	0.5	0.5	1	0.4
e	0.5	0.5	1	0.4
G	0.4	0.4	0.8	0.33
G	0.4	0.4	0.8	0.33
g	0.8	0.8	0.4	1
g	0.8	0.8	0.4	1

Appendix Figure 13. The image on the left depicts a sample of the Cross-modal pRSM for Motor Feature Overlap assuming the letter names activate uppercase letters. The image on the right is the same but assuming the names activate lowercase letters.

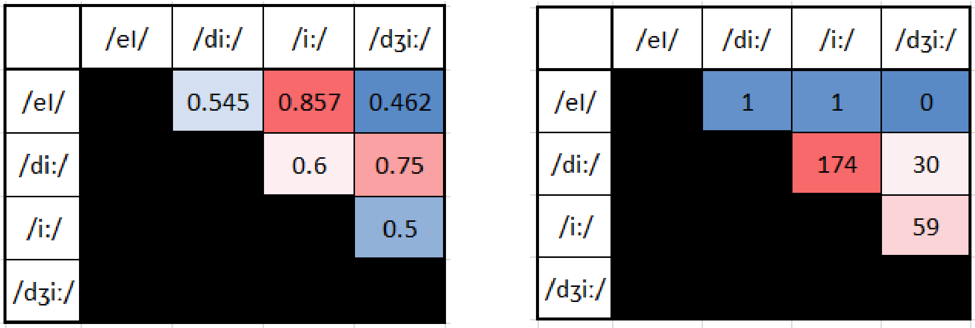

	/eI/	/di:/	/i:/	/dʒi:/
/eI/		0.545	0.857	0.462
/di:/			0.6	0.75
/i:/				0.5
/dʒi:/				

	/eI/	/di:/	/i:/	/dʒi:/
/eI/		1	1	0
/di:/			174	30
/i:/				59
/dʒi:/				

Appendix Figure 14. The image on the left depicts a sample of the Auditory pRSM for Phonetic Feature Overlap. The image on the right depicts a sample of the Auditory pRSM for Letter Name Confusability.

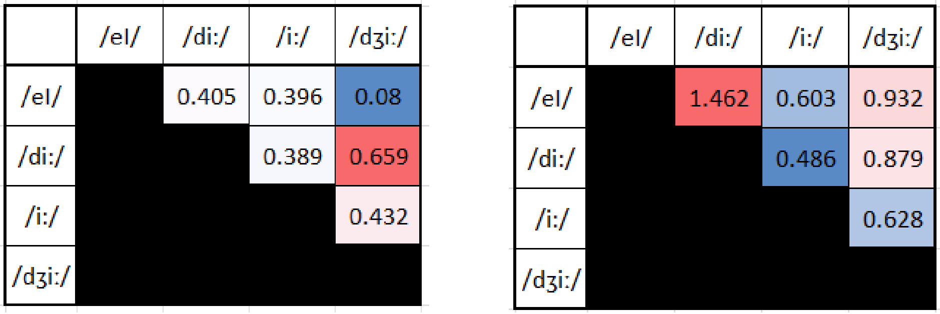

	/eI/	/di:/	/i:/	/dʒi:/
/eI/		0.405	0.396	0.08
/di:/			0.389	0.659
/i:/				0.432
/dʒi:/				

	/eI/	/di:/	/i:/	/dʒi:/
/eI/		1.462	0.603	0.932
/di:/			0.486	0.879
/i:/				0.628
/dʒi:/				

Appendix Figure 15. The image on the left depicts a sample of the Auditory pRSM for Visually Similarity assuming the letter names activate uppercase letters. The image on the right is the same but assuming the names activate lowercase letters. The values in each pRSM are standardized z-scores.

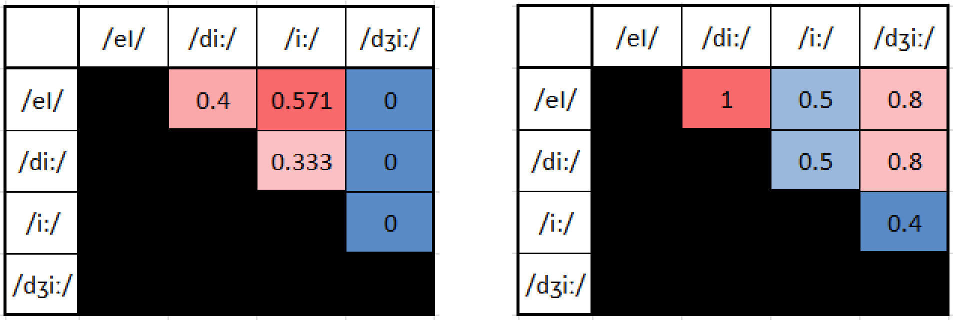

	/eI/	/di:/	/i:/	/dʒi:/
/eI/		0.4	0.571	0
/di:/			0.333	0
/i:/				0
/dʒi:/				

	/eI/	/di:/	/i:/	/dʒi:/
/eI/		1	0.5	0.8
/di:/			0.5	0.8
/i:/				0.4
/dʒi:/				

Appendix Figure 16. The image on the left depicts a sample of the Auditory pRSM for Motor Feature Overlap assuming the letter names activate uppercase letters. The image on the right is the same but assuming the names activate lowercase letters.

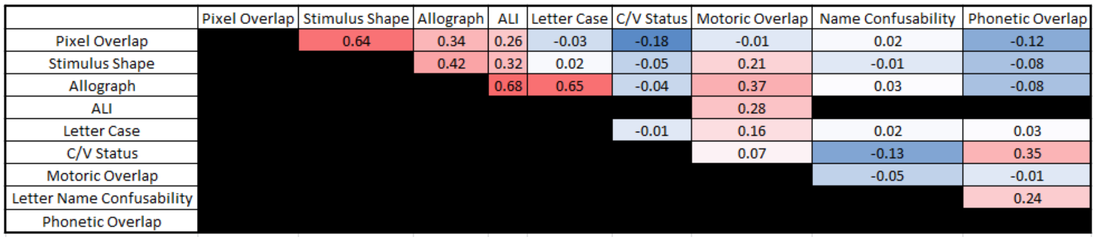

	Pixel Overlap	Stimulus Shape	Allograph	ALI	Letter Case	C/V Status	Motoric Overlap	Name Confusability	Phonetic Overlap
Pixel Overlap		0.64	0.34	0.26	-0.03	-0.18	-0.01	0.02	-0.12
Stimulus Shape			0.42	0.32	0.02	-0.05	0.21	-0.01	-0.08
Allograph				0.68	0.65	-0.04	0.37	0.03	-0.08
ALI							0.28		
Letter Case						-0.01	0.16	0.02	0.03
C/V Status							0.07	-0.13	0.35
Motoric Overlap								-0.05	-0.01
Letter Name Confusability									0.24
Phonetic Overlap									

Appendix Figure 17. The similarity matrix formed by cross correlating all of the pRSMs from the sensitivity analysis in Experiment 4.

CURRICULUM VITA

David William Rothlein was born on May 14, 1985 in Boston, MA. He moved to Danbury, CT a short 2 weeks later. He graduated from Danbury High school in 2003 and matriculated at Boston University from 2003-2005 before transferring to the University of Connecticut. He finished his undergraduate career at the University of Connecticut in 2007, graduating magna cum laude with a B.S. in Cognitive Science and a minor in Neuroscience. He subsequently started his graduate studies at the Johns Hopkins University in the Cognitive Science Department focusing on mental rotation and letter recognition under the mentorship of Michael McCloskey and Brenda Rapp. In the fall of 2015 he will be starting a postdoctoral position at the Veterans Affairs Health System in Boston, MA.